İSTANBUL UNIVERSITY-CERRAHPAŞA
INSTITUTE OF GRADUATE STUDIES

M.Sc. THESIS

THE BEHAVIOR OF ADJACENT SHALLOW FOUNDATIONS LOCATED ON OR IN SLOPES

Bashar BADAWI

SUPERVISOR
Assoc. Prof. Dr. Zülal AKBAY ARAMA

Civil Engineering Department

Civil Engineering Programme

June, 2023

THESIS ACCEPTANCE AND APPROVAL

This thesis titled **"Thesis Title"**, prepared by **Bashar BADAWI** under the supervision of **Assoc. Prof. Dr. Zülal AKBAY ARAMA** , was accepted as a **M.Sc. Thesis** after being **consensus** approved by our jury as a result of the exam held on **16/06/2023**.

Examining Committee Members

		Signature	Decision
SUPERVISOR	Assoc. Prof. Dr. Zülal AKBAY ARAMA İstanbul University-Cerrahpaşa Civil Engineering Department		☒ Accept ☐ Reject
MEMBER	Prof. Dr. İlknur BOZBEY İstanbul University-Cerrahpaşa Civil Engineering Department		☒ Accept ☐ Reject
MEMBER	Assist. Prof. Dr. Nazife Özge FERCAN Istanbul Kültür University Civil Engineering Department		☒ Accept ☐ Reject

DECLARATION

I hereby declare that this thesis is my own work, I have not had engaged in any unethical behavior at any of the stages from planning to the writing of the thesis, I have obtained all the information in this thesis within the limits of the academic and scientific ethical rules, I have cited all the information and comments being obtained in this thesis study, and I have included these references in the list of references. During the analysis and writing stages of this thesis, I accept that I have abided by the patent and copyright rights and therefore I myself take all kinds of legal responsibility.

Bashar BADAWI

To My Family… …

FUNDING

THE BEHAVIOR OF ADJACENT SHALLOW FOUNDATIONS LOCATED ON OR IN SLOPES

This thesis was supported by the project number - of the İstanbul University-Cerrahpaşa Scientific Research Projects Executive Secretariat.

ACKNOWLEDGEMENT

I would like to extend my heartfelt gratitude and sincere thanks to the individuals who have played a pivotal role in the completion of this thesis.

First and foremost, I am deeply grateful to my exceptional thesis supervisor Assoc. Prof. Dr. Zülal Akbay Arama. Their unwavering support, invaluable guidance, and expertise have been instrumental in shaping this research endeavor. I am truly fortunate to have had the opportunity to work under their mentorship.

I am also indebted to my loving family for their constant encouragement, understanding, and unwavering belief in my abilities. Their support and patience throughout this journey have been the cornerstone of my success. Their presence and motivation have kept me going even during the most challenging times.

To my family, my thesis supervisor, and my friends, I offer my deepest gratitude. Your unwavering support, guidance, and belief in me have been the driving force behind the culmination of this thesis.

June, 2023 Bashar BADAWI

CONTENTS

LIST OF FIGURES

Page

LIST OF TABLES

Page

LIST OF SYMBOLS AND ABBREVIATIONS

Symbols	Description
τ	: Represents the shear stress
c'	: Represents the cohesion force per unit weight
σ'	: Represents the effective normal stress per unit weight
φ'	: Represents the internal friction angle
φ	: Shear strenght angle
β	: Inclination angle of the slope
C	: Cohesion
ϕ	: Friction
γ	: The moist unit weight of the soil
γ_{sat}	: The saturated unit weight of the soil
H	: The slope height
B	: The foundation width
L	: The distance between the foundation and the top point of the slope
L_f	: The distance between the two foundations

Abbreviations	Description
FOS	: Factor Of Safety
Dr	: Relative Density
ULI	: Ultimate Load Intens
b/B	: Setback Ratio
S/B	: Spacing Ratio
SRM	: The Strength Reduction Method
EA	: Axial stiffness value
EI	: Inertia stiffness value

GENİŞLETİLMİŞ ÖZET

YÜKSEK LİSANS TEZİ

ŞEV ÜZERİNDE VEYA İÇİNDE YER ALAN KOMŞU YÜZEYSEL TEMELLERİN DAVRANIŞI

Bashar BADAWI

İstanbul Üniversitesi-Cerrahpaşa

Lisansüstü Eğitim Enstitüsü

İnşaat Mühendisliği Anabilim Dalı

İnşaat Mühendisliği Programı

Danışman : Doç. Dr. Zülal AKBAY ARAMA

Ülkemizde, özellikle büyük şehirlerimmizde, hızla artan nüfus oranı kentleşme ve istihdam imkanlarının sorgulanmasını zorunlu kılmıştır. Sınırlı iskan alanlarında yüksek kapasitede istihdam sağlamak amacı ile yatay mimariden ziyade dikey mimariye yönlenme başlamış ve aynı zamanda yapıların aralarında sınırlı bir mesafe bırakılarak veya bırakılmayarak bitişik nizam inşa süreci ile alan kazanımı mantığı artan bir hız kazanmıştır. Yakın mesafede inşa edilen bu binalar özellikle eğimli yüzeyler üzerinde yer almakta iseler temel elemanları yatayda etkileşimde bulunan temel elemanlarından daha farklı bir mekanizma ile deformasyon gösterebilirler ve taşıma güçleri yapının özelliklerine bağlı olarak farklılıklar içerebilmektedir. Literatürde, şevli yüzeyler üzerinde ve içerisinde yer alan binaları inceleyen analiz çalışmaları mevcuttur ancak süreci şevlerin başlangıç stabilitesinin irdelenmesinden başlayıp farklı tasarım özelliklerine bağlı olarak gerçekleşebilecek etkileşimin sorgulanması esasına dayanan çalışmalar sınırlıdır. Bu çalışma kapsamında, uyulama açısından sıklıkla karşımıza çıkan söz konusu problemin detaylı bir şekilde analiz edilmesi için kullanılan ticari iki boyutlu ve sonlu elemanlar yöntemi ile çalışan bir geoteknik mühendisiliği programından faydalanılmıştır.

Çalışma kapsamında saf kum temel zeminlerinden oluşan şevler göz önüne alınmış olup, kumun göreceli sıkılık değerinden faydalanılarak rijitlik ve kayma mukavemeti parametreleri elde edilmiştir. Toplamda yirmi farklı temel zemini kullanılarak yapılan birincil analizlerde göçmeden belirli bir güvenlik seviyesinde stabilitesini koruyabilecek olan şev kesitleri belirlenmiş ve olası en kritik göçme mekanizmaları belirlenmiştir. Çalışmanın ardışık aşamalarında sırası ile şev üzerinde yer alan tekil yüzeysel temeller, şev içerisinde yer alan tekil yüzeysel temeller, şev üzerinde yer alan iki komşu yüzeysel temel ve şev içerisinde yer alan iki komşu yüzeysel temel birleşimlerinden oluşan vakalar irdelenmiştir. Bu vakaların analiz edilmesi yolu ile şev üzerine farklı şekillerde nihai taşıma kapasitesi oranında yüklenerek şevi sınır göçme durumuna getiren limit durumlar incelenmiştir. Şevin başlangıçta belirli bir güvenlik seviyesinde sergilediği davranıştan tekil ve çoğul temeller inşası ile deformasyon ve güvenlik durumunun gelişimi takip edilmiş ve aynı zamanda farklı inşa koşulları söz konusu olması durumunda olası kritik göçme düzlemlerinin takibi yapılabilmiştir. Parametrik analizlerde temel zemini olan kumun geoteknik özelliklerinin değişiminin yanı sıra, temel boyutlarının, şevin yüksekliğinin, şev-temel etkileşim mesafesindeki farklılaşmanın ve temeller arasındaki mesafenin değişmesinin belirli vakalarda deformasyon durumu değişimine ve güvenlik sayısı ile mobilize olan kayma düzlemlerine etkisine odaklanılmıştır. Çalışmanın sonuçları, kum şevlerin içine veya üzerine inşa edilecek tekil veya çoklu temellerin deformasyon ve kayma mekanizmaları gözetilerek etkileşim mesafesinin belirlenmesinde, stabilite durumunu etkiyen koşulların değişiminin algılanmasında ve olası göçme mekanizmalarının tahmininde yol göstericidir.

Haziran 2023 , 106.. sayfa.

Anahtar kelimeler: Şev, Yüzeysel temel, Kum, Güvenlik

ABSTRACT

M.Sc. THESIS

THE BEHAVIOR OF ADJACENT SHALLOW FOUNDATIONS LOCATED ON OR IN SLOPES

Bashar BADAWI

İstanbul University-Cerrahpaşa

Institute of Graduate Studies

Department of Civil Engineering

Civil Enginering Programme

Supervisor : Assoc. Prof. Dr. Zülal AKBAY ARAMA

The rapidly increasing population rate, especially in our country's major cities, has necessitated questioning urbanization and employment opportunities. In order to provide high-capacity employment in limited residential areas, there has been a shift towards vertical architecture rather than horizontal architecture, and the logic of gaining space through the construction process of adjacent buildings with or without leaving a limited distance between them has accelarated. If these buildings constructed in close proximity are located on slopes, their foundation elements can undergo deformation with a mechanism different from the foundation elements that interact horizontally, and their load-bearing capacities can vary depending on the characteristics of the structure. There are analysis studies in the literature that examine buildings located on slopes, but studies based on questioning the interaction that can occur depending on different design features starting from the examination of the initial stability of the slopes are limited. In this study, a widely used commercial two-dimensional finite element method-based geotechnical engineering program was utilized to analyze the mentioned problem in detail from an implementation perspective. Slopes composed of pure sand foundation soils were considered in the study, and parameters such as stiffness and shear strength were obtained by utilizing the relative density value of the sand. In the primary analyses conducted using twenty different foundation soil profiles, slope sections that can maintain stability at a certain level of safety without failure were determined, and the possible critical failure mechanisms were identified. In the subsequent stages of the study, cases consisting of single shallow foundations on the slope, single shallow foundations within the slope, two adjacent shallow on the slope, and two adjacent shallow foundations within the slope were examined. Through the analysis of these cases, limit states were investigated by subjecting the slope to various loads in different ways to reach the ultimate bearing capacity ratio and induce failure. The deformation and safety conditions were monitored by observing the behavior of the slope from the initial level of safety to the construction of single and double foundations, and the tracking of potential critical failure planes was possible in the case of different construction conditions. In parametric analyses, the focus was on the change in deformation condition and the effect on the safety factor and mobilized shear planes in certain cases by varying not only the geotechnical properties of the sand foundation soil but also the foundation dimensions, slope height, differentiation in the slope-foundation interaction distance, and distance between the foundations. The results of the study provide guidance in determining the interaction distance, taking into account the deformation and shear mechanisms of single or multiple foundations to be constructed within or on sandy slopes. They also aid in detecting the changes in conditions that affect the stability state and predicting possible failure mechanisms.

June 2023, 106. pages.

Keywords: Slope, Shallow foundation, Sand, Safety

1. INTRODUCTION

A slope is an inclined surface with a height difference compared to a flat ground. A slope can occur naturally due to the natural inclination of the land or as a result of construction or engineering works. Slopes can be found in natural or artificial topographic features such as hills, cliffs, valleys, or sloping terrains. Slopes can have different types depending on the degree of inclination, shape, and stability. The degree of inclination indicates how steep or gentle the slope is. The shape refers to how the surface of the slope is inclined, such as a straight slope, concave slope, or convex slope. Stability indicates how stable the slope is in its natural state or with human intervention. In other words, slope is a term used in the construction industry and provide a potential area for building structures. However, it is important to construct slopes considering their stability and engineering calculations. Slope constructions done without proper design and safety measures can lead to issues such as erosion, soil sliding, or collapse. Within this context, Slope stability analysis involves engineering studies conducted to evaluate the stability of an inclined surface and identify potential hazards. These analyses assess the resistance of slopes to above mentioned stability issues. Slope stability analyses typically involve the following steps:

1. Determination of Soil Properties: Engineering properties of the soil on the slope, such as water content, unit weight, permeability of capillary water, etc., need to be determined. These data provide the fundamental information for the analyses.

2. Measurement of Geometry and Slope Parameters: Measuring the slope's geometry, including its inclination, height, width, and surface profile, is crucial. These measurements help determine the parameters used in the analyses.

3. Determination of Loads: The loads on the slope, including the weight of structural components, soil pressures, additional loads, etc., are considered in the analysis.

4. Application of Stability Analysis Methods: Various methods are employed for slope stability analyses. These methods may include hand analysis, limit equilibrium analysis,

curved failure surface analysis, finite element analysis, numerical modeling, and others. These analyses are used to assess the slope's stability and potential hazards.

5. Calculation of the Safety Factor: The analysis typically yields a safety factor, which indicates the slope's stability and level of safety. A high safety factor indicates a more stable and secure slope.

This leads us to question why engineers build on slopes. In fact, building on or near slopes is unavoidable, like what we have for highways, bridges and subways, in addition to some touristic reasons or due to land impediments. There are various reasons why slopes may be preferred for building construction:

1. Scenic beauty and natural aesthetics: Slopes are often located at higher positions, providing magnificent views. Building on slopes allows for better appreciation of natural beauty, cityscapes, or sea views.

2. Land utilization: Limited space in cities makes building on slopes attractive. Buildings constructed on slopes can vertically ascend and provide more living space, optimizing land utilization.

3. Aesthetic value: Buildings on slopes can be architecturally striking and intriguing. Such structures can add a unique appearance to the city skyline and enhance urban charm.

4. Climate advantages: Slopes can offer advantages in terms of climate factors. For example, increased exposure to sunlight and natural wind protection can enhance energy efficiency and improve building performance.

5. Topographic compatibility: Slopes can be a suitable construction area in various terrain structures and sloping regions. Building designs can better integrate with the natural topography of slopes.

6. Subterranean utilization: Slopes can sometimes provide access to underground areas. For instance, underground levels such as parking lots or storage spaces can be incorporated beneath slopes.

Hence, a foundation built on slope conducts a reduction in the bearing capacity of the foundation and threatening the stability of the slope itself. In that case we have two modes of failure; bearing capacity failure when the shear surface does not intersect the slopes, where bearing capacity theories for horizontal ground surface are applicable to such modes of failure. The second mode of failure is the slope failure, where the critical shear surface extends beyond the crest and therefore involves part of the slope. Even if the above-mentioned reasons show the positive aspects of building on slopes, there are also some disadvantages for structures built on slopes. Potential differential risks that may be encountered when a structure is built on a slope are listed below:

1. Geotechnical challenges: Buildings constructed on slopes carry certain risks related to stability and soil strength. Construction without proper soil investigation and engineering calculations can lead to problems such as erosion, sliding, and settlement.

2. Safety concerns: Buildings on slopes are exposed to various natural hazards. Especially during disasters like earthquakes, the safety of buildings on slopes can be a significant concern. Construction processes and structural integrity must be taken into account.

3. Maintenance difficulties: Maintenance and repair of buildings on slopes can be more challenging compared to other structures. Due to difficult access and steep terrain, maintenance tasks can be costly and time-consuming.

4. Stability: The stability of buildings within a slope is of utmost importance. Slopes may pose risks such as erosion, soil sliding, or collapse. Appropriate engineering calculations and structural reinforcement measures are necessary to ensure stability.

5. Construction costs: Building within a slope can sometimes entail a more complex and costly construction process. Constructing on an inclined surface may involve earthwork modifications, reinforcement measures, and accessibility challenges, all of which can increase costs.

These problems encountered in the structures built on the slope are also valid for the structures built inside the slope. In both of these cases, it is necessary to consider the structure-soil interaction and evaluate all parameters that can influence the behavior. Within the scope of literature studies, these topics have been addressed in a limited manner, and there is a need for research that can provide guidance by evaluating and consolidating all parameters that can potentially affect the behavior in a single source.

Within this context, the scope of this thesis is intended to address two important and fundamental points related to building structures on or in a slope; to examine the ultimate bearing capacity of a shallow foundation placed near or within a slope and to consider the inevitable reduction in bearing capacity due to the presence of the slope. A separate and important objective of this thesis is to investigate the effects on the stability behavior of single foundations located on or within the slope, as well as a limited number of buildings constructed in contiguous order. For this purpose, within the scope of this thesis, firstly, the geometric criteria that should be applied to maintain the stability of the slopes at certain heights were determined by parametric analysis. Numerical analyses were carried out using a commercial software that works with finite element method. The second phase of the thesis is the analysis of single foundations to be built on the slope under stable conditions by using different loading, foundation and soil properties. In the third stage, the interaction mechanisms of the neighboring foundations on the slope and the interaction mechanisms with the slope were investigated using variable parameters. In the fourth stage, the single shallow foundations in the slope were analyzed and in the fifth stage, the adjacent shallow foundation buildings in the slope were analyzed. In all of the analyses, slopes consisting of sand soils were analyzed, but with different stiffness and strength values depending on different relative stiffnesses of interest.

2. CONCEPTUAL FRAMEWORK

Within the context of the mentioned information, there are several literature studies performed to investigate the overall behavior of foundations located on slopes.

Meyerhof, according to his 1957 paper, examined the ultimate bearing capacity of foundations on slopes. He proposed that his bearing capacity theory published in 1951 can be combined with the theory of slope stability to encompass this loading condition (Meyerhof 1957). Meyerhof investigated two different scenarios for the bearing capacity of foundations on slopes. The first scenario is the bearing capacity of a foundation on the face of the slope, and the second scenario is the bearing capacity of a foundation on the top of the slope. According to Meyerhof, when a foundation is loaded and fails on a slope surface, the plastic flow zone in the soil on the slope side is smaller compared to a similar foundation on flat ground, and consequently, the ultimate bearing capacity decreases. For a material, the shear strength is given as follows:

$\tau_f = c + \sigma \tan \varphi$……………………………………………………………… Eq. 2.1

Here:

- τ represents the shear stress.
- c' represents the cohesion force per unit weight.
- σ' represents the effective normal stress per unit weight.
- φ' represents the internal friction angle.

In this equation, the effective normal stress, cohesion force, and internal friction angle are used to calculate the plastic flow zone along the slope. According to Meyerhof, the plastic flow zone in the soil on the slope side is smaller compared to a similar foundation on flat ground. This occurs due to the lateral support effect of the soil on the vertical face. Therefore, when the plastic flow zone decreases, the shear strength decreases, and the ultimate bearing capacity decreases.

The bearing capacity of a foundation on a slope with an inclination β can be expressed using Terzaghi's equation (Terzaghi, 1943).

$q = cN_c + P_0N_q + \gamma(BN / 2)_\gamma$…………………………………………………….. Eq. 2.2

Or, the bearing capacity of a foundation on a slope can be presented using Meyerhof's equation (Meyerhof, 1951).

$q = cN_{cq} + \gamma(BN / 2)_{\gamma q}$……………………………………….…………………. Eq. 2.3

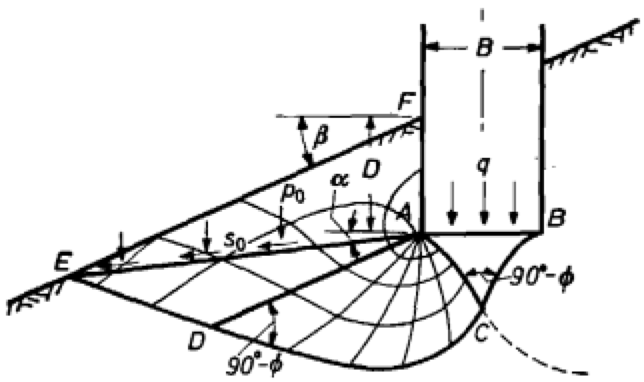

Figure 2.1. The plastic zones occurred near rough strip foundation (Meyerhof, 1957)

A study was conducted to determine the bearing capacity factors for foundations placed on or near slopes in two different types of soil: purely cohesive (φ=0) and cohesionless (c=0) materials. The bearing capacity factors were found to decrease as the slope inclination increased, reaching a minimum at β=90° for purely cohesive materials and β=φ for cohesionless soils. When the slope angle (β) is less than 30°, the decrease in bearing capacity is relatively small for clays but significant for sands and gravels. This is because the bearing capacity of cohesionless soils decreases approximately in a parabolic manner as the slope angle increases.

In the case of submerged soil, the unit weight (ɣ) is replaced by the submerged unit weight (ɣ') of the soil. For situations involving rapid drawdown of the water table, the bearing capacity can be determined using Meyerhof's equation with a reduced angle of friction, as in the case of unloaded slopes (Terzaghi, 1943). These findings highlight the importance of considering the slope angle and soil type when assessing the bearing capacity of foundations placed on or near slopes. Different factors come into play depending on the cohesive or cohesionless nature of the soil, as well as the presence of water or changes in the water table.

$$\phi' = \tan^{-1}((\gamma'/\gamma)\tan\varphi) \qquad \text{Eq. 2.4}$$

In cohesive materials where the angle of shearing resistance is small or nonexistent, the bearing capacity of a foundation may be restricted by the stability of the entire slope, with a potential slip surface intersecting the toe or base of the slope. In the case of slopes in purely cohesive soil that have considerable depth, base failure of an unloaded slope occurs along a critical mid-point circle (Fellenius, 1927). This means that foundations positioned below the mid-point section enhance the overall stability of the slope, while those above it decreases the stability. The upper limit of the bearing capacity can be estimated using the following equation:

$$q = cN_{cq} + \gamma D \qquad \text{Eq. 2.5}$$

In the same study, Meyerhof presented the bearing capacity of a foundation on top of a slope using his well-known equation.

$$q = cN_{cq} + \gamma(BN\,/\,2)_{\gamma q} \qquad \text{Eq. 2.6}$$

In Meyerhof's analysis, the resultant bearing capacity factors Ncq and Nɣq are influenced by several factors, including the distance (b) from the edge of the slope, the slope inclination (β), the internal friction angle (φ), and the ratio of embedment depth to foundation width (D/B). These factors collectively determine the bearing capacity of a foundation on top of a slope. The bearing capacity factors decrease as the slope inclination increases. However, they increase significantly as the distance from the foundation to the edge of the slope becomes greater. Beyond a certain distance, typically ranging from 2 to 6 times the foundation width (depending on φ and D/B), the bearing capacity becomes independent of the slope inclination. At this point, it reaches a value equivalent to that of a foundation on a large horizontal ground surface. The theory of bearing capacity for foundations on level ground can be extended and combined with slope stability theory to analyze the stability of foundations on slopes. When a foundation is located on the face of a slope or near the top edge of a slope, the bearing capacity decreases with a greater slope inclination, especially in cohesionless soils. However, as the distance from the edge of the slope increases, the bearing capacity decreases significantly with a greater height of the slope. In such cases, the overall stability of the slope governs the bearing capacity behavior of the foundation.

In 1988, Graham et al. proposed an analysis method for determining the bearing capacity of shallow foundations placed in cohesionless slopes. Their analysis took into account the stress conditions directly beneath the footing. The method utilized the concept of stress characteristics and incorporated sand properties based on a critical state model. The stress characteristics method considered various stress levels, different placement densities of the sand, and the compressibility of the soil. It also accounted for the transition from strain softening to strain hardening behavior that occurs as the stress levels increase. This means that the method captured the changes in soil behavior as the stresses acting on it increased. The critical state model, which describes the behavior of sand under different stress conditions, played a key role in this analysis method. By incorporating these soil properties and stress characteristics, Graham et al. aimed to provide a more accurate estimation of the bearing capacity of shallow foundations in cohesionless slopes. The work by Graham in 1986 likely provided further insights into the sand compressibility and the transition between strain softening and strain hardening behavior in cohesionless soils, which were integral to the proposed analysis method for determining the bearing capacity in cohesionless slopes.

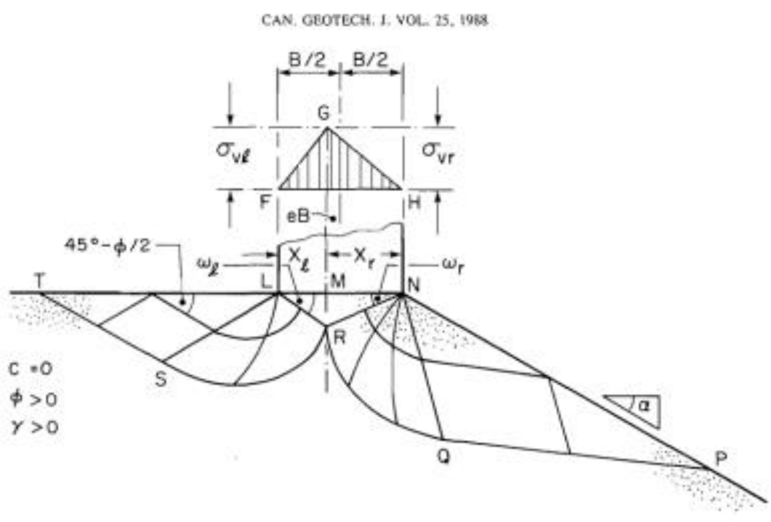

Figure 2.2. Failure zones defined by Graham et al. (1988)

In their study published in 1990, Narita and Yamaguchi focused on determining the bearing capacity of foundations located near slopes using log-spiral sliding surfaces. This study was an extension of their earlier work, which investigated the bearing capacity of strip foundations on level ground using the same analysis method. The researchers employed log-spiral sliding surfaces to analyze the failure mechanisms near slopes. Specifically, they considered a strip footing with a width of B = 2b, positioned at a distance of L = λB from the edge of a slope inclined at an angle β. The sliding surface was assumed to follow a logarithmic spiral shape. Narita and Yamaguchi aimed to examine the applicability and validity of their proposed technique for practical engineering problems. To accomplish this, they conducted a comparative study that involved analyzing and comparing their results with other analytical methods and experimental findings. By conducting this research, Narita and Yamaguchi aimed to provide insights into the bearing capacity of foundations near slopes and to verify the effectiveness of their log-spiral analysis technique in practical engineering scenarios. The representative equation of a log spiral is given as:

$r = r_0 \exp(\mu\theta)$………………………………………………………………… Eq. 2.7

Where μ=tan φ (φ is the shear strenght angle) and ro = OA

The log-spiral sliding surface used by Narita and Yamaguchi can be defined by specifying sets of values related to the footing condition (β, λ) and the location of the pole O (ro, α).

1. Footing condition:

- β represents the inclination angle of the slope.
- λ represents the distance of the strip footing from the edge of the slope, expressed as a multiple of the footing width (B = 2b).

2. Location of the pole O:

- ro represents the radial distance of the pole O from the origin or the center of the log-spiral.
- α represents the angular position or angle of the pole O.

By specifying these sets of values, the log-spiral sliding surface can be precisely defined and utilized in the analysis of the bearing capacity of foundations near slopes. The log-spiral shape provides a mathematical representation of the failure mechanism and allows for the assessment of stability and load-bearing capacity in these scenarios. It is important to refer to the specific study by Narita and Yamaguchi (1990) for further details on the calculation and utilization of these parameters in their log-spiral analysis method for foundations near slopes. In the log-spiral method of analysis, each component of the ultimate load Q (Q_c, Q_q, and Q_γ) is determined by minimizing the corresponding footing load, which is derived individually from the equilibrium of moments about the pole O.

To calculate each component, the equilibrium of moments is established by considering the forces and moments acting on the strip footing. By minimizing the moments about the pole O, the values of Q_c (related to cohesion), Q_q (related to surcharge load), and Q_γ (related to unit weight) can be determined. In cases where the height of the fill is relatively small, denoted as H = hB, and base failure is likely to be the dominant failure mechanism, the equations for toe and slope failure can be applied with some modifications. These modifications take into account the specific conditions and factors associated with base failure in relatively small fill heights.

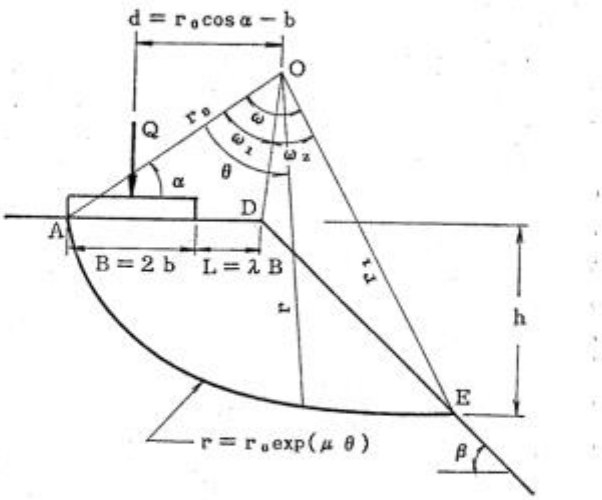

Figure 2.3. Log-spiral failure surface (Narita and Yamaguchi, 1990)

The authors of the study have reached three main conclusions:

1. The log-spiral analysis tends to overestimate the bearing capacity values compared to the upper bound and simplified Bishop solutions. The errors involved are around 20% at maximum and vary depending on the angle of internal friction (ø) and slope inclination (β).

2. In the case of purely cohesive soils, the log-spiral solution becomes close to other analytical solutions, with a maximum error of 5% at most.

3. For cohesionless soils, both the log-spiral and upper bound solutions show a gradual increase in the $N\gamma$ value (bearing capacity factor related to unit weight) as the distance between the footing and the edge of the slope increases.

In general, the log-spiral solution provides acceptable agreement with other analytical solutions, especially when base failure is expected. It yields a lower value for the ultimate load compared to the upper bound solutions within a certain range of slope height. These findings suggest that the log-spiral method can be a reliable and effective approach for analyzing the bearing capacity of foundations near slopes, although it may have some limitations and discrepancies compared to other analytical solutions.

In their study, Shiau et al. (2011) investigated the undrained stability of footings on slopes and concluded that the ultimate bearing capacity of the footing in such systems is controlled by either the foundation bearing capacity or the overall stability of the slope. The combination of these two factors makes the problem challenging to solve.

To address this combined problem, there are several methods available, including:

1. Slip-line methods: These methods, pioneered by Sokolovski in 1960, involve analyzing the slip-line patterns to determine the bearing capacity and stability of the footing on the slope.

2. Limit equilibrium techniques: These techniques, such as those proposed by Meyerhof in 1957 and Narita et al. in 1990, involve establishing equilibrium conditions to assess the bearing capacity and stability of the footing on the slope.

3. Yield design theory: This theory considers the yielding behavior of the soil and applies plasticity concepts to analyze the bearing capacity and stability of the footing on the slope.

4. Upper and lower bounds: Davis and Booker in 1973 proposed the use of upper and lower bounds to approximate the bearing capacity and stability of the footing on the slope.

5. Analytical upper bound solutions: Kusakabe et al. in 1981 developed analytical upper bound solutions that provide estimates of the maximum bearing capacity and stability of the footing on the slope.

These methods offer different approaches to tackle the challenging problem of analyzing the combined bearing capacity and stability of footings on slopes. The choice of method depends on factors such as the specific conditions of the problem, available data, and desired level of accuracy.

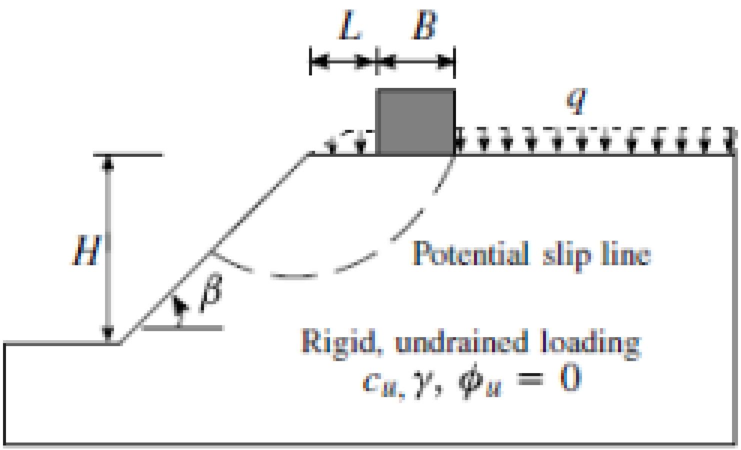

Figure 2.4. Potential failure surface and mechanism (Shiau et al., 2011)

The slip-line analysis, although mathematically rigorous, can be challenging to apply, particularly for problems with complex geometry or complicated loading conditions. On the other hand, limit equilibrium methods are less strict and can handle various complex boundary conditions, soil properties, and loading conditions. However, their accuracy is sometimes questioned. The lower and upper bound theorems are based on the concept of statically admissible stress fields and kinematically admissible velocity fields. In practice, the upper bound theorem is more commonly used because it is easier to develop a kinematically admissible failure mechanism than a statically admissible stress field. In contrast, finite element-based methods have been introduced by researchers such as Sloan, Kleeman, and Lyamin. These methods allow for the solution of large two-dimensional problems on a standard personal computer.

In their study, Shiau et al. (2011) focused on the undrained bearing capacity of a rigid strip footing placed near a slope on a homogeneous clay soil. They used finite element-based limit analysis formulations of the lower and upper bound theorems. The soil behavior was assumed to be undrained, with a shear strength represented by C_u. The study revealed that for foundations near slopes, the soil's unit weight has a significant impact on the bearing capacity. In contrast, on level ground, the unit weight of the soil does not affect the ultimate bearing capacity. The study also considered a fixed H/B ratio of 3 throughout the analysis, which resulted in toe failure. Overall, the study by Shiau et al. provides insights into the undrained bearing capacity of foundations near slopes and highlights the importance of considering soil properties and geometry in the analysis.

Chakraborty and Kumar (2013) conducted a study on the bearing capacity of foundations on slopes. They observed that for footings placed on level ground, the bearing capacity factor Nγ, which is influenced by the soil unit weight, is affected by the roughness condition of the footing. However, the bearing capacity factors N_c and N_q remain unaffected by the roughness condition. The impact of footing roughness on the values of N_c, N_q, and N_γ for foundations on sloping ground was not known. Most of the existing analyses for footings on sloping ground rely on assumptions regarding the geometry of the failure surface, except for those employing the displacement-based finite element limit analysis technique. When a material follows an associated flow rule, the solution obtained from limit analysis in conjunction with finite elements closely approximates the true solution. In their paper, Chakraborty and Kumar calculated the bearing capacity factors N_c, N_q, and N_γ for both smooth and rough strip footings with a width B placed on sloping ground with an inclination angle β relative to the horizontal. They utilized the lower bound finite element limit analysis technique in combination with nonlinear programming. The soil was considered to be plastic and followed the Mohr-Coulomb failure criterion and an associated flow rule. By employing this approach, Chakraborty and Kumar aimed to obtain accurate values of the bearing capacity factors for foundations on sloping ground, accounting for the influence of footing roughness and the plastic behavior of the soil.

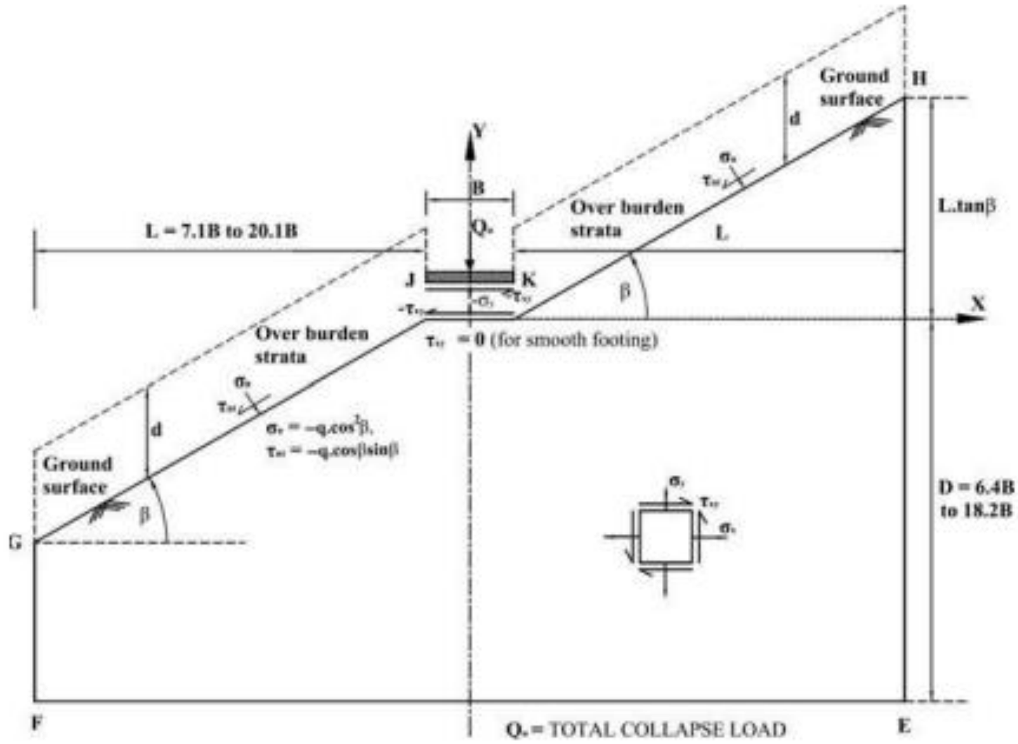

Figure 2.5. Selected domain and the stress boundary conditions (Chakraborty and Kumar, 2013)

The study by Chakraborty and Kumar (2013) revealed that the bearing capacity factors Nc, Nq, and Nγ decrease as the slope angle increases and increase with an increasing soil friction angle. In the case of rough footings, the bearing capacity factors show a significant increase compared to smooth footings.

It is important to note that the lower bound theorem of limit analysis can provide a true lower bound solution only if the material satisfies an associated flow rule.

The conclusions drawn from the study are as follows:

- Along a sloping ground surface, the bearing capacity factors are significantly higher for rough footings compared to smooth footings.
- The extent of the plastic zone around the footing base is also greater for rough footings.
- As expected, the value of the bearing capacity factors decreases significantly with an increase in the inclination of the ground surface.

Baah-Frempong and Shuklas’ (2018) study focuses on conducting a finite element analysis of a sandy soil slope that supports an embedded footing. The analysis is performed using Plaxis 2D, a commercially available finite element software. The objective is to investigate the impact of slope geometry, soil properties, and footing locations on the slope's stability, specifically in terms of the factor of safety. The used model geometry is given in Figure 1.6.

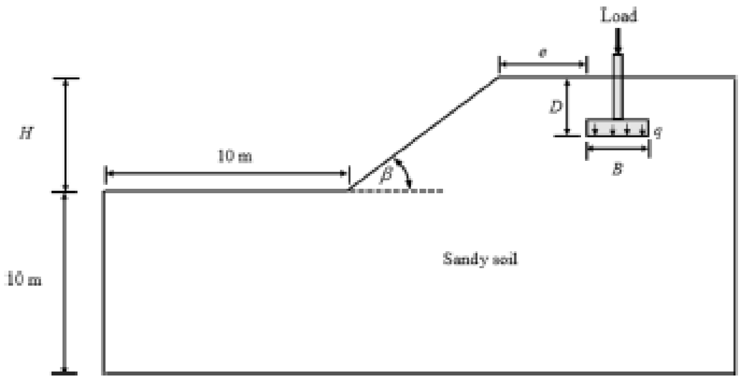

Figure 2.6. The model geometry (Baah-Frempong and Shukla, 2018)

The results ot the study of Leshchinsky (2015) are obtained using an upper-bound limit state plasticity failure discretization scheme called Discontinuity Layout Optimization (DLO). This method incorporates a non-assumptive failure geometry under translational kinematics in its formulation. The presented values highlight significant factors to consider in determining the bearing capacity of strip footings placed adjacent to slopes with c` -ϕ` soils. Specifically, the relationship between soil strength properties, slope height to footing width ratio, slope angle, and critical collapse mechanism are examined. To facilitate practical application, a set of reduction coefficients is provided, which can be directly applied to the classical bearing capacity formulation. These coefficients allow for easier implementation of the findings in engineering practice.

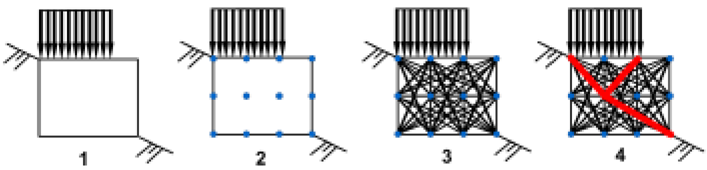

Figure 2.7. The application of DLO scheme (Leshchinsky, 2015)

Javdanian (2017) focuses on assessing the bearing capacity of shallow strip foundations constructed on a geosynthetic-reinforced sand slope using the finite difference program FLAC. The study investigates the effects of various geometric and resistivity parameters of the reinforcement layers to determine the optimal values that result in maximum bearing capacity Figure 1.8 Additionally, the influence of the strength properties of the sand embankment, foundation position, and slope angle on the behavior of strip foundations resting on a reinforced soil slope is examined. The findings reveal that the use of geosynthetic reinforcement layers significantly enhances the bearing capacity of shallow foundations.

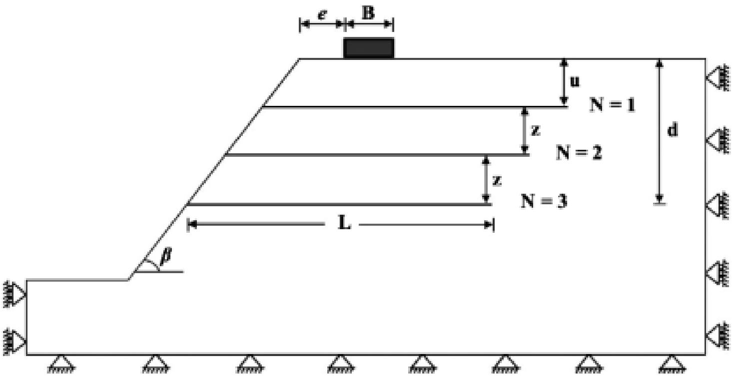

Figure 2.8. Schematic geometrical model of the analysis (Javdanian, 2017)

Yang et al. (2019) presents the derivation of an analytical approach for evaluating the bearing capacity of shallow foundations affected by the presence of a slope. The results are presented as dimensionless bearing capacity factors (N_{cs}, $N_{\gamma s}$, and N_{qs}), allowing for the consideration of cohesion, soil weight, and embedment in the calculation of bearing capacity near slopes. The analytical nature of the study provides insights into the influence of the critical kinematically admissible failure mechanism, categorized as surface failure, toe failure, base failure, or crest failure, which can occur due to slope stability or bearing capacity considerations. A series of design charts are provided for ease of application within the conventional bearing capacity formulation.

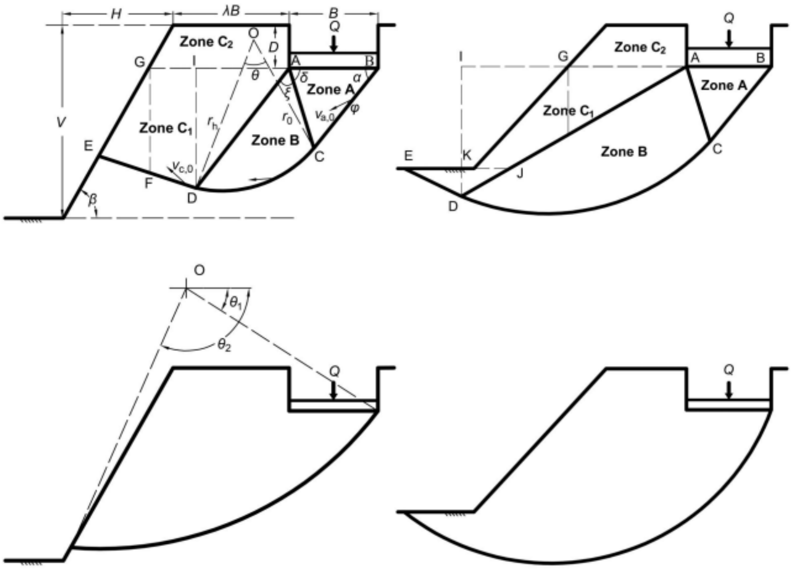

Figure 2.9. Failure mechanisms and failure models (Yang et al., 2019)

Qarmout et al. (2020) utilize Finite Element Limit Analysis to accurately determine lower and upper bounds for the bearing capacity of an embedded strip footing adjacent to a sand soil slope. The analysis results are compared with existing analytical methods found in literature. Parametric studies are conducted to investigate the influence of various factors on the bearing capacity, including slope angle, soil friction angle, footing location, and embedded depth. Figure 1.10 represents the model geometry and generated mesh. The results demonstrate that when the strip footing is positioned adjacent to the sand slope, the bearing capacity is reduced, depending on the relative location of the footing to the slope crest. Furthermore, the bearing capacity of the slope increases as the embedded depth of the footing and the soil strength increase, while it decreases with an increase in the slope angle. To facilitate practical applications, the numerical findings are presented in design charts, which can be utilized by engineers for analysis and design purposes. These design charts provide valuable insights and guidance for engineers in determining the bearing capacity of strip footings adjacent to sand slopes.

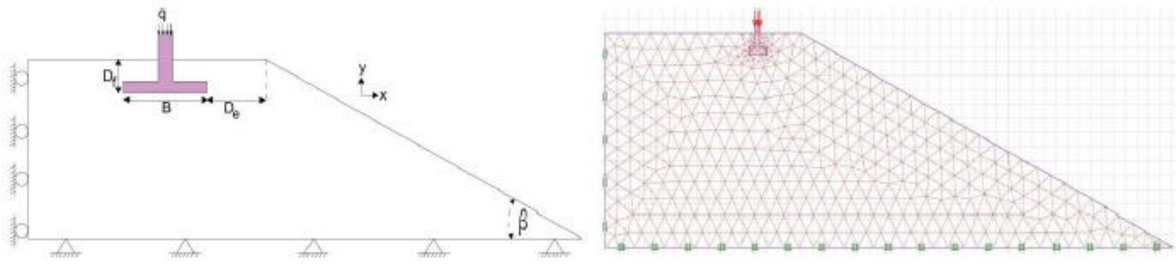

Figure 2.10. The model geometry and generated mesh (Qarmout et al., 2020)

In addition to all these, in many developed cities around the world, the need to maximize land utilization due to limited construction areas has led to the continued process of vertical architecture or constructing buildings in an adjacent manner. This approach provides advantages in obtaining additional living space, office areas, or commercial utilization. By building vertically or in an adjacent manner, it becomes possible to optimize land usage and accommodate the growing population and urban needs. This trend has become increasingly popular as cities strive to make the most efficient use of available land while meeting the demands of urbanization.

Adjacent buildings are buildings that are tightly connected to each other and share a common wall. They are often preferred in urban areas due to the advantages of density and land utilization. Here are some features of adjacent buildings:

1. Efficient land utilization: Adjacent buildings allow for the maximum use of land. By constructing buildings side by side, they make efficient use of minimum land area, providing more residential or commercial units.

2. Sound and thermal insulation: Adjacent buildings benefit from shared walls, which provide advantages in terms of sound and thermal insulation. The shared wall reduces noise transmission from neighboring buildings and enhances energy efficiency.

3. Security: Adjacent buildings offer security advantages through proximity to neighbors. Having buildings adjacent to each other can help reduce crime rates and foster a sense of community among residents.

4. Aesthetic integrity: Adjacent buildings can create a visually cohesive appearance. By using a common design language or similar exterior materials, they enhance the overall street and neighborhood aesthetics.

5. Ease of transportation: Adjacent buildings provide convenience in terms of transportation, particularly in city centers or densely populated areas. Being closer to public transportation and other infrastructure allows residents to meet their transportation needs more easily.

However, there are some disadvantages to adjacent buildings:

1. Noise and privacy: Shared walls can transmit noise from neighboring buildings and, in some cases, compromise privacy.
2. Maintenance and repairs: Maintenance and repair of adjacent buildings can be associated with coordinating efforts with neighboring buildings. Shared walls may require coordinated maintenance and repair procedures.
3. Fire risk: Fires in one building can spread to adjacent infill buildings, increasing the risk of fire spread.

When the aforementioned issues are considered within the scope of geotechnical engineering discipline, slope stability, safety of foundations, behavior of adjacent buildings have their own analysis and design criteria with different methods. The presence of all of these problems in the same case is a completely separate research topic and requires analysis with a method that includes integrated behavioral analysis. In this context, it is necessary to solve the problem of interaction of different structures with each other, and the large number of parameters affecting the behavior in these analyzes requires the comparison of balance elements with advanced methods and tools.

Raj et al. (2018) examines the response of soil slopes beneath adjacent embedded strip foundations subjected to increased vertical loads due to the gravity load of buildings. The study also considers slopes beneath closely spaced adjacent buildings. Additionally, the effects of horizontal seismic loading are addressed using a simplified pseudostatic method. The response of two representative slopes Fig. 1.11 is investigated using nonlinear two-dimensional finite element limit analysis and the strength reduction method. The effects of the interaction between the building, foundation, and slope are explored in terms of the slip surface, factor of safety (FOS), and ultimate load intensity (ULI). Furthermore, the influence of the integrated movement of the building frame on slope-building interaction is investigated. It is found that buildings/foundations mostly induce local migration of stable slopes under gravity and seismic loads. Consequently, the FOS of the slope is found to be sensitive to the foundation loading intensity, but relatively insensitive to the number and spacing of adjacent foundations and buildings in the considered cases.

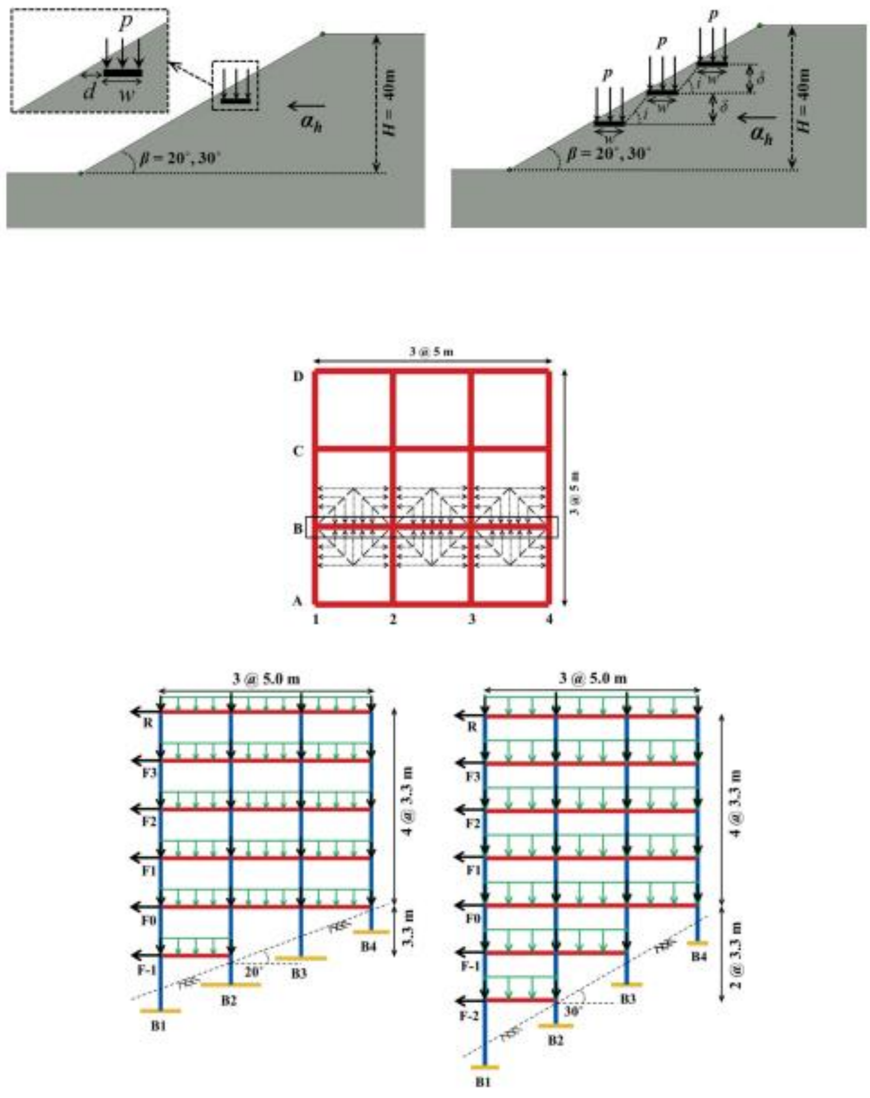

Figure 2.11. The locations of the foundations and section and elevations of the buildings (Raj et al., 2018)

Acharyya and Day (2018) studied the ultimate bearing capacity of isolated and interfering surface strip footings at the crest of a c-φ soil slope, a series of finite element analyses were conducted using Plaxis 3D software. The formed model of the study is given in Fig. 1.12.

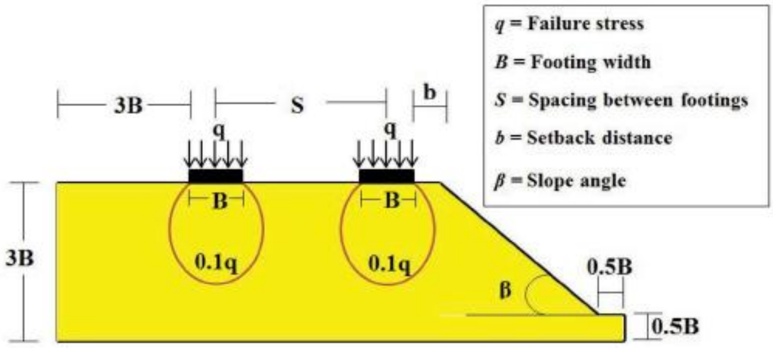

Figure 2.12. The model geometry of the study (Acharyya and Day, 2018)

The numerical analysis aimed to investigate the effects of different geo-parameters on the ultimate bearing capacity of the footings. Various factors such as slope inclination, soil properties, and footing geometry were considered in the analysis. The results of the analysis revealed the failure mechanisms of the footings. It was observed that the slope angle had a significant impact on the ultimate bearing capacity. Additionally, for interfering strip footings, the influence of interference disappeared when the setback ratio (b/B) exceeded a critical value of 6. Similarly, the influence of interference vanished when the spacing ratio (S/B) exceeded a critical value of 3. These findings provide valuable insights into the behavior of strip footings placed at the crest of a slope. They suggest that beyond certain setback and spacing ratios, the effect of slope inclination and interference becomes negligible in determining the ultimate bearing capacity of the footings.

The analysis results indicate that the factor of safety of the slope increases when the footing edge distance, footing depth, and soil relative density are increased. On the other hand, the factor of safety decreases as the slope angle and applied pressure on the footing increase. To facilitate practical engineering applications, the study includes the development of design charts. These charts aim to assist practicing engineers in understanding and utilizing the factors influencing slope stability. Additionally, an illustrative example is provided to demonstrate how these charts can be effectively employed in engineering practice.

Dey et al. (2019) integrated lots of studies about the subject of foundations on slopes. Their study offers a comprehensive and up-to-date review of the responses of shallow foundations placed on or near the face of a sloping surface. The review is organized into three main categories: experimental, theoretical, and numerical approaches. In the experimental category, various experimental studies investigating the behavior of shallow foundations on slopes are discussed. This includes laboratory tests, field measurements, and model tests, providing insights into the performance of such foundations under different conditions. The theoretical category focuses on the development of analytical models and theoretical frameworks to analyze the behavior of shallow foundations on sloping surfaces. Different theoretical approaches and methodologies used in predicting bearing capacity, settlement, and stability are examined and compared. The numerical category explores the use of numerical methods, such as finite element analysis and finite difference methods, to simulate the behavior of shallow foundations on slopes. The advantages and limitations of numerical modeling techniques are discussed, along with examples of their applications in studying foundation responses. Finally, the study provides a critical appraisal of the current state-of-the-art practice in analyzing shallow foundations on sloping surfaces. It highlights the strengths and weaknesses of existing approaches and identifies areas that require further investigation. The study concludes by outlining the potential avenues for future research in this field.

Xiao et al. (2020) presents a closed-form analytical solution for the ultimate bearing capacity of a footing-on-slope system. The solution is obtained based on a bilaterally admissible failure mechanism that satisfies the requirements of the combination. The failure mechanism used in the context of this study is given in Fig. 1.13.

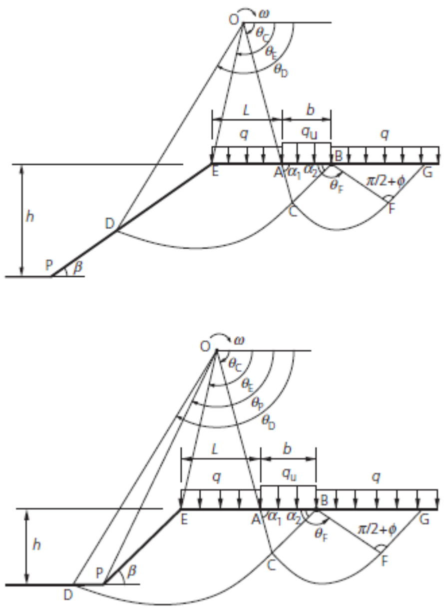

Figure 2.13. The failure mechanism of the method (Xiao et al., 2020)

The analysis is conducted using the upper-bound theorem of kinematical limit analysis. The proposed method allows for a quantitative understanding of how the failure mode of the footing-on-slope system changes as the horizontal distance ratio of the footing from the slope edge relative to the footing width increases. The study demonstrates that the failure mode transitions from the slope side to the non-slope side as this distance ratio increases. To validate the proposed method, several examples are considered. The results obtained using the proposed method are compared with those obtained from other analytical and numerical methods, as well as laboratory model tests. The comparison shows good agreement, indicating the accuracy and reliability of the proposed method. Furthermore, the study explores the influences of shear strength parameters of the soil and the safety factor of the slope on the bearing capacity. These influences are discussed and analyzed within the context of the provided examples.

Acharyya and Day (2020), describes a numerical two-dimensional finite element-based study that investigates the failure mechanism and bearing capacity of interfering strip footings located on the face of a slope. The used analysis model is given in Figure 1.14 The study demonstrates that the behavior of interfering footings is influenced by factors such as soil type, footing width, slope inclination, and the relative elevation between the footings. The study findings indicate that increasing the footing width by two times leads to a 33% increase in the bearing capacity of the interfering footing, even though the interfering mechanism remains the same. Additionally, for every successive increase in slope inclination by 5 degrees, the interfering bearing capacity decreases by 37%. The study also reveals that the maximum interference between strip footings occurs when their relative height of separation (in terms of footing width) is around 2, while the interference completely disappears when the relative height of separation is 8 or more. These findings provide valuable insights for the analysis and design of foundations on slope faces, aiding in decision-making regarding the consideration of interference effects.

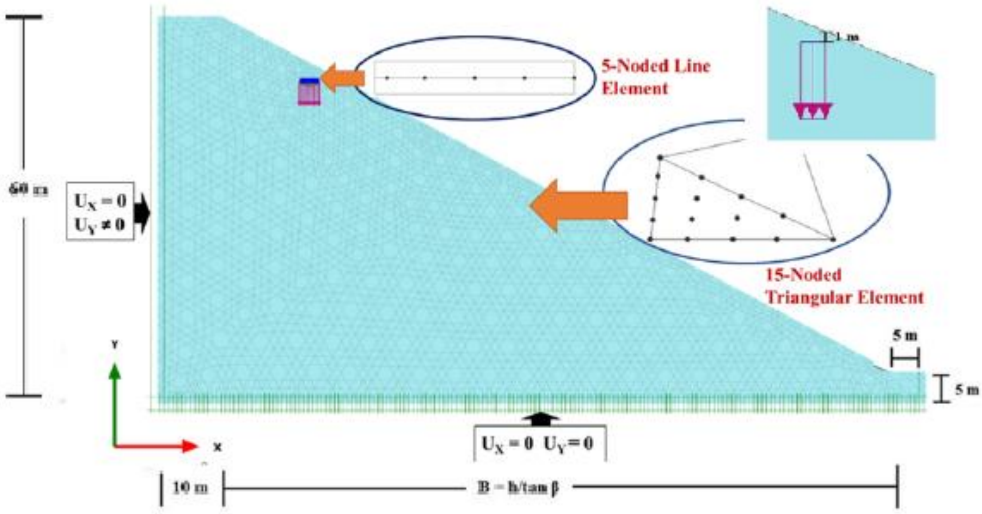

Figure 2.14. The model conditions and generated mesh (Acharyya and Day, 2020)

Haghgouei et al. (2021) invesgigated the effect of interference between closely spaced foundations resting on a slope on elastic settlement using a semi-analytical solution. The distribution of stress caused by footing pressure on the slope is calculated using a proposed Airy stress function, and then the displacements of the footings are computed using the finite difference method. The results obtained demonstrate that as the distance between the foundations increases, the influence of interference on settlement ratio diminishes. However, this behavior is highly dependent on the characteristics of the slope. For a slope with a height 10 times the footing width, beyond an S/B ratio greater than 10, the interference effect becomes negligible and the footings behave as isolated foundations. By decreasing the slope height, this behavior occurs at a lower S/B ratio.

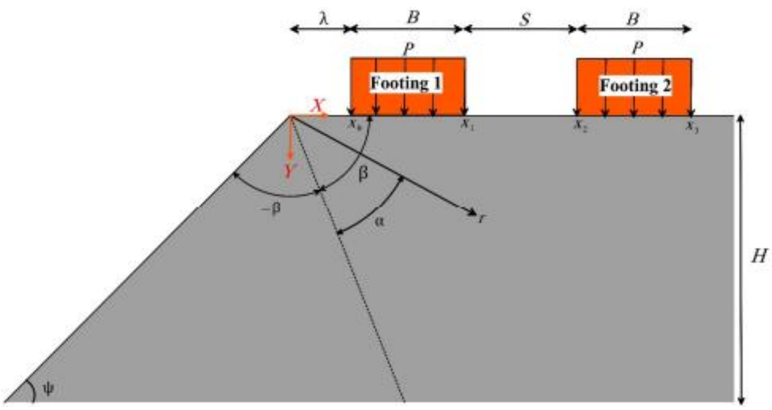

Figure 2.15. The illustration of slope-foundation system (Haghgouei et al., 2021)

In the study of Chen and Xiao (2022) shallow rigid strip foundations located near slopes are analyzed in terms of five bilateral failure modes. Kinematically admissible velocity fields are constructed using a generalized log-spiral shear mechanism, which improves upon traditional failure mechanisms by incorporating a geometric factor. The upper-bound solution for the bearing capacity of foundations near slopes is derived based on this approach. The minimum value among the five failure modes is considered the desired solution, and the corresponding failure mode is accepted. Numerical examples demonstrate that the proposed results closely align with those obtained through other theoretical and numerical methods, as well as laboratory model tests. In most cases, the geometric parameter of the generalized mechanism falls between 0.7 and 1, indicating a significant optimization of the failure mechanisms of the systems. The influence of various factors, such as slope height, foundation depth and width, distance from the foundation to the slope crest, and soil properties, on the transformation among these failure modes is investigated. The analysis results indicate that the bearing capacity of foundations near slopes does not strictly exhibit a linear relationship with cohesion or footing depth. Additionally, a comprehensive factor table is provided to facilitate the consideration of slope effects on the bearing capacity for practical applications.

Haghgoue et al. (2022) employed a semi-analytical method to determine the elastic and viscoelastic settlement of a foundation resting on a slope. The proposed method is developed based on the theory of elasticity by combining a transformed Airy stress function with the finite difference method. To facilitate the use of the proposed solution and investigate the influence of slope characteristics and footing geometry on settlement, a series of elastic and time-dependent settlement charts are proposed. The results indicate that the slope angle, normalized footing distance from the crest, and slope height significantly affect the settlement behavior of the foundation. Increasing the normalized footing distance or decreasing the slope angle leads to more uniform settlement along the edges of the foundation, resembling the behavior of a foundation on a horizontal ground surface. Additionally, as the slope height decreases, this behavior, resembling that of a foundation on a half-space, occurs at smaller normalized footing distances.

3. METHOD

Within the scope of this thesis, parametric studies were conducted to model the shallow foundation on the slope, model the adjacent shallow foundations on the slope, model the shallow foundation within the slope, and analyze the adjacent shallow foundations within the slope, starting from slope stability analyses. The aim of these modeling efforts is to examine the differences in the failure and deformation behavior of structures located on or within the slope, and to investigate the effects of these behaviors on neighboring (adjacent) buildings. For this purpose, parametric analyses were conducted using an infrastructure based on the finite element method, utilizing "Plaxis 2D Ultimate (Version 2023)" software, which is a commercially preferred software in the design of geotechnical engineering structures. The parametric analyses followed a five-step process. Below, each of these steps is explained, and the details of the process are described in Figure 3.1.

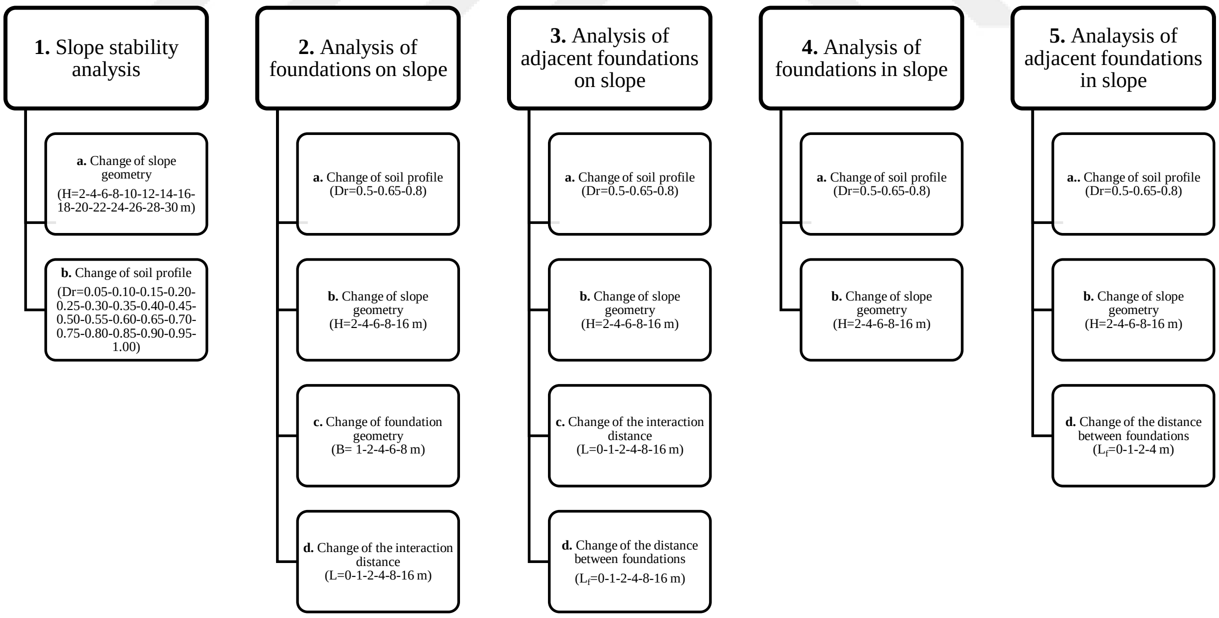

Figure 3.1. The analyses process.

Throughout the entire analysis process consisting of five steps, pure sandy soils were chosen as the foundation soil, and the properties of sandy soils were calculated based on their relative densities (D_r) using the study by Brinkgreve et al. (2010). Brinkgreve et al. (2010) developed empirical formulas to support geotechnical engineers in the selection of soil model parameters for the Hardening Soil model, specifically the parameters related to small-strain stiffness (HSsmall). These formulas are derived based on a characteristic property (relative density for sands and plasticity index for clays). The authors of the study demonstrate a validation of the formulas for sands derived from published soil test data in their publications. The primary purpose of the empirical formulas is to provide a reasonable first-order approximation of soil behavior in finite element model calculations covering a wide range of sands. The authors have shown that the recommended relationships work reasonably well in obtaining an initial estimate of deformations and stress development for a real project in a selected case study. Therefore, within the scope of the thesis, material model parameters were obtained using the relationships proposed by Brinkgreve et al. (2010) for sandy soils. In this context, relative density can already be estimated by using the following formulas in practical applications to estimate the unit weight of sand:

$\gamma_{unsat} = 15 + 4.0\,RD/100\ \ [kN\ /\ m^3]$ .... Eq. 3.1

$\gamma_{sat} = 19 + 1.6\,RD/100\ \ [kN\ /\ m^3]$.. Eq. 3.2

The HSsmall model includes four different stiffness parameters that measure the reference stiffness at a specific stress path for a given reference stress level (p_{ref}). For a detailed description of the HSsmall model and the definition of its parameters, references can be made to Benz (2007) and Brinkgreve et al. (2008).

It is assumed that the stiffness of (specially quartz sand) sand approximately varies with relative density. The following formulas are proposed by assuming p_{ref} = 100 kPa for the reference stiffness parameters:

$E_{50}^{\mathrm{ref}} = 60000\,RD/100\ \ [kN\ /\ m^2]$.. Eq. 3.3

$E_{oed}^{\mathrm{ref}} = 60000\,RD/100\ \ [kN\ /\ m^2]$.. Eq. 3.4

$E_{ur}^{\mathrm{ref}} = 180000\,RD/100\ \ [kN\ /\ m^2]$.. Eq. 3.5

$G_{0}^{\mathrm{ref}} = 60000 + 68000\ \ RD/100\ \ [kN\ /\ m^2]$.. Eq. 3.6

It has been observed that the stress dependency ratio, m, is negatively correlated with density. The following equation is proposed for m:

$m = 0.7 - RD/320\ [-]$.. Eq. 3.7

For unloading and reloading, the Poisson's ratio, νur, is assumed to be 0.2. The parameter $\gamma_{0.7}$, which links the modulus reduction curve to the cyclic shear strain level, can be calculated using the following equation:

$\gamma_{0.7} = (2 - RD/100) \cdot 10^{-4}$.. Eq. 3.8

For strength-related properties, the following formulas are suggested:

$\varphi' = 28 + 12.5\ RD/100\ [^0]$.. Eq. 3.9

$\Psi = -2 + 12.5\ RD/100\ [^0]$.. Eq. 3.10

$R_f = 1 - RD/800\ [-]$.. Eq. 3.11

It has to be noted that, although the analysis conducted within the scope of this study explores a parametric process that provides a generalized approach, it is not appropriate to abandon detailed soil investigation by relying solely on general empirical formulas for selecting model parameters. These formulas cannot provide sufficient accuracy for a final design, and a more detailed soil investigation is definitely necessary. However, an initial analysis based on these formulas can provide insights into dominant stress paths and critical locations in the project, thereby assisting in defining a detailed soil investigation plan.

Within the scope of the thesis, the parameters to be used have been examined for relative density values ranging from 0 to 100 with increments of 5, and all relevant parameters have been calculated. The analysis parameters obtained based on the relative density values with the empirical equations suggested by Brinkgreve et al. (2010) are presented in Table 3.1.

Table 3.1. The parameters based on the relative density values and the empirical equations

Density definition	D_r	γ_{unsat}	γ_{sat}	E_{50ref}	m	$\gamma_{0.7}$	ϕ'	R_f	ν_{ur}	k_x=k_y
Unit	%	kN/m^3	kN/m^3	kN/m^2	-	-	°	-	-	m/sec
Very loose	0	15.0	19.0	0	0.70	0.00020	28.0	1.00	0.2	0.000001
	5	15.2	19.1	3000	0.68	0.00020	28.6	0.99	0.2	0.000001
	10	15.4	19.2	6000	0.67	0.00019	29.3	0.99	0.2	0.000001
Loose	15	15.6	19.2	9000	0.65	0.00019	29.9	0.98	0.2	0.00001
	20	15.8	19.3	12000	0.64	0.00018	30.5	0.98	0.2	0.00001
	25	16.0	19.4	15000	0.62	0.00018	31.1	0.97	0.2	0.00001
	30	16.2	19.5	18000	0.61	0.00017	31.8	0.96	0.2	0.00001
Medium	35	16.4	19.6	21000	0.59	0.00017	32.4	0.96	0.2	0.0001
	40	16.6	19.6	24000	0.58	0.00016	33.0	0.95	0.2	0.0001
	45	16.8	19.7	27000	0.56	0.00016	33.6	0.94	0.2	0.0001
	50	17.0	19.8	30000	0.54	0.00015	34.3	0.94	0.2	0.0001
	55	17.2	19.9	33000	0.53	0.00015	34.9	0.93	0.2	0.0001
	60	17.4	20.0	36000	0.51	0.00014	35.5	0.93	0.2	0.0001
Dense	65	17.6	20.0	39000	0.50	0.00014	36.1	0.92	0.2	0.001
	70	17.8	20.1	42000	0.48	0.00013	36.8	0.91	0.2	0.001
	75	18.0	20.2	45000	0.47	0.00013	37.4	0.91	0.2	0.001
Very dense	85	18.4	20.4	51000	0.43	0.00012	38.6	0.89	0.2	0.001
	90	18.6	20.4	54000	0.42	0.00011	39.3	0.89	0.2	0.01
	95	18.8	20.5	57000	0.40	0.00011	39.9	0.88	0.2	0.01
	100	19.0	20.6	60000	0.39	0.00010	40.5	0.88	0.2	0.01

Slope stability analyses are preliminary analyses and serve as a means to control the overall system, including foundations on the slope. Therefore, in these preliminary analyses, the elastic-perfectly plastic material model is selected for the analysis. The elastic-perfectly plastic material model is described using the Mohr-Coulomb material model, and the stiffness parameters such as Young's modulus and Poisson's ratio, as well as strength parameters such as cohesion and angle of internal friction, are sufficient to define its characteristics.

Sand soils have been classified based on relative density values in Bowles (1998). The relevant classification is provided in Table 3.2 and these limits have been used to define sand soils.

Table 3.2. Classification of Sandy soils

Relative Density %	Descriptive Term -
0-15	Very Loose
15-35	Loose
35-65	Medium
65-85	Dense
85-100	Very Dense

Furthermore, the permeability coefficients of sand soils classified according to their densities have been selected based on Bowles (1998). The figure below Figure 3.1 provides the permeability characteristics for different soil types. In the analyses, considering isotropic conditions, the horizontal and vertical permeability coefficients have been chosen to be numerically equal.

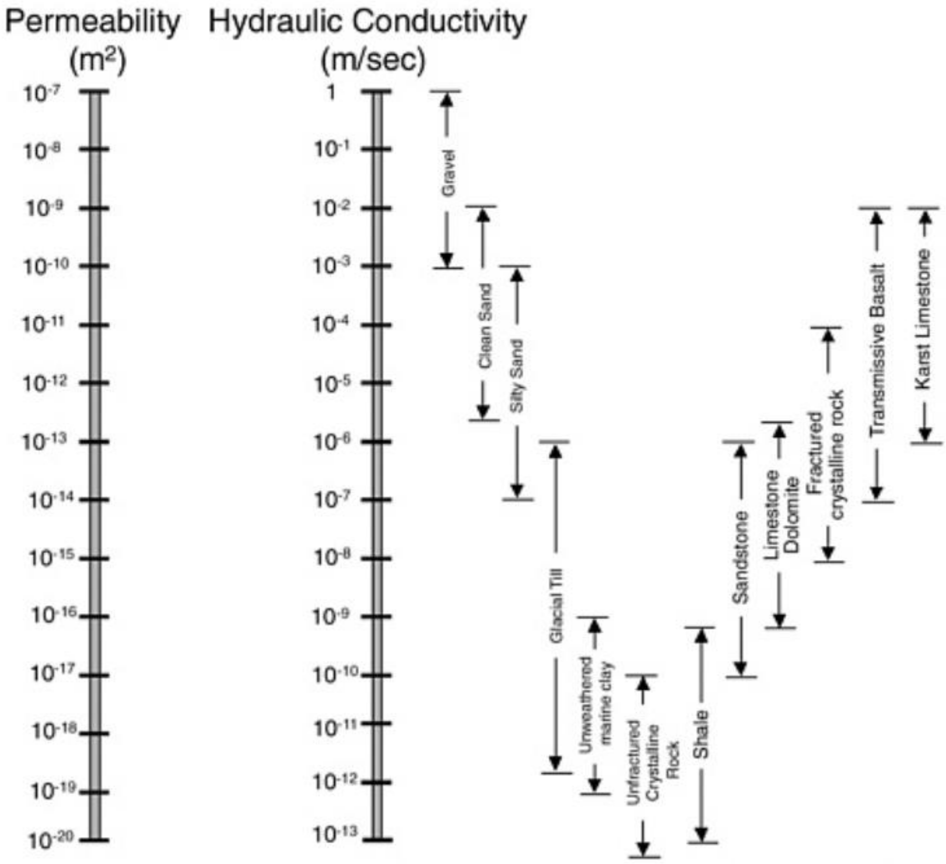

Figure 3.2. The permeability characteristics for different soil types.

In all the initial stage slope stability analyses conducted, the slope geometry was modified according to the slope height, while the slope inclination was kept constant. The slope inclination ratio used in all the analyses was vertical/horizontal = 1/2. In addition, in the initial stage of the study, cases with different slope heights were modeled. The aim of this stage is to demonstrate that the slopes can maintain their stability at a certain level of safety. The slope height in the analyses is denoted by the parameter H, with numerical values assumed to be 2-4-6-8-10-12-14-16-18-20-22-24-26-28-30 meters in sequence. Finite element analysis with plane strain conditions and 15-node elements have been preferred to evaluate slope stability conditions. The boundaries of the system have been selected wide enough for each analysis to allow for the restriction of stress and strain distributions and/or propagation. Slopes have been modeled in the "structures" menu, and analyses have been repeated with different parameters in the Mohr Coulomb material model for a total of 20 different soil profiles. Fine mesh has been preferred in the analyses. None of the models created within the scope of the study include groundwater, and the analyses have been conducted under static conditions. Three phases have been used in these analyses evaluating slope stability. Initial phase gravity loading conditions have been used to examine stability conditions. The gravity loading option in Plaxis refers to the capability of the program to simulate the effects of gravity on non-horizontal layers in geotechnical analyses. When analyzing soil or rock structures, the weight of the materials can significantly impact their behavior and stability. By enabling the gravity loading option in Plaxis, the program takes into account the vertical forces exerted by the self-weight of the soil or rock layers. This allows for a more realistic representation of the system's response to gravitational forces. The gravity loading option in Plaxis considers the distribution of stresses induced by the weight of the materials, which can influence the deformation and stability of the analyzed structure. It helps in accurately modeling the behavior of slopes, retaining walls, foundations, and other geotechnical systems under the influence of gravity. By incorporating the gravity loading conditions into the analysis, engineers and geotechnical professionals can obtain more reliable results and make informed decisions regarding the design and stability of their structures. The second phase involves observing slope behavior under plastic loading effects, and the third phase is considered as the safety phase. The Strength Reduction Method (SRM) is a commonly used technique in Plaxis for safety analysis. It is a numerical approach that helps assess the factor of safety and determine the critical failure mechanism of geotechnical structures. Plaxis incorporates the SRM in its software to evaluate the stability of various soil-structure systems. The strength reduction parameters, also known as the reduction factors or mobilization factors, are defined in Plaxis. These factors represent the reduction in the soil strength properties (e.g., shear strength parameters) during the analysis. They are gradually reduced until a failure mechanism is activated. A preliminary analysis is performed using Plaxis, considering the initial strength properties and loading conditions. The initial factor of safety is calculated based on the soil strength parameters and applied loads. Plaxis then performs an iterative analysis with the Strength Reduction Method. The analysis involves reducing the soil strength properties by multiplying them with the reduction factors. This reduction is applied incrementally until the factor of safety reaches a specified target value (usually close to 1). During the iterative analysis, as the strength properties are progressively reduced, the failure mechanism within the soil mass starts to activate. The activation of the failure mechanism is identified by reaching the target factor of safety. The final analysis step determines the critical failure mechanism. Plaxis identifies the specific failure mode, such as slope failure, bearing capacity failure, or retaining wall failure, that corresponds to the activated mechanism with the lowest factor of safety. From the safety phase, safety factors obtained for the current analysis and the most reasonable critical failure mechanisms that the program can predict are obtained using the incremental displacements option in the menu. This sequence allows for a comprehensive safety analysis and aids in optimizing the design and mitigating risks associated with projects including slope stability problems.

As a result of investigating the safety of the slope at specific heights under different soil conditions, slope designs with a specific level of safety, which will be built upon, have been obtained. Carefully designed slopes were aimed to have a factor of safety above 1.5. In the second step of the study, analyses were conducted for a shallow single foundation on the slope under different design conditions. In the second step of the study, the aim was to investigate how the obtained factor of safety values and the failure mechanisms were affected when a single foundation was present on the slope. The analysis focused on evaluating the influence of the foundation on the factor of safety and the stability mechanisms of the slope. In this phase of the study, not all the sections analyzed in the first phase were continued. The soil profile was limited to relative density values of 0.5, 0.65, and 0.8. The effects of the foundation characteristics and other factors that could influence the behavior of the slope-foundation interaction were individually examined for each of these relative density values. In this context, the dimensions (width) of the added shallow foundation as a structural element were analyzed in a subsequent sub-phase, with widths of 1, 2, 4, 6, and 8 meters being considered. The slope heights were set to be multiples of the foundation width, with values of 2, 4, 6, 8, and 16 meters taken into account. The distance between the analyzed foundation and the top point of the slope, denoted by the symbol L, was considered as a separate variable. The L dimension was evaluated as 0, 1, 2, 4, 8, and 16 meters, also being multiples of the foundation width. As a result of the analyses, similar to the outputs of the first phase, the factor of safety, in addition to the failure mechanism, was examined along with deformation values. The analyzed case and variable parameters are symbolically represented in Figure 3.3.

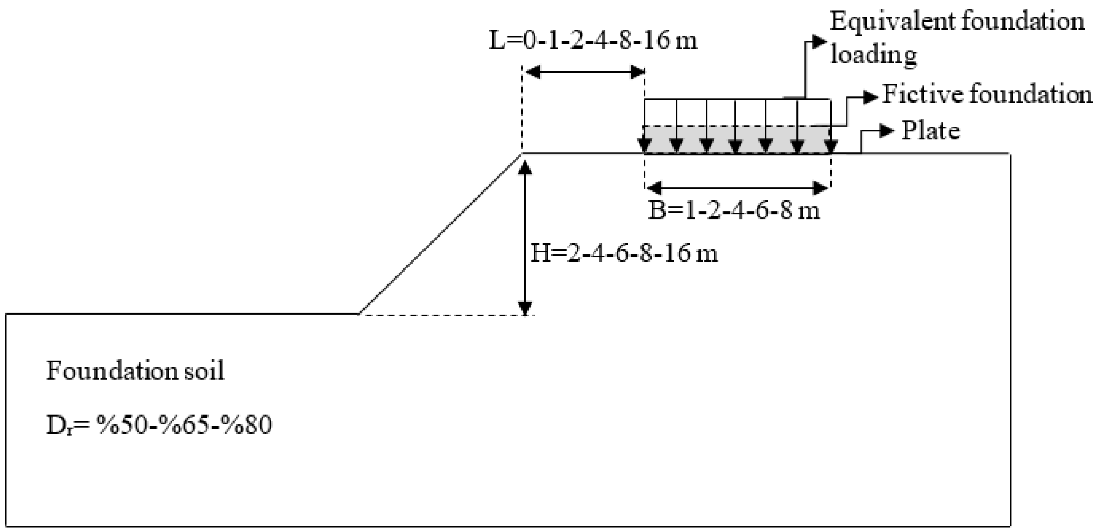

Figure 3.3. The cases of the modeled foundation on the slope.

In the analysis conducted in the finite element program for the second stage analysis, the assumption was made that the individual shallow foundation is a flexible foundation. The modeling includes a plate element with a certain stiffness and an equivalent load on it, which is equivalent to the foundation load. The plate element represents a 50 cm thick. The calculated axial stiffness value (EA) is $13.9*10^6$, and the moment of inertia stiffness value (EI) is $289.6*10^3$. The unit weight of the foundation is calculated as 12.5 kN/m/m, and a Poisson's ratio of 0.15 is assumed. A fine mesh density is used for the system, and a representative visual of the mesh created with the system elements is presented in Figure 3.4.

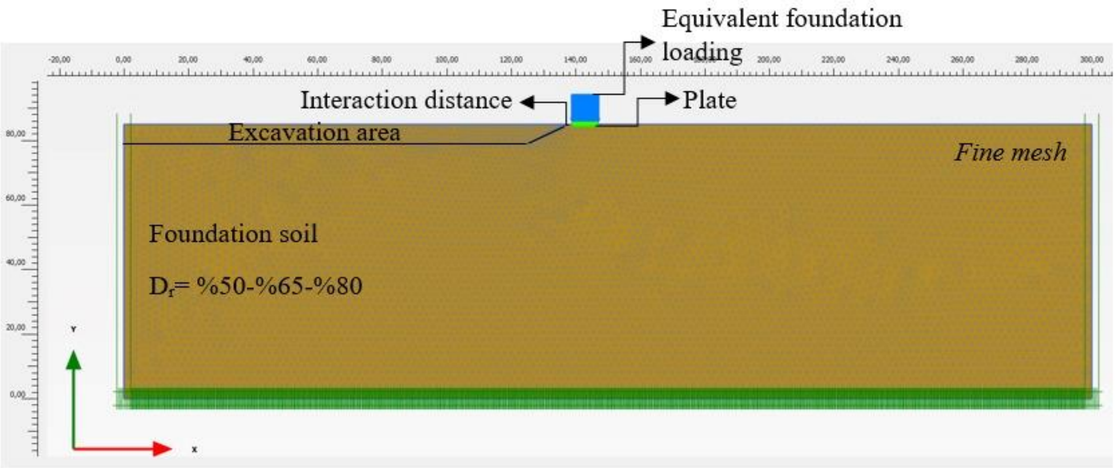

Figure 3.4. A representative visual of the mesh created with the system elements.

For the modeling of the construction stages, the initial phase is modeled according to the K_o procedure. In this condition, it is assumed that there is no slope in the environment and that the environment is in a horizontally layered state. However, in the second phase, with the displacements set to zero, it is assumed that slope excavation is performed, and therefore, the area defined as the excavation area is deactivated. In the subsequent phases, the condition where the foundation system is loaded more than its ultimate load-carrying capacity is modeled. In this way, the maximum load-carrying capacity of the foundation is determined and loaded with the maximum load it can carry. The aim is to bring the environment consisting of the slope and foundation pair to a limit equilibrium state and thus control the mechanisms in the limit safety condition. Therefore, additional safety analyses were added to the end of each phase, such as slope excavation and loading of the foundation load, to examine both the safety factors and the mechanisms obtained from incremental displacements menu. The definition of the phases in the Plaxis program is also given visually in Figure 3.5.

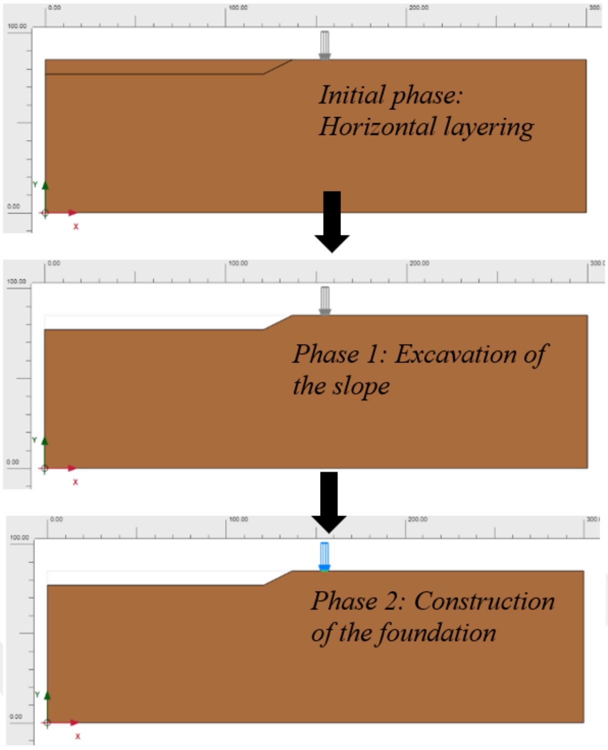

Figure 3.5. The definition of the phases in the Plaxis program.

In the third step of the thesis, a critical aspect of the research involves conducting an in-depth analysis of single foundations situated within the slope. This analysis plays a crucial role in assessing slope stability and informing foundation design decisions. To ensure the stability and optimal performance of structures, an exhaustive analysis was carried out to thoroughly investigate the behavior of single foundations positioned within the slope. The analysis took into account essential factors, including soil characteristics, slope inclination, and foundation loading, as these elements significantly influence the foundation's response and overall stability. The assessment of single foundations within the slope employed numerical modeling techniques to evaluate their behavior and performance. By employing such modeling techniques, it was possible to simulate various scenarios and accurately assess the foundation's response to different loadings and slope conditions. As a result, the analysis of single foundations located within the slope has been carried out. In these analyses, a similar process was conducted by modeling the foundations within the slope, and the analyses were shaped based on specific cases where the relative density value of the foundation soil was determined as 50%, 65%, and 80%. The slope height was repeated for all analyses at 2, 4, 6, 8, and 16 meters. In the analyses, it was assumed that the single foundation is located at a vertical distance equal to half of the slope height at the center of the slope. The variation in foundation size was not considered, and the analyses were only applied for a 1-meter foundation size. The case of the modeled foundation within the slope is visualized in Figure 3.6.

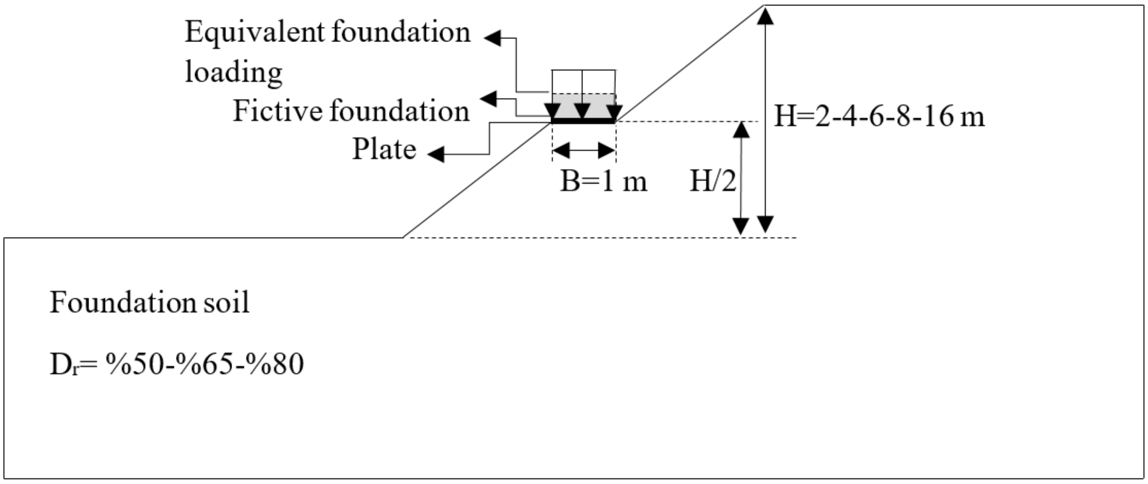

Figure 3.6. The cases of the modeled foundation within the slope.

In the modeling conducted in the Plaxis program, careful consideration was given to the selection of system boundaries. To ensure accurate results, the system boundaries were chosen to be wide enough so as not to have a significant effect on the propagation of stresses and deformations within the model. This ensured that the boundaries did not introduce any limitations that could affect the overall behavior of the analyzed system. A fine mesh was used as the grid structure, By using a fine mesh, smaller-scale features and potential localized effects could be captured and evaluated accurately, enabling a more comprehensive understanding of the behavior and performance of the single foundations within the slope (Liu,2013). Figure 3.7 shows the mesh obtained from the analysis of the single foundation within the slope.

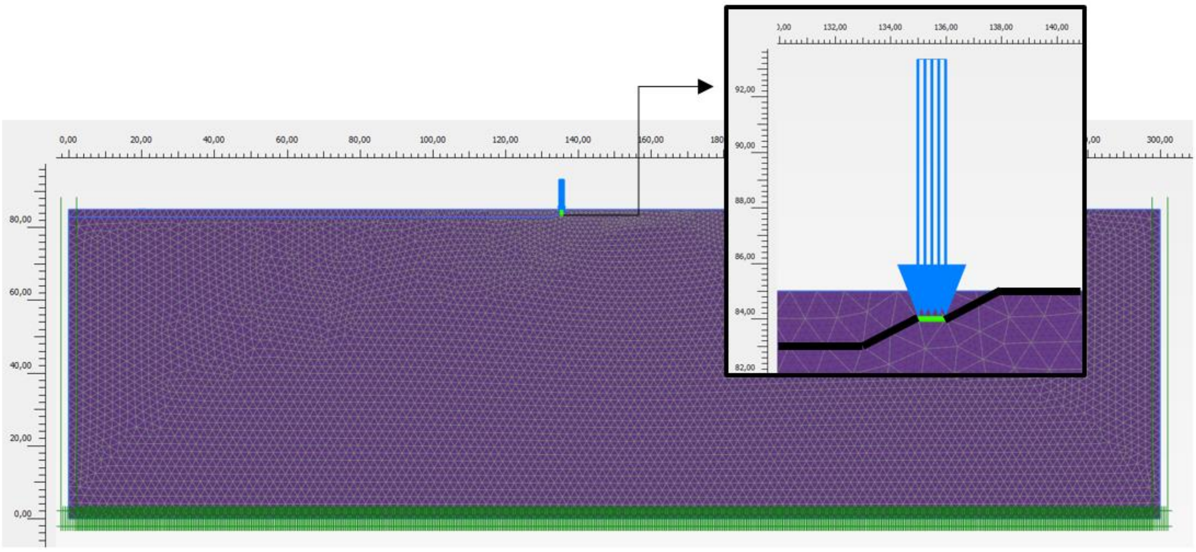

Figure 3.7. The mesh obtained from the analysis of the single foundation within the slope.

The construction phases (stages) used in the analyses are presented in Figure 3.8 The steps are the same as the foundations located on the slope. The initial phase was obtained based on the K_0 procedure, assuming a completely horizontal layering condition. The slope geometry was obtained in the first phase. In the second phase, the individual foundation located at the center of the slope was constructed. For the construction of the single foundation, the load value that would lead to system failure was calculated. The system was loaded with a value very close to this calculated load, aiming to bring the system to a state of equilibrium at the system boundary. In this phase, the focus was on achieving a safety factor of 1.0. In the first phase, during the formation and subsequent loading of the slope, safety phases were added to examine safety factors and critical failure planes.

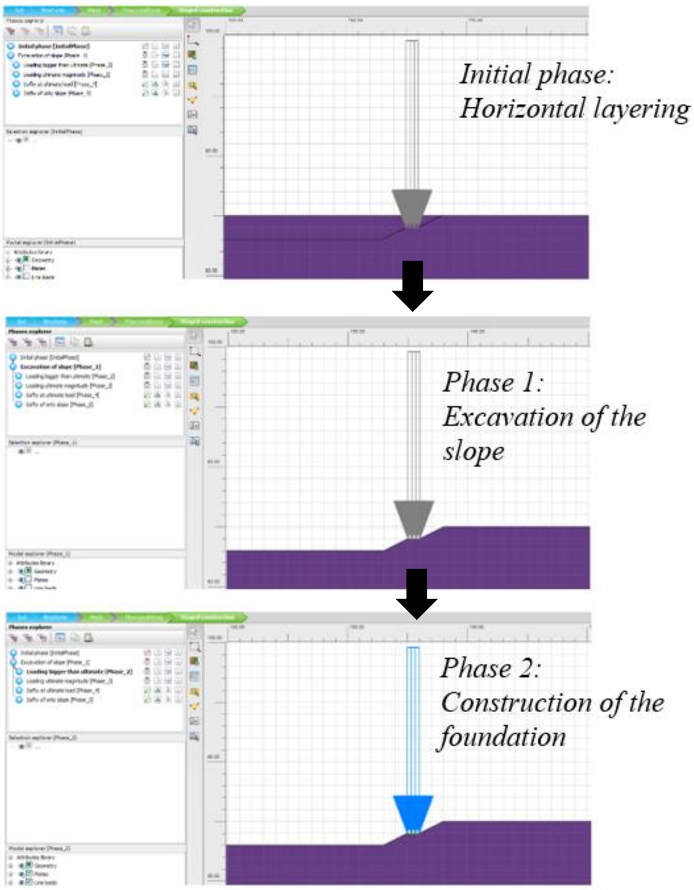

Figure 3.8. The construction stages used in the analyses.

In the fourth step of the analysis, the subject of adjacent foundations was studied. In this stage, the analysis of adjacent foundations located on the slope was conducted, This analysis aimed to investigate the interaction and potential influence between neighboring foundation systems. By considering multiple soil profiles, and once again similar to the previous steps, all analyses were repeated for three different soil profiles. In these analyses, the relative density values of the foundation soil were assumed to be 50%, 65%, and 80% respectively. Both foundations had a size of 1 meter. The slope height was selected as 2, 4, 6, 8, and 16 meters. Additionally, the positions of the foundations relative to the slope were also considered as evaluated parameters. The distance of the first foundation close to the slope crest was considered to be 0, 1, 2, 4, 8, and 16 meters. What makes the analysis of adjacent foundations special is the consideration of a defined distance between the two foundations. In cases where the distance between the two foundations (L_f) was 0, 1, 2, 4, 8, and 16 meters, the analyses were repeated, and the results were evaluated accordingly.

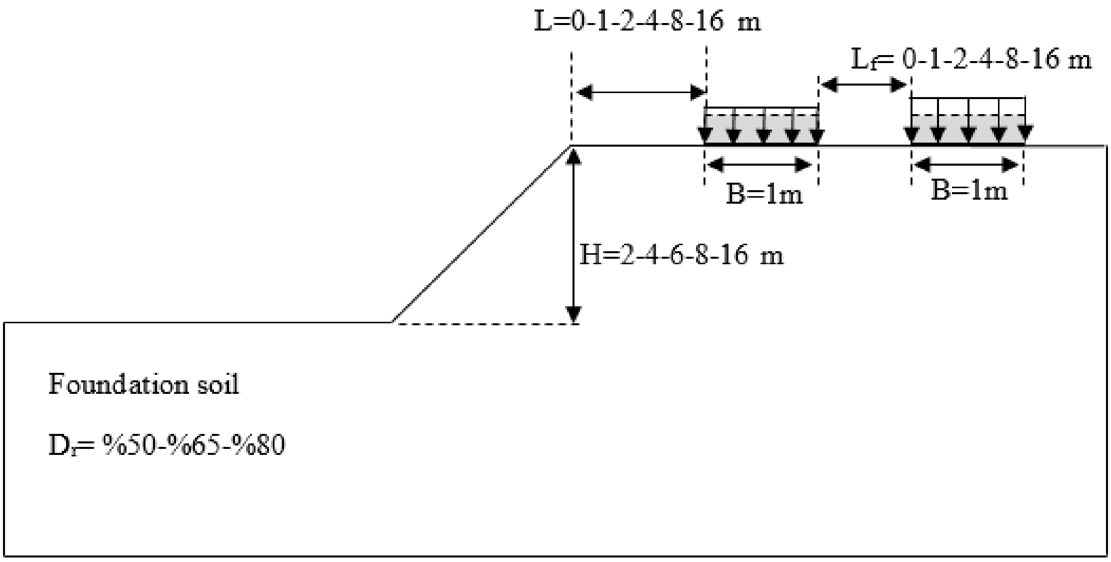

Figure 3.9. The cases of the modeled Adjacent foundations on the slope.

The cross-section used in the Plaxis analyses is presented in Figure 3.10 The modeling phases are similar in nature to the analysis cycle in the previous step. However, additional analyses are conducted to investigate the effect of the distance variation between the foundations.

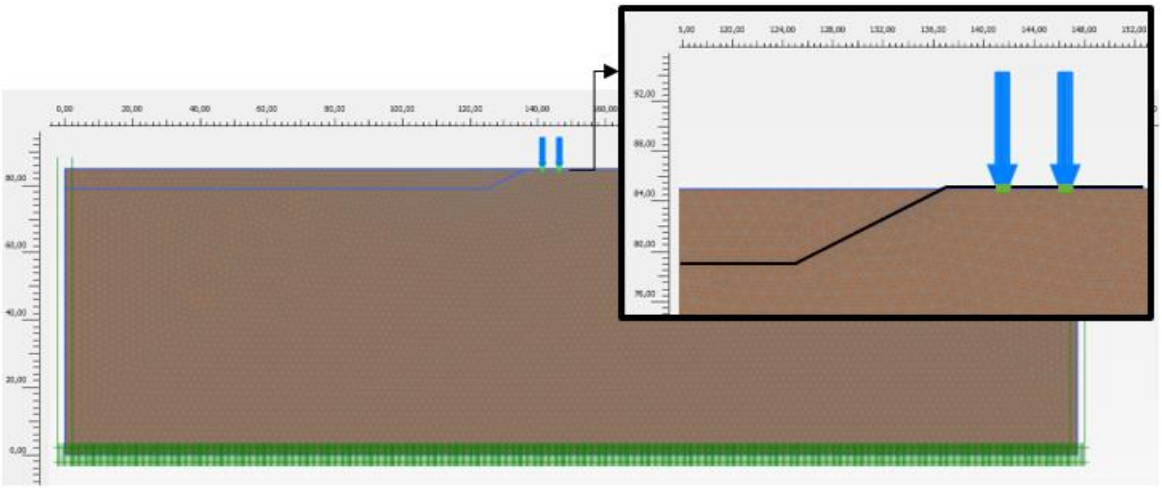

Figure 3.10. The cross-section used in the Plaxis analyses of the adjacent foundations.

The phases used in the analysis of double foundations are presented in Figure 3.11 In the case of having two foundations on the slope, the foundation loadings were analyzed with an intermediate phase, where the loading values were adjusted to bring the slope safety to a critical state. Subsequently, these values were applied in the loading phase of the analysis.

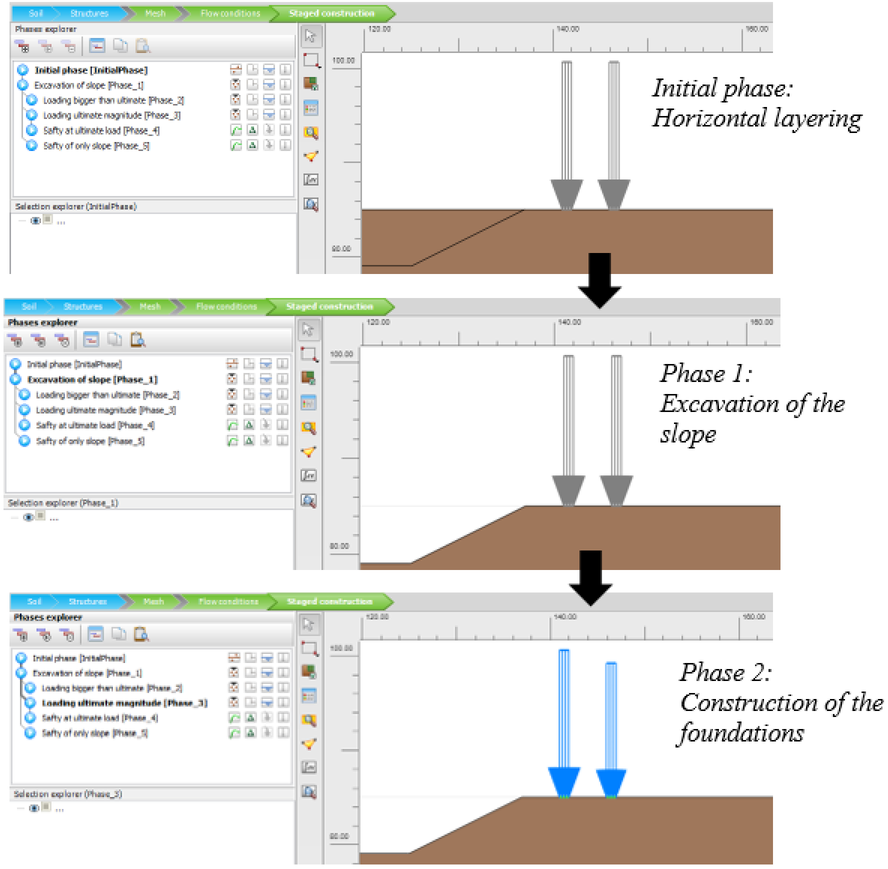

Figure 3.11. The phases used in the analysis of double foundations.

In the fifth step of the analysis, the situation where adjacent foundations are present within the slope was evaluated. In this scenario, the foundation widths were considered constant and set at 1 meter each. The foundations were positioned at half of the slope height. This placement allowed for a comprehensive assessment of the interaction between the foundations and the surrounding soil, considering the influence of the slope's geometry. The foundation-soil system was examined in three different profiles. Calculations were repeated for slope heights of 2, 4, 6, 8, and 16 meters, and the distance between the two foundations was sequentially expanded at 0, 1, 2, and 4 meters, and the analyses were continued. A representative section is provided for the analyses used in Step 5 in Figure 3.12.

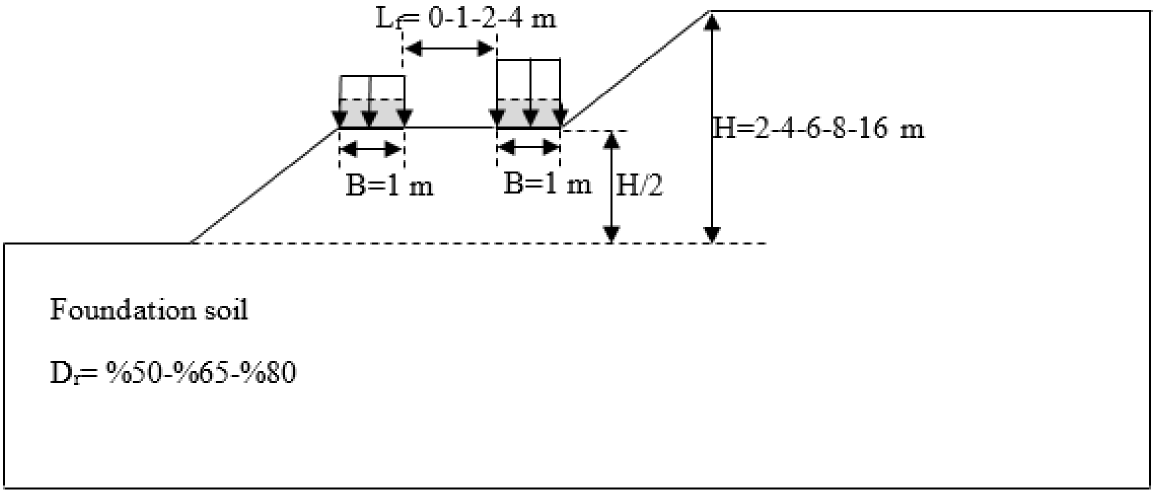

Figure 3.12. The cases of the modeled Adjacent foundations within the slope.

The mesh and representative loading conditions obtained in finite element analyses are presented in Figure 3.13.

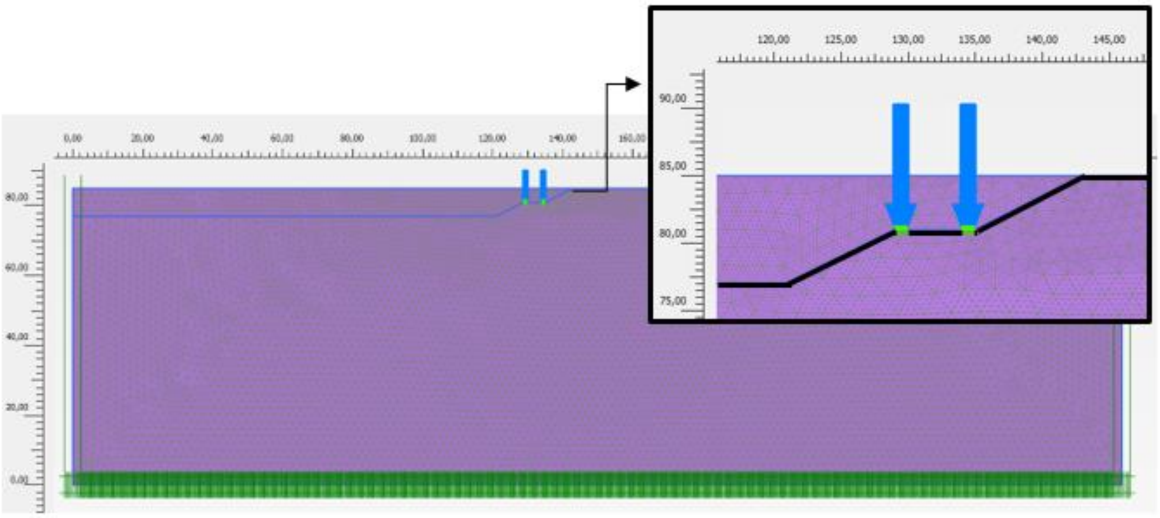

Figure 3.13. The mesh and representative loading conditions obtained in finite element analyses.

The phases in which the adjacent foundations within the slope are analyzed are provided in Figure 3.14 Logically, in analyses carried out using the same iterative process, the important point is to investigate the foundation loads that will lead to slope boundary loading conditions through trial and error method during intermediate phases.

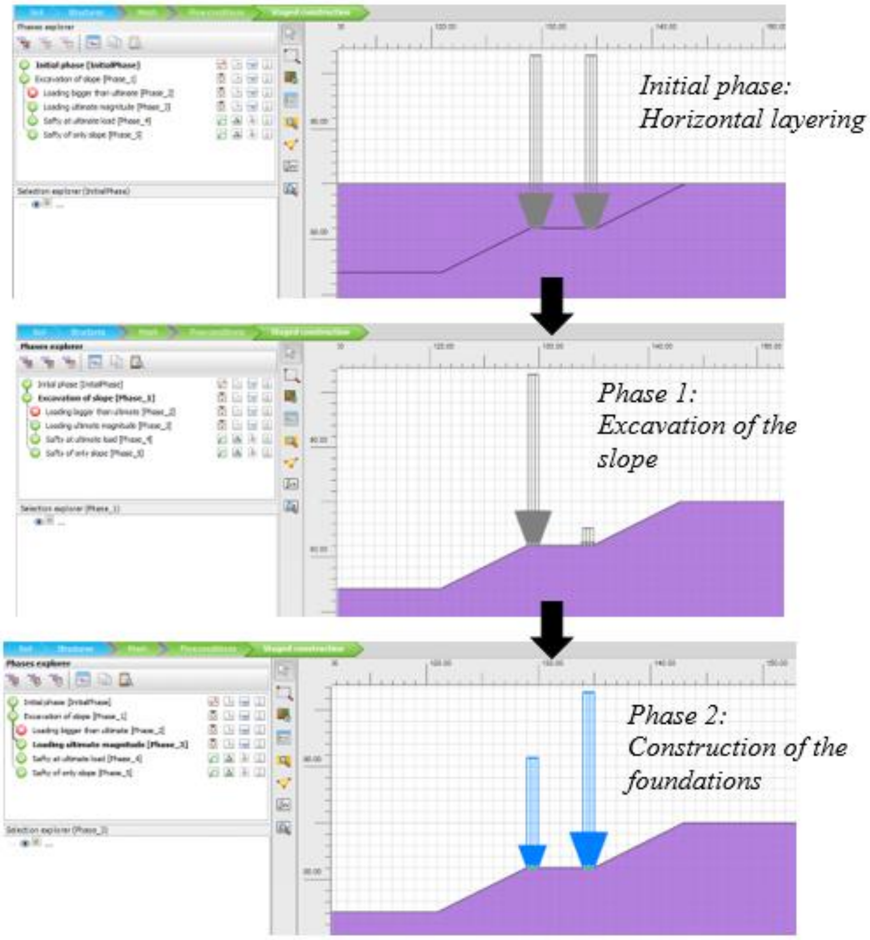

Figure 3.14. The phases of analysis of the adjacent foundations within the slope.

In this section of the thesis, the details of the cases to be evaluated within the scope of the analyses have been explained. Based on the provided information, parametric analyses were conducted, resulting in focused analysis outputs, safety factors, and critical failure planes being determined.

4. RESULTS

In the previous section, it was stated that the thesis work consists of five main steps. In the first step of the study, stability analyses of geometries adjusted at different heights for a slope with a constant gradient were conducted using the gravity loading option. The safety factors obtained from the analyses and the evaluation of the most critical shear planes were taken into consideration. The obtained factor of safety values (FoS or FS_{slope}) from the analyses were evaluated based on different relative density conditions, and the variation of the factor of safety with respect to the slope height (H) is shown in Figure 4.1. The Figure demonstrates that the factor of safety decreases as the slope height increases, as expected, it increases with increasing relative density values. The rate of increase in the factor of safety corresponds proportionally to the rate of increase in relative density. An important observation in the figure is the significant change in the factor of safety when the slope height increases from 2 meters to 4 meters. Another notable observation is that there is no significant change in the factor of safety when the slope height exceeds 8 meters.

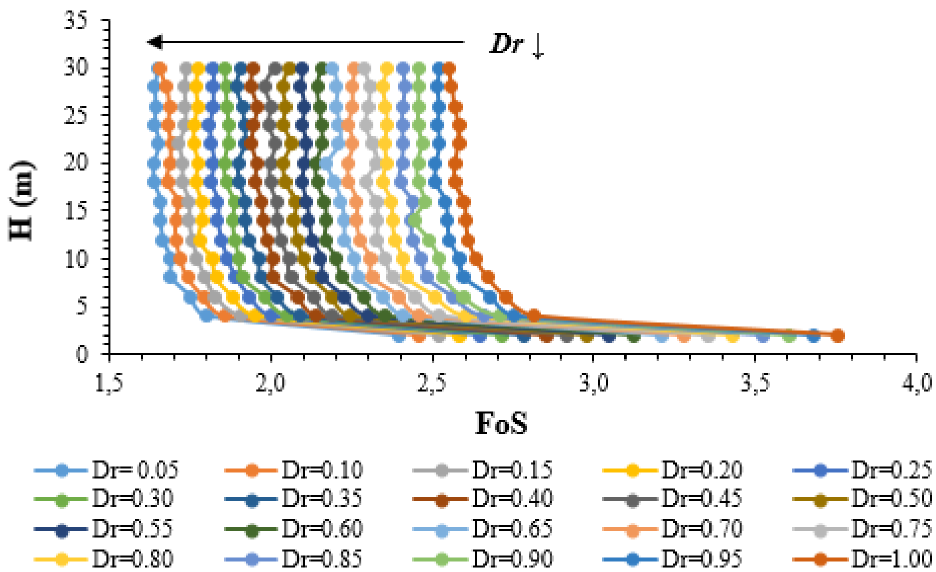

Figure 4.1. Factor of safety based on different relative density conditions, and the variation the slope height

In addition, possible critical failure mechanisms were obtained for each different relative density values and slope heights. Figure 4.2, shows the critical failure mechanisms obtained for selected reference relative density and slope height values. The obtained mechanisms are presented in the program output at the same scale, and the boundaries of the mechanism are emphasized with a thick red line for clarity.

H	D_r= %25	D_r= %50	D_r= %75	D_r= %100
2	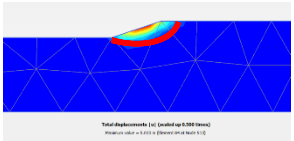	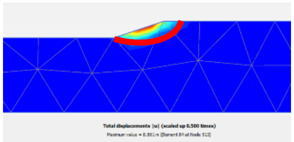	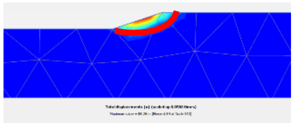	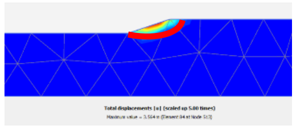
4	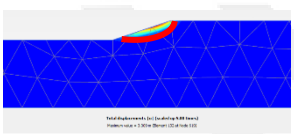	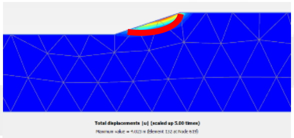	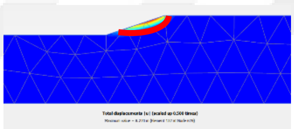	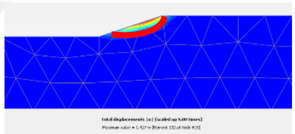
8	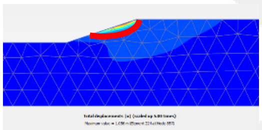	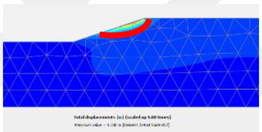	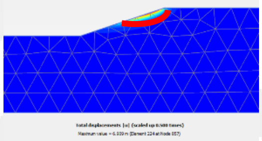	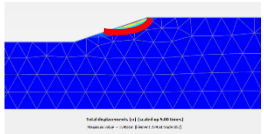
12	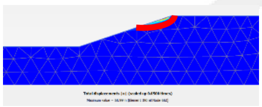	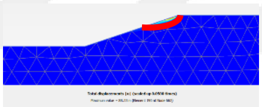	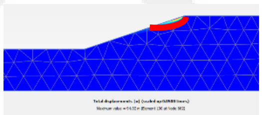	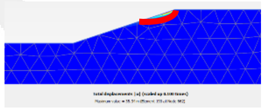
16	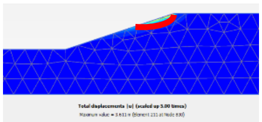	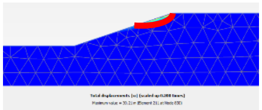	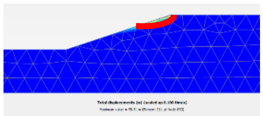	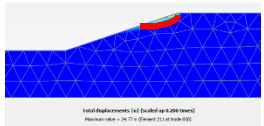
20	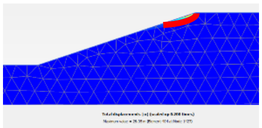	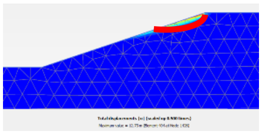	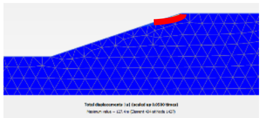	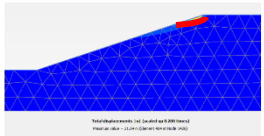
24	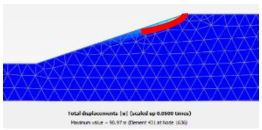	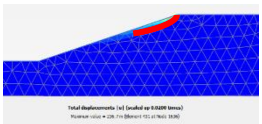	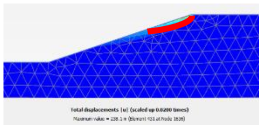	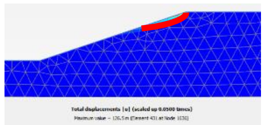
30	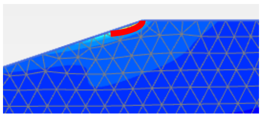	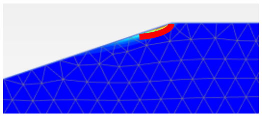	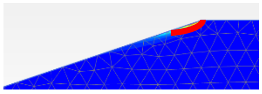	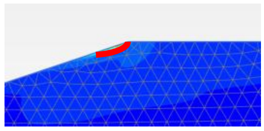

Figure 4.2. The critical failure mechanisms obtained for selected reference relative density and slope height values.

When the slope height is low, the critical displacement behavior occurs in a way that scans the entire slope. As the slope height increases, the critical failure plane shifts towards the upper point of the slope. When evaluating the intensity of the resulting deformation, it can be observed that the activated mechanisms become shallower proportionally to the slope height. An increase in relative density, in each case, has led to a narrowing of the failure surface, showing an inverse relationship with density as the height increases.

In the first stage of the study, slopes with a certain level of safety were obtained in terms of geometry. In the subsequent stages of the study, these slopes were re-modeled by incorporating shallow foundations constructed on or within them, and the safety level checks were updated accordingly. Additionally, in the discussion section of the thesis, for the selected specific cases, comparisons of possible failure mechanisms for single and double foundation analyses will be made with the mechanisms presented in Figure 4.2.

The subsequent steps of the study will focus on the slope-shallow foundation interaction, considering the soil-structure interaction problem. In this context, the second and third steps of the analysis addressed single shallow foundations, and the variations in safety levels for several anticipated scenarios and factors influencing the most critical shear plane were thoroughly examined in relation to changes in parameters. With this logic, in this section of the thesis, the results obtained from each analysis have been interpreted within their own context, and the findings have been presented separately for each case.

Table 4.1, presents the variation of L interaction distance depending on the FS_{slope} values and q_{ult} values when the foundation width is 1 meter. The analyses were conducted for three different soil profiles. The soil profiles were defined according to the definitions presented in Table 4.1, The sandy soil with a relative density value of 50% represents medium dense conditions, the sandy soil with a relative density value of 65% represents dense conditions, and the sandy soil with a relative density value of 85% represents very dense conditions, which are boundary values. The L, foundation-slope interaction distance represents the distance from the top of the slope to the closest corner of the foundation. In this context, L=0 represents a foundation resting on the top of the slope, which constitutes the most critical condition in terms of loading. The L distance is gradually increased to represent certain proportions of the foundation size. Interaction distances of B, 2B, 4B, 8B, and 16B were used, and the slope heights were differentiated as 2B, 4B, 6B, 8B, and 16B. In this way, the aim was to obtain the ultimate load value that would bring the slope to the limit state of safety, considering the safety factor before and after the foundation loading. The evaluations that can be made as a result of sequentially examining Table 4.1, are as follows. As mentioned in all the literature sources, an increase in slope height leads to a decrease in the factor of safety of the slope. When the factor of safety is examined with decimal precision, it is evident that their magnitudes are the same in all cases where the height and density values remain constant. It can be said that an increase in relative density has positively affected slope stability and has caused significant changes in the factor of safety values. Specifically, between Dr values of 50% and 65%, there has been a variation of up to 14% in certain cases, and between values of 50% and 80%, there has been a variation of up to 21.5% in certain cases.

In the subsequent stages of the study, the loading level that brings the factor of safety to its limit state was determined solely for the slope. In the applied analyses, a loading was imposed on the system beyond the ultimate value, and the load value that induced system failure was controlled using stress-strain curves. In the following phase, this limit load value obtained was defined as the foundation load in the slope-foundation system, and the possible most critical failure plane for the slope loaded at the limit state was determined. The comparison of the behavior of the slope-foundation system under these conditions was performed by comparing the possible critical failure planes obtained from the "incremental displacements" section and added to the subsequent sections of the study. When examining the effects of variations in relative density on the ultimate load value for a fixed interaction distance, it can be said that there is a significant difference of up to 93%, especially when the interaction distance is 0. However, this percentage tends to decrease as the slope height increases. Additionally, an increase in the interaction distance tends to reduce the variation caused by the increase in relative density. When examining the difference resulting from the variation in interaction distance under the same relative density effect, it can be observed that the ultimate load value increases with an increase in slope height. As the structure moves away from the top of the slope, the load that can be sustained increases, and approximately when the distance of movement reaches four times the foundation size, the load capacity is calculated in similar proportions. This indicates a decrease in the slope-foundation interaction when the interaction distance is 4B. To verify the accuracy of the situation, the analyses were repeated with different foundation widths.

Table 4.1. Change of FSslope and qult values for B= 1 m condition according to L

		B=1 m					
		D_r= 50%		D_r= 65%		D_r= 80%	
L (m)	*H (m)*	FS_{slope}	q_{ult} (kPa)	FS_{slope}	q_{ult} (kPa)	FS_{slope}	q_{ult} (kPa)
0.0	*2.0*	1.5	82.0	1.6	111.0	1.6	147.0
	4.0	1.4	77.0	1.5	96.0	1.6	131.0
	6.0	1.4	68.0	1.5	87.0	1.6	124.0
	8.0	1.4	62.0	1.5	83.0	1.6	119.0
	16.0	1.3	58.0	1.4	81.0	1.5	112.0
		D_r= 50%		D_r= 65%		D_r= 80%	
L (m)	*H (m)*	FS_{slope}	q_{ult} (kPa)	FS_{slope}	q_{ult} (kPa)	FS_{slope}	q_{ult} (kPa)
1.0	*2.0*	1.5	149.0	1.5	215.0	1.7	249.0
	4.0	1.4	142.0	1.5	211.0	1.6	243.0
	6.0	1.4	138.0	1.5	208.5	1.6	238.0
	8.0	1.4	135.0	1.5	201.0	1.6	231.0
	16.0	1.3	132.0	1.4	189.0	1.5	226.0
		D_r= 50%		D_r= 65%		D_r= 80%	
L (m)	*H (m)*	FS_{slope}	q_{ult} (kPa)	FS_{slope}	q_{ult} (kPa)	FS_{slope}	q_{ult} (kPa)
2.0	*2.0*	1.5	237.0	1.6	311.0	1.7	331.0
	4.0	1.4	233.0	1.6	302.0	1.6	327.0
	6.0	1.4	229.0	1.5	297.5	1.6	322.0
	8.0	1.4	227.0	1.5	292.0	1.6	318.0
	16.0	1.3	223.0	1.4	284.0	1.5	311.0
		D_r= 50%		D_r= 65%		D_r= 80%	
L (m)	*H (m)*	FS_{slope}	q_{ult} (kPa)	FS_{slope}	q_{ult} (kPa)	FS_{slope}	q_{ult} (kPa)
4.0	*2.0*	1.5	307.0	1.5	420.0	2.7	479.0
	4.0	1.4	302.0	1.5	411.0	2.5	474.0
	6.0	1.4	299.0	1.5	402.0	2.5	470.0
	8.0	1.4	288.0	1.5	382.0	1.5	463.0
	16.0	1.3	254.0	1.4	341.0	1.5	457.0
		D_r= 50%		D_r= 65%		D_r= 80%	
L (m)	*H (m)*	FS_{slope}	q_{ult} (kPa)	FS_{slope}	q_{ult} (kPa)	FS_{slope}	q_{ult} (kPa)
8.0	*2.0*	1.5	311.0	1.5	429.0	2.7	503.0
	4.0	1.4	309.0	1.5	383.0	2.5	497.0
	6.0	1.4	306.0	1.5	369.0	2.5	492.0
	8.0	1.4	296.0	1.5	358.0	1.5	489.0
	16.0	1.3	289.0	1.4	353.0	1.5	486.0
		D_r= 50%		D_r= 65%		D_r= 80%	
L (m)	*H (m)*	FS_{slope}	q_{ult} (kPa)	FS_{slope}	q_{ult} (kPa)	FS_{slope}	q_{ult} (kPa)
16.0	*2.0*	1.4	315.0	1.6	432.0	2.6	519.0
	4.0	1.4	310.0	1.5	396.0	2.5	511.0
	6.0	1.4	308.0	1.5	387.0	2.5	505.0
	8.0	1.4	272.0	1.5	349.0	1.5	466.0
	16.0	1.3	262.0	1.5	338.0	1.5	463.0

The results obtained when using a foundation width of 2 meters are provided in Table 4.2, Since the factor of safety is only related to the stability of the slopes, the factor of safety values were obtained at the same value in all cases, regardless of the variation in foundation width. The changes in the ultimate load due to an increase in foundation width are similar in nature to the case of B=1 meter. The key point to note here is the numerical changes in the load values between the B=1 meter case and the B=2 meter case. When comparing the ultimate loading values for B=1 meter and B=2 meter cases, it can be observed that when there is no interaction distance, there is an increase of up to 100% in the load-bearing capacity. The results of the analyses conducted for the cases where the foundation width increases to 4 and 8 meters respectively are provided in Table 4.2, and Table 4.3. In the cases where the foundation width increases from 1 meter to 4 meters, an increase in the interaction distance is observed to result in an increase in the load-bearing capacity of the foundation. Similarly, an increase in relative density allows for an increase in the load-bearing capacity. When examining the mentioned tables, an interesting observation is that, especially when the foundation width reaches 8B, if the interaction distance is more than 4 meters, the ultimate load values that can be achieved at the limit state of stability decrease. The reasons behind this occurrence can be identified through evaluating possible failure mechanisms. In similar cases, where B=2 m and B=4 m, with Dr=80% and L=8m, this situation applies to all slope heights. For both cases, the generated critical failure surfaces obtained from safety analysis have been investigated. For the discussion of B= 4 m and B=8 m condition Figure 4.3, and fort he discussion of B=2 m and B=4 m condition Figure 4.4, have been taken. To verify this situation, the incremental displacements in the safety phases were compared for the cases of B=4 m, H=2 m, L=4 m, D_r= 80%, and B=8 m, H=2 m, L=4 m, D_r=80%, as shown in Figure 4.3, In these cases, the effect of the foundation width is examined. In the case of B=4 m, the largest displacements occur near the edge of the foundation, and the overall system failure occurs with a mechanism reaching the slope toe. In the case of B=8 m, with the increase in foundation width, the affected area and the distribution of deformations have increased, resulting in the mobilization of a deeper failure surface that includes the slope toe. In these cases, the values of moment (M), shear force (Q), and normal force (N) in the foundation section were also examined. It can be observed that these effects increase and exert more stress on the section when B=8 m, indicating a decrease in the load-carrying capacity of the foundation compared to the B=4 m condition.

Table 4.2. Change of FSslope and qult values for B= 2 m condition according to L

		B=2 m					
		D_r= 50%		D_r= 65%		D_r= 80%	
L (m)	*H (m)*	FS_{slope}	q_{ult} (kPa)	FS_{slope}	q_{ult} (kPa)	FS_{slope}	q_{ult} (kPa)
0.0	*2.0*	1.5	154.0	1.6	207.0	1.6	269.0
	4.0	1.4	138.0	1.5	195.0	1.6	249.0
	6.0	1.4	135.0	1.5	188.0	1.6	242.0
	8.0	1.4	131.0	1.5	183.0	1.6	229.0
	16.0	1.3	128.0	1.4	177.0	1.5	223.0
		D_r= 50%		D_r= 65%		D_r= 80%	
L (m)	*H (m)*	FS_{slope}	q_{ult} (kPa)	FS_{slope}	q_{ult} (kPa)	FS_{slope}	q_{ult} (kPa)
1.0	*2.0*	1.5	201.0	1.5	300.0	1.7	354.0
	4.0	1.4	198.0	1.5	265.0	1.6	293.0
	6.0	1.4	195.0	1.5	257.5	1.6	285.0
	8.0	1.4	191.0	1.5	249.0	1.6	281.0
	16.0	1.3	188.0	1.4	243.0	1.5	273.0
		D_r= 50%		D_r= 65%		D_r= 80%	
L (m)	*H (m)*	FS_{slope}	q_{ult} (kPa)	FS_{slope}	q_{ult} (kPa)	FS_{slope}	q_{ult} (kPa)
2.0	*2.0*	1.5	324.0	1.6	445.5	1.7	469.0
	4.0	1.4	294.0	1.6	389.5	1.6	454.0
	6.0	1.4	289.0	1.5	380.0	1.6	448.0
	8.0	1.4	284.0	1.5	371.5	1.6	439.0
	16.0	1.3	279.0	1.4	349.0	1.5	428.0
		D_r= 50%		D_r= 65%		D_r= 80%	
L (m)	*H (m)*	FS_{slope}	q_{ult} (kPa)	FS_{slope}	q_{ult} (kPa)	FS_{slope}	q_{ult} (kPa)
4.0	*2.0*	1.5	437.0	1.5	647.0	2.7	697.0
	4.0	1.4	433.0	1.5	611.0	2.5	684.0
	6.0	1.4	428.0	1.5	577.0	2.5	672.0
	8.0	1.4	421.0	1.5	556.0	1.5	664.0
	16.0	1.3	418.0	1.4	539.0	1.5	657.0
		D_r= 50%		D_r= 65%		D_r= 80%	
L (m)	*H (m)*	FS_{slope}	q_{ult} (kPa)	FS_{slope}	q_{ult} (kPa)	FS_{slope}	q_{ult} (kPa)
8.0	*2.0*	1.5	543.0	1.5	816.0	2.7	903.0
	4.0	1.4	538.0	1.5	809.0	2.5	894.0
	6.0	1.4	531.0	1.5	805.0	2.5	886.0
	8.0	1.4	525.0	1.5	796.0	1.5	879.0
	16.0	1.3	519.0	1.4	772.0	1.5	868.0
		D_r= 50%		D_r= 65%		D_r= 80%	
L (m)	*H (m)*	FS_{slope}	q_{ult} (kPa)	FS_{slope}	q_{ult} (kPa)	FS_{slope}	q_{ult} (kPa)
16.0	*2.0*	1.4	553.0	1.6	766.0	2.6	904.0
	4.0	1.4	549.0	1.5	845.0	2.5	898.0
	6.0	1.4	546.0	1.5	885.0	2.5	891.0
	8.0	1.4	542.0	1.5	955.0	1.5	885.0
	16.0	1.3	539.0	1.5	911.0	1.5	877.0

Table 4.3. Change of FSslope and qult values for B= 4 m condition according to L

		B=4 m					
		D_r= 50%		D_r= 65%		D_r= 80%	
L (m)	*H (m)*	FS_{slope}	q_{ult} (kPa)	FS_{slope}	q_{ult} (kPa)	FS_{slope}	q_{ult} (kPa)
0.0	*2.0*	1.5	303.0	1.6	427.0	1.6	478.0
	4.0	1.4	227.0	1.5	306.0	1.6	394.0
	6.0	1.4	221.0	1.5	282.0	1.6	380.0
	8.0	1.4	204.0	1.5	277.0	1.6	358.0
	16.0	1.3	139.0	1.4	207.0	1.5	246.0
		D_r= 50%		D_r= 65%		D_r= 80%	
L (m)	*H (m)*	FS_{slope}	q_{ult} (kPa)	FS_{slope}	q_{ult} (kPa)	FS_{slope}	q_{ult} (kPa)
1.0	*2.0*	1.5	341.0	1.5	467.0	1.7	479.0
	4.0	1.4	328.0	1.5	452.0	1.6	412.0
	6.0	1.4	309.0	1.5	437.0	1.6	409.0
	8.0	1.4	273.0	1.5	376.0	1.6	403.0
	16.0	1.3	267.0	1.4	369.0	1.5	399.0
		D_r= 50%		D_r= 65%		D_r= 80%	
L (m)	*H (m)*	FS_{slope}	q_{ult} (kPa)	FS_{slope}	q_{ult} (kPa)	FS_{slope}	q_{ult} (kPa)
2.0	*2.0*	1.5	482.0	1.6	573.0	1.7	636.0
	4.0	1.4	436.0	1.6	556.0	1.6	633.0
	6.0	1.4	392.0	1.5	485.0	1.6	578.0
	8.0	1.4	374.0	1.5	473.0	1.6	539.0
	16.0	1.3	357.0	1.4	444.0	1.5	501.0
		D_r= 50%		D_r= 65%		D_r= 80%	
L (m)	*H (m)*	FS_{slope}	q_{ult} (kPa)	FS_{slope}	q_{ult} (kPa)	FS_{slope}	q_{ult} (kPa)
4.0	*2.0*	1.5	591.0	1.5	672.0	2.7	685.0
	4.0	1.4	579.0	1.5	647.0	2.5	682.0
	6.0	1.4	538.0	1.5	641.0	2.5	604.0
	8.0	1.4	509.0	1.5	607.0	1.5	603.0
	16.0	1.3	489.0	1.4	571.0	1.5	598.0
		D_r= 50%		D_r= 65%		D_r= 80%	
L (m)	*H (m)*	FS_{slope}	q_{ult} (kPa)	FS_{slope}	q_{ult} (kPa)	FS_{slope}	q_{ult} (kPa)
8.0	*2.0*	1.5	737.0	1.5	639.0	2.7	463.0
	4.0	1.4	724.0	1.5	585.0	2.5	462.0
	6.0	1.4	708.0	1.5	546.0	2.5	459.0
	8.0	1.4	672.0	1.5	509.0	1.5	454.0
	16.0	1.3	604.0	1.4	505.0	1.5	452.0
		D_r= 50%		D_r= 65%		D_r= 80%	
L (m)	*H (m)*	FS_{slope}	q_{ult} (kPa)	FS_{slope}	q_{ult} (kPa)	FS_{slope}	q_{ult} (kPa)
16.0	*2.0*	1.4	911.0	1.6	950.0	2.6	955.0
	4.0	1.4	899.0	1.5	943.0	2.5	649.0
	6.0	1.4	893.0	1.5	937.0	2.5	647.0
	8.0	1.4	887.0	1.5	924.0	1.5	634.0
	16.0	1.3	879.0	1.5	895.0	1.5	629.0

Table 4.4. Change of FSslope and qult values for B= 8 m condition according to L

		B=8 m					
		D_r= 50%		D_r= 65%		D_r= 80%	
L (m)	*H (m)*	FS_{slope}	q_{ult} (kPa)	FS_{slope}	q_{ult} (kPa)	FS_{slope}	q_{ult} (kPa)
0.0	*2.0*	1.5	514.0	1.6	568.0	1.6	419.0
	4.0	1.4	411.0	1.5	541.0	1.6	418.0
	6.0	1.4	349.0	1.5	527.0	1.6	416.0
	8.0	1.4	321.0	1.5	376.0	1.6	413.0
	16.0	1.3	212.0	1.4	142.0	1.5	299.0
1.0	*2.0*	1.5	535.0	1.5	664.0	1.7	413.0
	4.0	1.4	529.0	1.5	629.0	1.6	412.0
	6.0	1.4	488.0	1.5	554.0	1.6	410.0
	8.0	1.4	461.0	1.5	539.0	1.6	352.0
	16.0	1.3	432.0	1.4	496.0	1.5	349.0
2.0	*2.0*	1.5	593.0	1.6	709.0	1.7	746.0
	4.0	1.4	562.0	1.6	699.0	1.6	715.0
	6.0	1.4	548.0	1.5	683.0	1.6	707.0
	8.0	1.4	406.0	1.5	658.0	1.6	291.0
	16.0	1.3	255.0	1.4	569.0	1.5	278.0
4.0	*2.0*	1.5	286.0	1.5	472.0	2.7	436.0
	4.0	1.4	604.0	1.5	469.0	2.5	418.0
	6.0	1.4	348.0	1.5	463.0	2.5	413.0
	8.0	1.4	581.0	1.5	451.0	1.5	409.0
	16.0	1.3	539.0	1.4	446.0	1.5	407.0
8.0	*2.0*	1.5	295.0	1.5	340.0	2.7	403.0
	4.0	1.4	662.0	1.5	336.0	2.5	401.0
	6.0	1.4	322.0	1.5	333.0	2.5	398.0
	8.0	1.4	453.0	1.5	325.0	1.5	393.0
	16.0	1.3	428.0	1.4	313.0	1.5	389.0
16.0	*2.0*	1.4	834.0	1.6	780.0	2.6	397.0
	4.0	1.4	734.0	1.5	377.0	2.5	395.0
	6.0	1.4	727.0	1.5	373.0	2.5	394.0
	8.0	1.4	719.0	1.5	366.0	1.5	391.0
	16.0	1.3	691.0	1.5	358.0	1.5	388.0

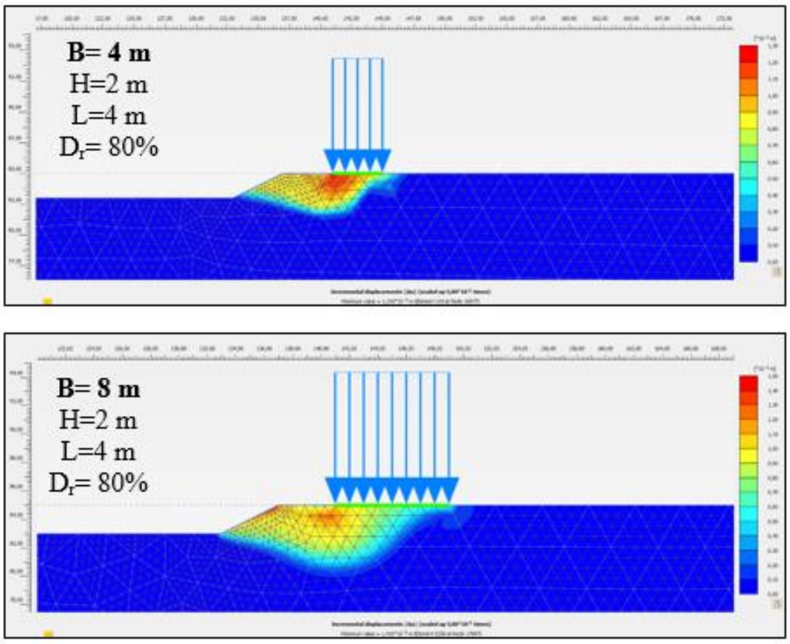

Figure 4.3. The discussion of B= 4 m and B=8 m condition

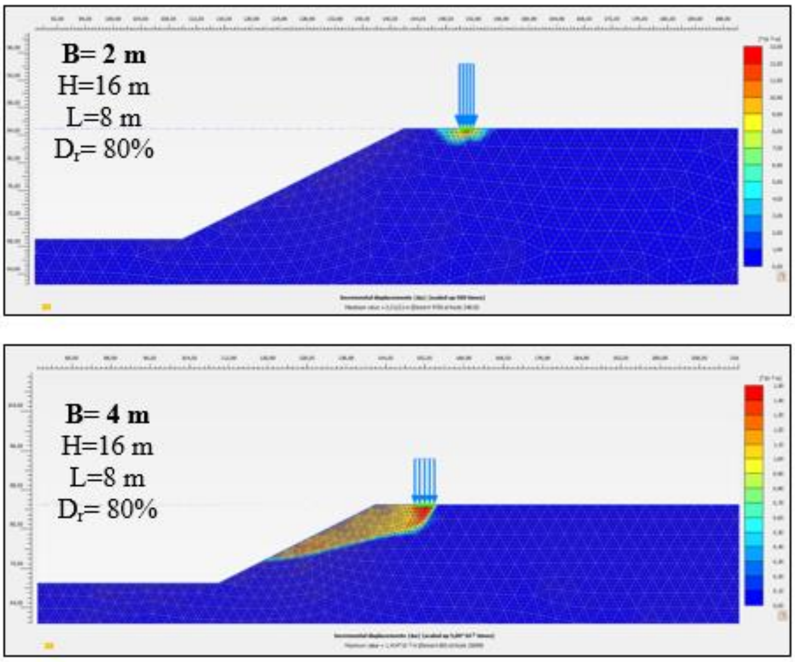

Figure 4.4. The discussion of B=2 m and B=4 m condition

Additionally, when comparing the cases of B=2 m, L=8 m, H=16 m, Dr=80% and B=4 m, L=8 m, H=16 m, Dr=80% as shown in Figure 4.4, a similar and more distinct mechanism can be observed. In the case of B=2 m, there is sufficient distance between the slope crest and the corner of the foundation, allowing the slope to remain stable at a certain level of safety without being affected by the foundation loading. However, in the case of B=4 m, the slope has interacted with the foundation loading, exhibiting a combined behavior. This condition has prevented the formation of a passive zone in the foundation (as mentioned in the literature sources) and led to a decrease in the load-carrying capacity of the foundation.

When constructing a building on or within slopes, the foundation's bearing capacity (ultimate load it can support) is influenced not only by the soil profile and geotechnical properties but also by the geometry of the slope (Keskin and Laman, 2013). In such cases, the ultimate bearing capacity is governed by either the foundation's capacity or the overall stability of the slope. The combination of slope stability and bearing capacity presents a challenging problem for modeling and analysis (Moayedi and Hayati, 2018).

The theories used to calculate the ultimate bearing capacity of a foundation on horizontal soil layers can be expanded and combined with slope stability theory to encompass the stability of foundations located on slopes. Based on the analysis conducted so far, it is understood that the ultimate bearing capacity of foundations located within or on slopes decreases as the slope angle increases, particularly for granular (cohesionless) soils. At a greater distance from the crest of a slope, the bearing capacity significantly decreases with a steeper slope and is primarily governed by overall slope instability.

In shallow foundations, according to literature sources, the allowable bearing capacity is predominantly governed by the settlement of the foundation. Therefore, according to Skempton and MacDonald (1956), when the maximum allowable settlement is 32 mm for sand and 45 mm for clay, it has been observed that settlement exceeding these values leads to inadequate bearing capacity and the occurrence of failure due to excessive settlement. In addition, according to IS-1904 (1966), the allowable maximum settlement for isolated foundations is 40 mm for sandy soils and 65 mm for clayey soils. For raft foundations constructed on clayey soil, the allowable settlement range is 65-100 mm, while for those constructed on sandy soil, it is 65 mm. The FHWA Geotechnical Engineering Circular No. 6, Shallow Foundations (2002), states that in practice, total settlements are typically limited to the order of 25 mm (1 inch), and the differential settlements are limited to approximately half of the total settlement. According to Uzuner (1995), for single-strip footings, the recommended maximum differential settlement is 4.0 cm for clayey soil and 2.5 cm for sandy soil. The maximum total settlement is recommended to be 6.5 cm for clayey soil and 4.0 cm for sandy soil. For raft foundations, the maximum differential settlement value is 4.0 cm for clayey soil and 2.5 cm for sandy soil. The maximum total settlement value is within the range of 6.5-10 cm for clayey soil and 4.0-6.5 cm for sandy soil. When considering the literature studies mentioned above, it is generally observed that for single footings located on sandy soils, a maximum settlement limit of 4.0 cm is recommended when settling onto sandy soil. In this context, within the scope of the thesis, deformation analyses will consider a settlement limit of 4.0 cm as the maximum allowable settlement.

Due to insufficient bearing capacity followed by slope instability, a distinct failure mode can be observed in slope-foundation interaction systems. In this case, the ultimate bearing capacity of the foundation reaches its ultimate (or allowable) value in terms of vertical displacement of the soil beneath the foundation, while the slope is still stable and achieves an acceptable factor of safety of at least $FS_{slope} = 1.3$ for design purposes. In geotechnical engineering designs, an acceptable factor of safety of a minimum of 1.3 is commonly adopted for slopes, and a factor of safety less than this is considered to indicate slope instability. In geotechnical engineering software used for analysis, particularly based on limit equilibrium methods, a factor of safety of 1.0 is assumed to represent the occurrence of failure, and the applied load magnitude under this condition represents the limit load condition.

As an additional category of failure observed in slope-foundation integrated systems, the opposite of what was described above can also occur. In this case, with an increase in the applied load level, a continued slope instability may develop following a loss of foundation bearing capacity.

With this context, the following (deformation) analysis can be made to control the above-mentioned situations. The analysis of single foundations on the slope involves the control of maximum displacements occurring with the ultimate load value. The relevant displacement measurements were taken from the midpoint of the footing and a representative point is shown in Figure 4.5, The variations of displacements with loading were examined step by step. For the analysis, it is crucial to consider how the displacements on the footing change in response to loading. This information provides insights into the stability and behavior of the foundation.

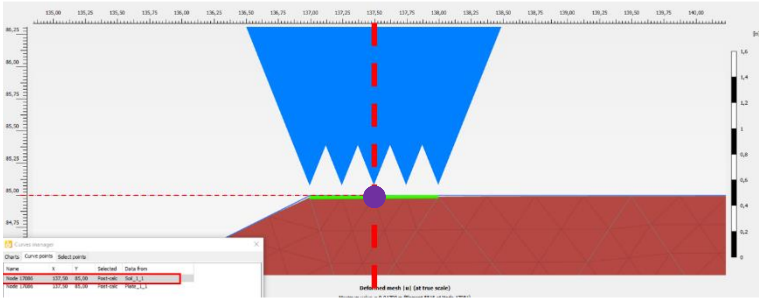

Figure 4.5. The displacement measurements

The graphs presented below are arranged in triple columns, where the first column represents the condition of D_r=50%, the second column represents D_r=65%, and the third column represents D_r=80%. It should be noted that the axes of the graphs are not scaled equally. Therefore, the evaluations based on each graph are presented below in order.

In Figure 4.6, under the condition of D_r=50%, the maximum displacement occurs at H=2 m under the maximum load that the foundation can bear. For slope heights other than H=2 m, a clear failure point can be identified, indicating a distinct location of slope failure. However, at H=2 m, the deformation appears to have reached a peak. On the other hand, at H=16 m, the system experiences the highest level of load that it can sustain without failure (hardening behavior), but the deformation remains at a relatively low level.

With an increase in the D_r value to 65%, the relationship between load and deformation has become linear, and except for H=16 m, the qult values have been close to each other for other slope heights. An increase in relative density has led to a decrease in the maximum displacement values occurring in the ultimate bearing capacity. When D_r=80%, the stress-strain relationship has started to exhibit an elastoplastic trend. The lowest ultimate load value was obtained again at the highest slope height.

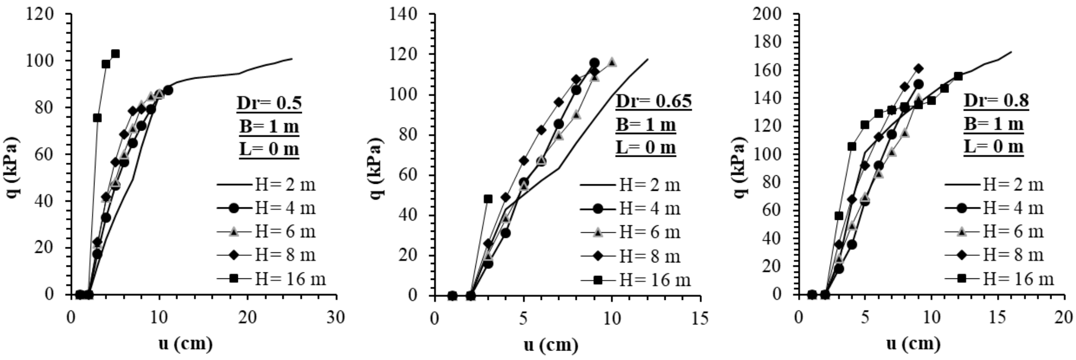

Figure 4.6. The change of displacement via the applied ultimate load magnitude for B=1 m and L= 0 condition

The relationship between stress and displacement was obtained by considering the variations in slope heights with the aim of achieving different relative densities when B=1 m and L=1 m. As the foundation moves away from the slope, the ultimate load value obtained for the foundation has started to increase in all analyses for different slope heights and relative density values. This situation has also led to an increase in the displacements occurring relative to the foundation resting on the slope. However, the stress-displacement relationship has differed from the relationships defined under the condition of L=0, especially for relatively low relative density values.

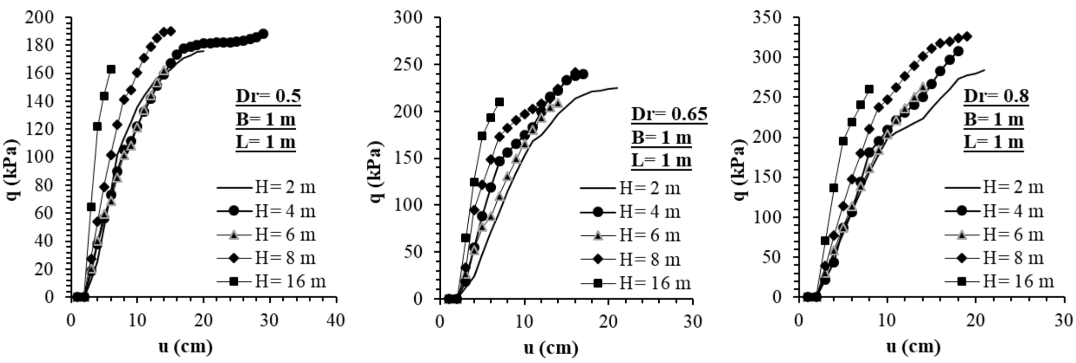

Figure 4.7. The change of displacement via the applied ultimate load magnitude for B=1 m and L= 1 m condition

The relationship between stress and displacement was obtained by considering the variations in slope heights with the aim of achieving different relative densities when B=1 m and L=2 m. This condition represents the situation where the foundation moves away from the slope top by a distance equal to twice its width. In this case, an increase in the relative density value leads to a significant increase in the ultimate load value. Moreover, the foundation moving away from the slope surface also increases the ultimate load value and particularly reduces the displacements occurring, especially for low relative density values. In the cases of D_r=65% and

D_r=80%, there is an increase in the ultimate load values for both L=1 m and L=2 m conditions, but the magnitudes of the displacements are not as much influenced as they are by D_r=50%.

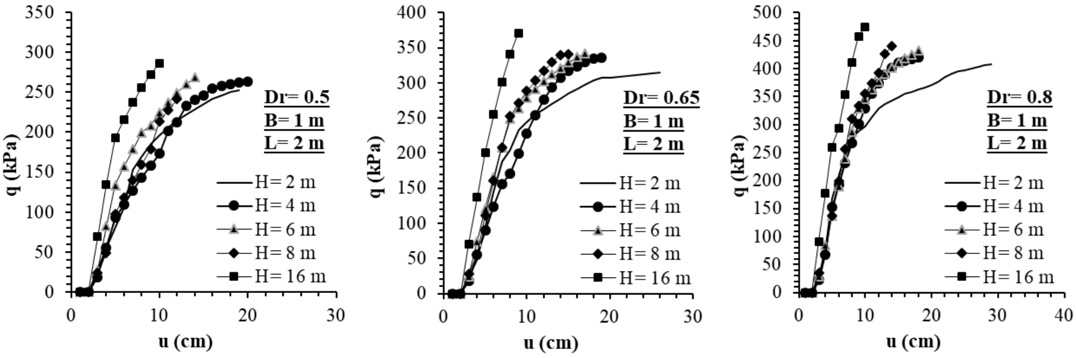

Figure 4.8. The change of displacement via the applied ultimate load magnitude for B=1 m and L= 2 m condition

The relationship between stress and displacement was obtained by considering the variations in slope heights with the aim of achieving different relative densities when B=1 m and L=4 m in Figure 4.9, When examining the case of D_r=50% in the figures, it can be observed that similar behavior is exhibited for H=2-4-6 meter slope heights. The stress-strain behavior progresses in an elastic-plastic manner, and the critical failure load can be clearly determined at the respective heights. However, with an increase in the D_r value, particularly for H=2 and 4 meter slope heights, the system's failure behavior differentiates, and the anticipated maximum allowable displacement of the single footing tends to be exceeded. In this case, it should be considered that the resulting settlement may be caused by the foundation deformations and subsequently lead to overall slope failure. To make this situation meaningful, it is essential to evaluate it together with the critical failure surface in the corresponding condition.

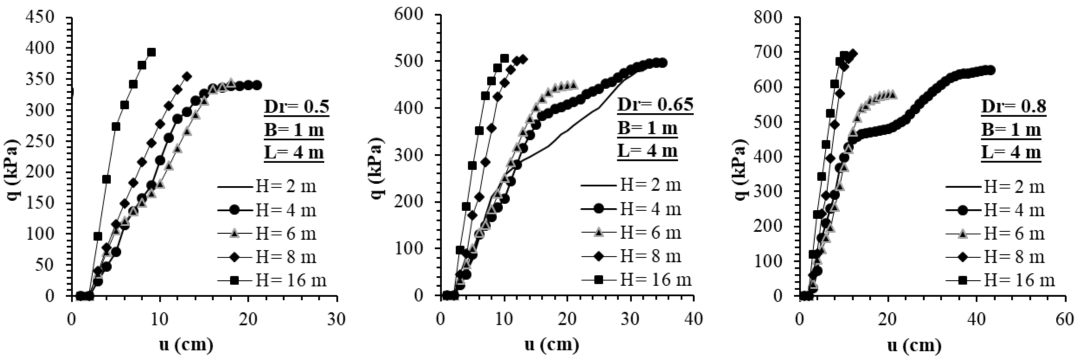

Figure 4.9. The change of displacement via the applied ultimate load magnitude for B=1 m and L= 4 m condition

The relationship between stress and displacement was obtained by considering the variations in slope heights with the aim of achieving different relative densities when B=1 m and L=8 m in Figure 4.10.

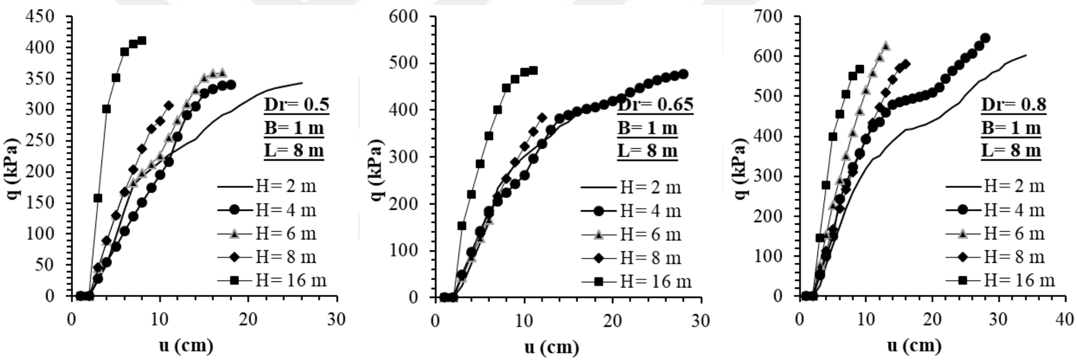

Figure 4.10. The change of displacement via the applied ultimate load magnitude for B=1 m and L= 8 m condition

The relationship between stress and displacement was obtained by considering the variations in slope heights with the aim of achieving different relative densities when B=1 m and L=16 m in Figure 4.11, In this case, a similar behavior is observed for all relative density values in the L=4 m scenario. Particularly for slope heights of H=6-8-16 m, the failure behavior appears to be related to the foundation's bearing capacity, while for other slope heights, there might be a deficiency in bearing capacity due to slope-foundation interaction.

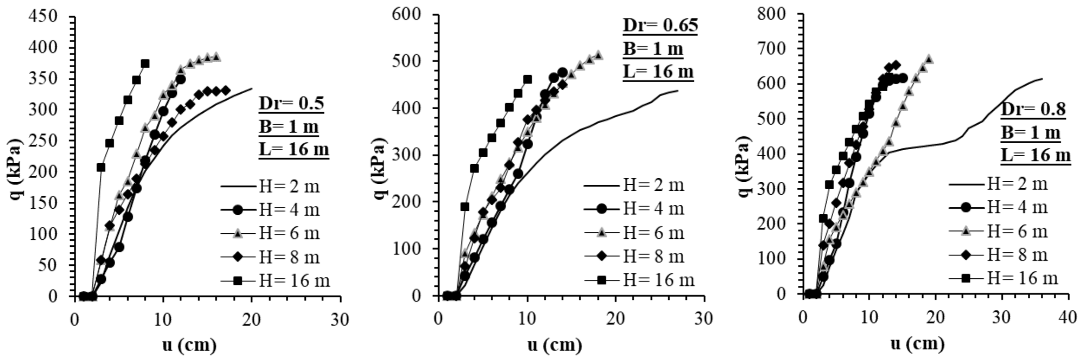

Figure 4.11. The change of displacement via the applied ultimate load magnitude for B=1 m and L= 16 m condition

The relationship between stress and displacement was obtained by considering the variations in slope heights with the aim of achieving different relative densities when B=2 m and L=0 m in Figure 4.12 With the increase in foundation width, even if the foundation is located at the top of the slope, there has been an increase in the ultimate load value compared to the other cases examined. This has subsequently led to an increase in deformations as well. The number of analyses and their outputs conducted in the scope of the thesis are extensive, and it is not possible to present all of them. Therefore, additional analysis sections and information are provided only for critical cases like this. In this particular case, incremental displacements were monitored in the safety phase at D_r=65% for each different height. In Figure 4.12, the analysis outputs are presented collectively, representing the most critical shear planes depending on the heights.

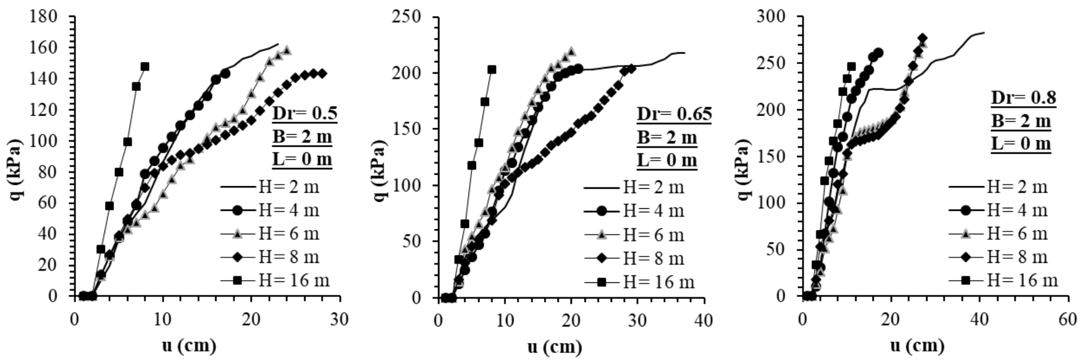

Figure 4.12. The change of displacement via the applied ultimate load magnitude for B=2 m and L= 0 condition

Upon examining Figure 4.12, a distinct stress-strain behavior can be observed for slope heights of H=2 and 4 meters. This behavior is also present in previous cases, but the displacements observed did not exceed the predicted limit values. In this case, it can be said that the realized displacement value occurred at the predicted displacement limit ratio (especially for H=2 m). In order to understand the reason behind this, stress-strain graphs will be interpreted along with the analysis results representing the potential critical failure plane. In this context, when examining the shaded mechanisms presented in Figure 4.13, it can be suggested that in low slope heights, where the deformations mobilized due to foundation loading are present in a slope environment with a lower height compared to the foundation width, both the foundation bearing capacity and slope stability issues may occur on the mobilized critical shear plane. However, when the slope height reaches three times the foundation width, the mobilization of the aforementioned mechanism changes, and slope stability ceases to be a balancing factor.

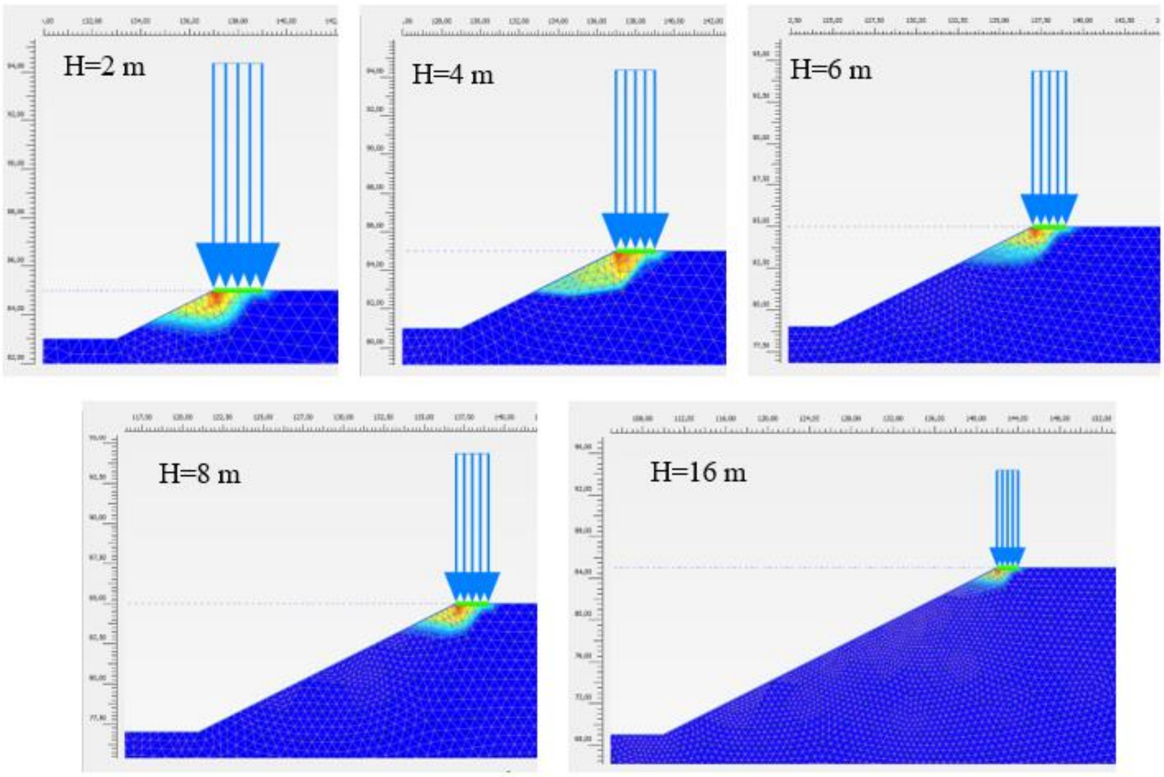

Figure 4.13. The potential critical failure plane

The relationship between stress and displacement was obtained by considering the variations in slope heights with the aim of achieving different relative densities when B=2 m and L=1 m in Figure 4.14, The notable point in this regard is the observation of minimum displacement followed by failure when the D_r values are at 50% and 80%, for H=2m with applied load. This phenomenon can be interpreted as the occurrence of slope failure following the settlement caused by the foundation's bearing capacity.

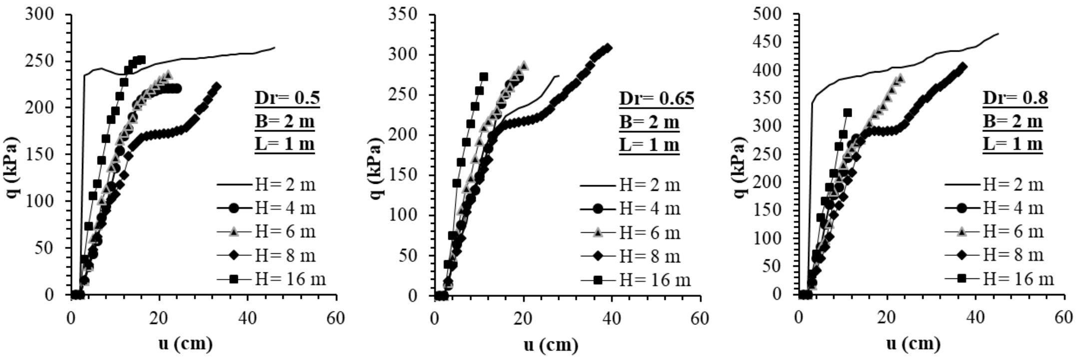

Figure 4.14. The change of displacement via the applied ultimate load magnitude for B=2 m and L= 1 m condition

The relationship between stress and displacement was obtained by considering the variations in slope heights with the aim of achieving different relative densities when B=2 m and L=2 m in Figure 4.15, When compared with the previous figure, it can be observed that increasing the foundation-slope interaction distance results in the occurrence of foundation bearing capacity failure as a form of settlement at D_r=50% for H=2 m. However, in this condition, for D_r=65% and H=16m, the occurrence of foundation bearing capacity failure can be added to the varying conditions compared to the previous figure. Below, the necessary details will be provided to explain the differences in the presented trends of these graphs when considering all the variables involved in the second phase of the thesis study.

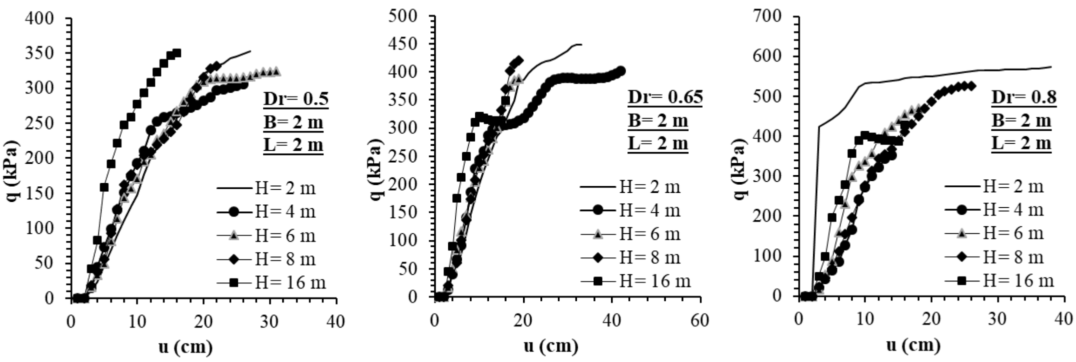

Figure 4.15. The change of displacement via the applied ultimate load magnitude for B=2 m and L= 2 m condition

The relationship between stress and displacement was obtained by considering the variations in slope heights with the aim of achieving different relative densities when B=2 m and L=4 m in Figure 4.16.

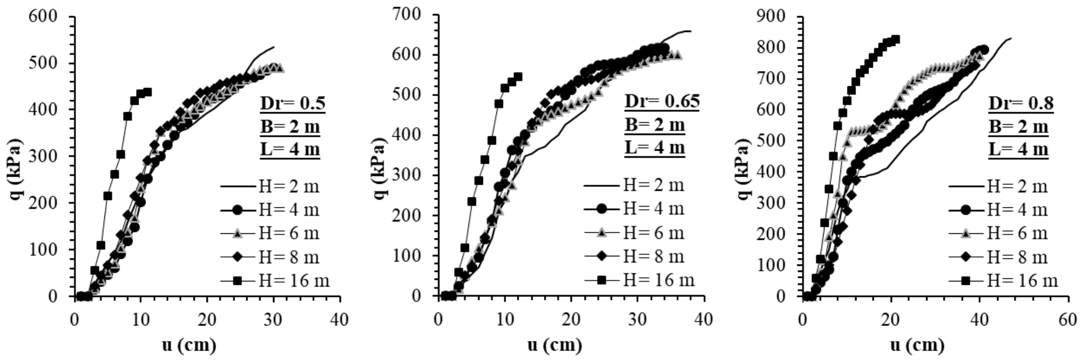

Figure 4.16. The change of displacement via the applied ultimate load magnitude for B=2 m and L= 4 m condition

The relationship between stress and displacement was obtained by considering the variations in slope heights with the aim of achieving different relative densities when B=1 m and L=8 m in Figure 4.17.

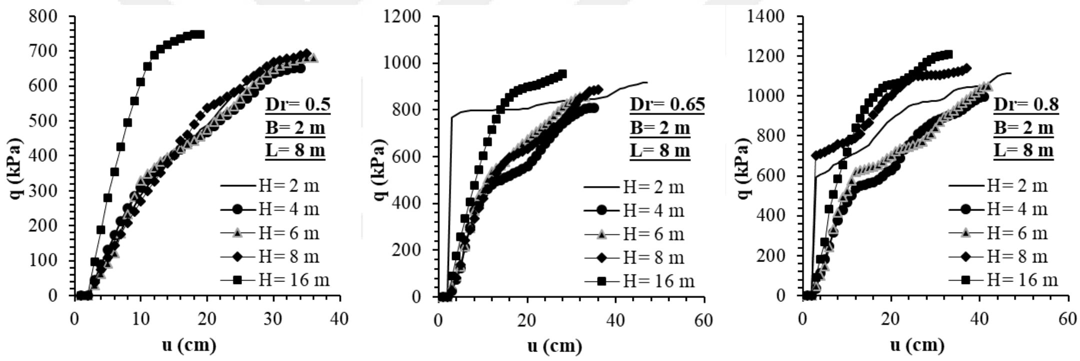

Figure 4.17. The change of displacement via the applied ultimate load magnitude for B=2 m and L= 8 m condition

The relationship between stress and displacement was obtained by considering the variations in slope heights with the aim of achieving different relative densities when B=1 m and L=16 m in Figure 4.11. In Figure 4.18, a significant difference in behavior can be observed. Regardless of the change in relative density, this condition is characterized by the occurrence of only bearing capacity failure in H=2 m.

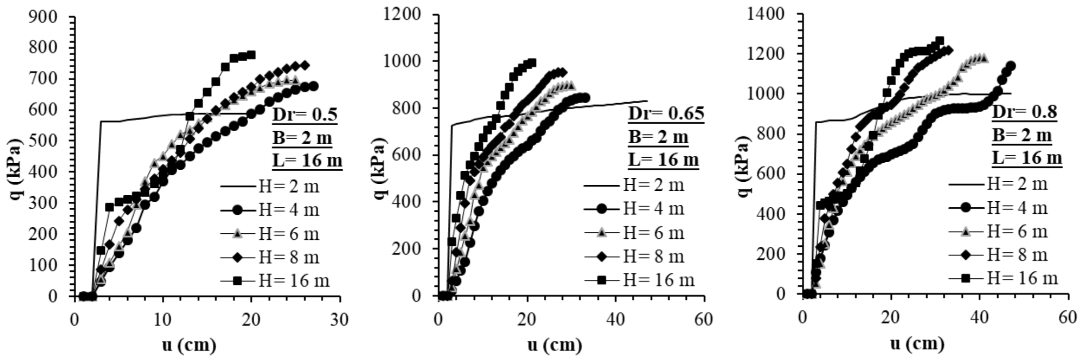

Figure 4.18. The change of displacement via the applied ultimate load magnitude for B=2 m and L= 16 m condition

The relationship between stress and displacement was obtained by considering the variations in slope heights with the aim of achieving different relative densities when B=4 m and L=0 m in Figure 4.19. As a result of the increase in foundation width, a different stress-strain behavior is observed in Figure... compared to the overall trend. In this case, it can be stated that a limit state is reached due to the bearing capacity in H=2-4-6-8 meter values. The increasing interaction distance value of B=4 m and L has led to similar results in consecutive graphs.

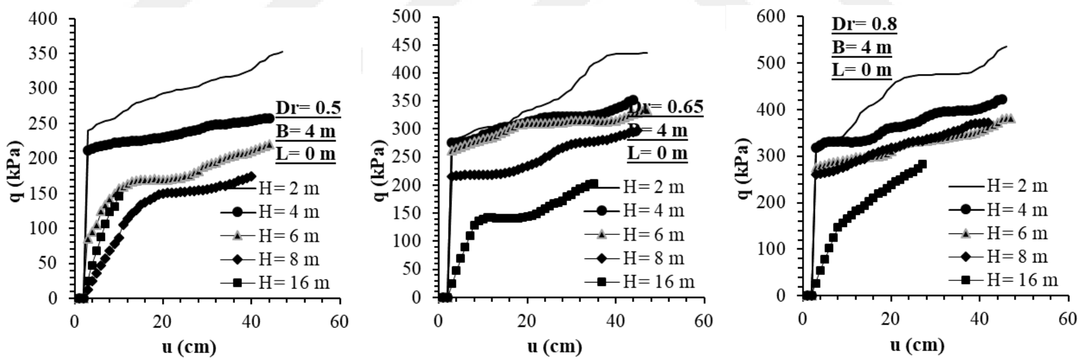

Figure 4.19. The change of displacement via the applied ultimate load magnitude for B=4 m and L= 0 condition

The relationship between stress and displacement was obtained by considering the variations in slope heights with the aim of achieving different relative densities when B=4 m and L=1 m in Figure 4.20.

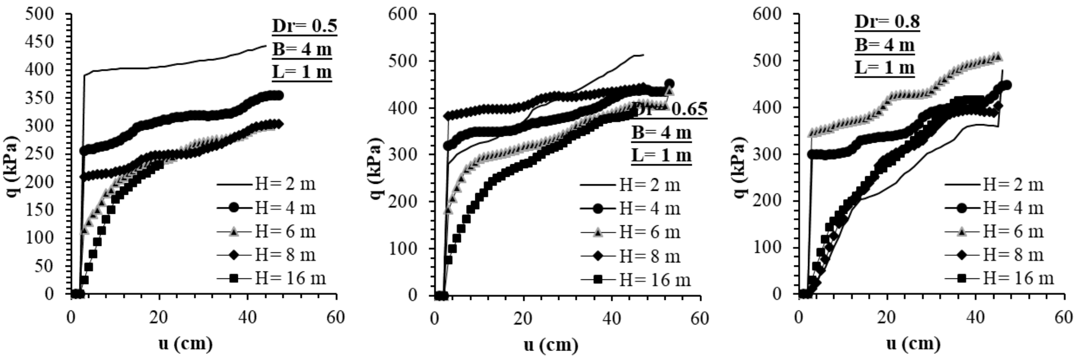

Figure 4.20. The change of displacement via the applied ultimate load magnitude for B=4 m and L= 1 m condition

The relationship between stress and displacement was obtained by considering the variations in slope heights with the aim of achieving different relative densities when B=4 m and L=2 m in Figure 4.21.

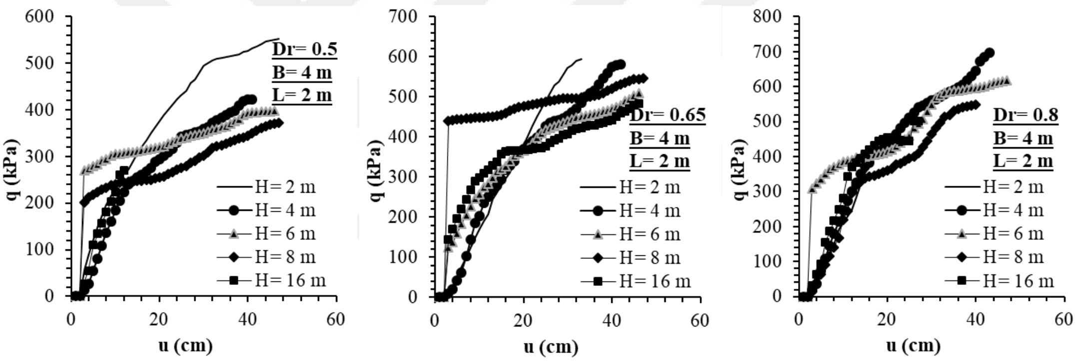

Figure 4.21. The change of displacement via the applied ultimate load magnitude for B=4 m and L= 2 m condition

The relationship between stress and displacement was obtained by considering the variations in slope heights with the aim of achieving different relative densities when B=4 m and L=4 m in Figure 4.22.

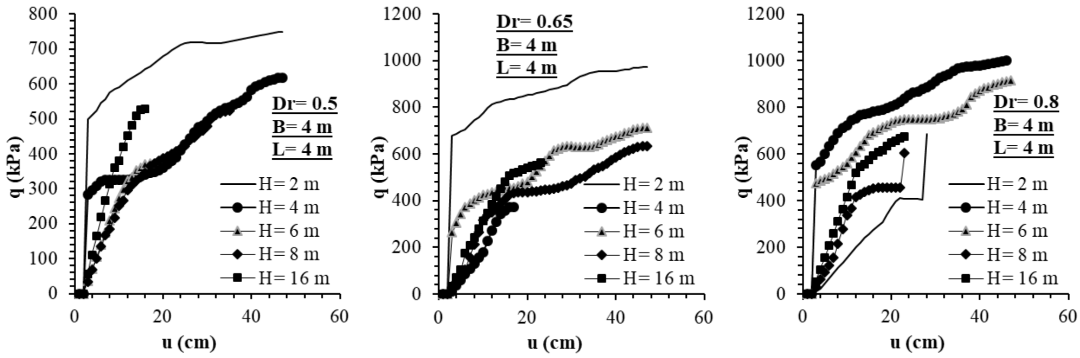

Figure 4.22. The change of displacement via the applied ultimate load magnitude for B=4 m and L= 4 m condition

The relationship between stress and displacement was obtained by considering the variations in slope heights with the aim of achieving different relative densities when B=4 m and L=8 m in Figure 4.23.

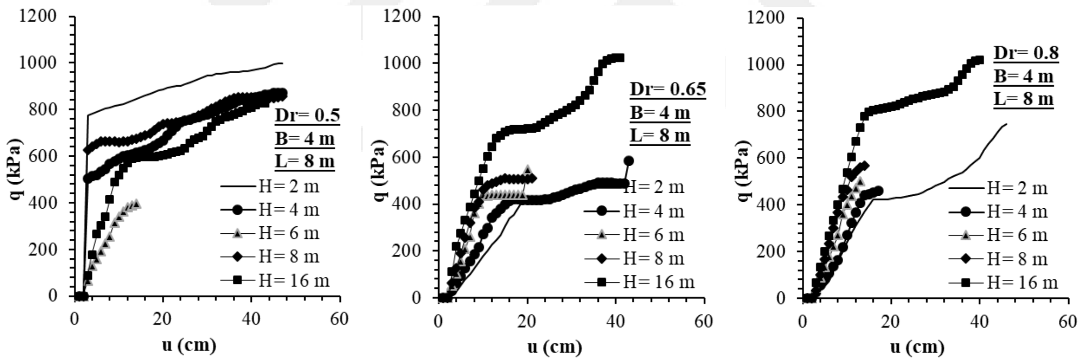

Figure 4.23. The change of displacement via the applied ultimate load magnitude for B=4 m and L= 8 m condition

The relationship between stress and displacement was obtained by considering the variations in slope heights with the aim of achieving different relative densities when B=4 m and L=16 m in Figure 4.24.

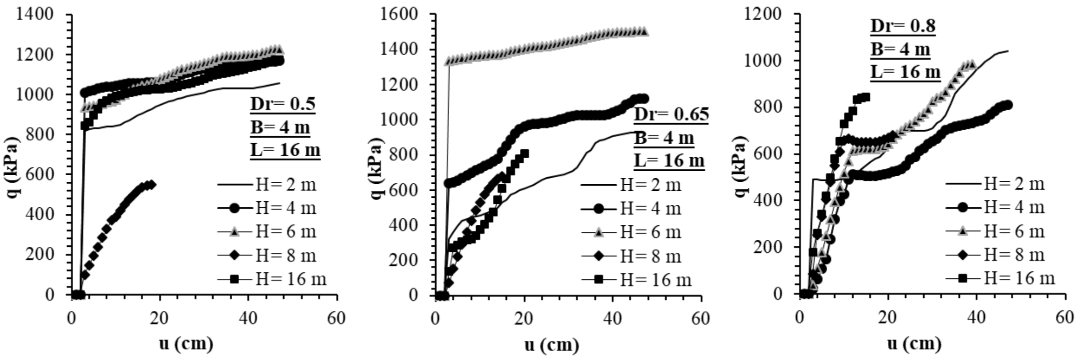

Figure 4.24. The change of displacement via the applied ultimate load magnitude for B=4 m and L= 16 m condition

The relationship between stress and displacement was obtained by considering the variations in slope heights with the aim of achieving different relative densities when B=8 m and L=0 m in Figure 4.25.

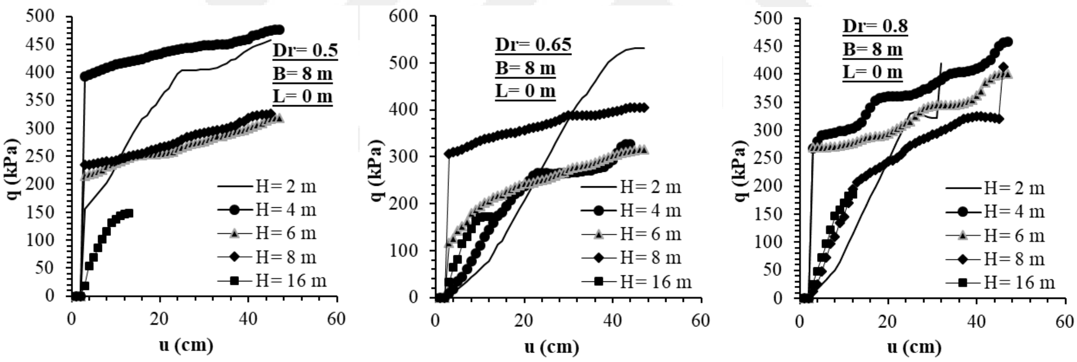

Figure 4.25. The change of displacement via the applied ultimate load magnitude for B=8 m and L= 0 condition

The relationship between stress and displacement was obtained by considering the variations in slope heights with the aim of achieving different relative densities when B=8 m and L=1 m in Figure 4.26.

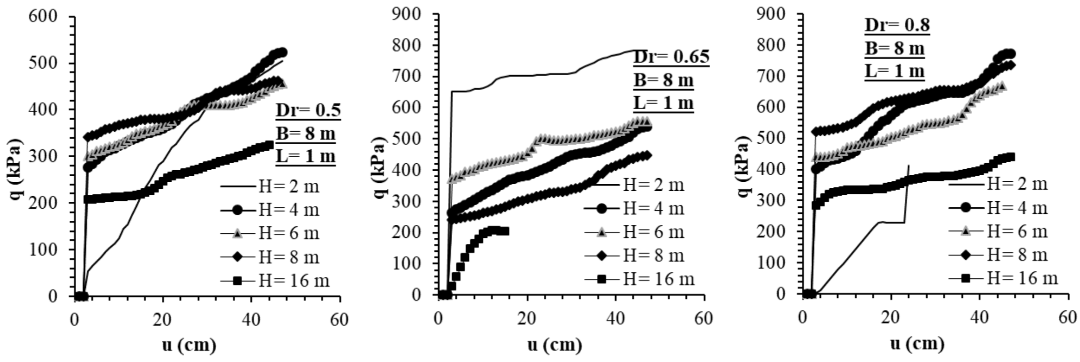

Figure 4.26. The change of displacement via the applied ultimate load magnitude for B=8 m and L= 1 m condition

The relationship between stress and displacement was obtained by considering the variations in slope heights with the aim of achieving different relative densities when B=8 m and L=2 m in Figure 4.27.

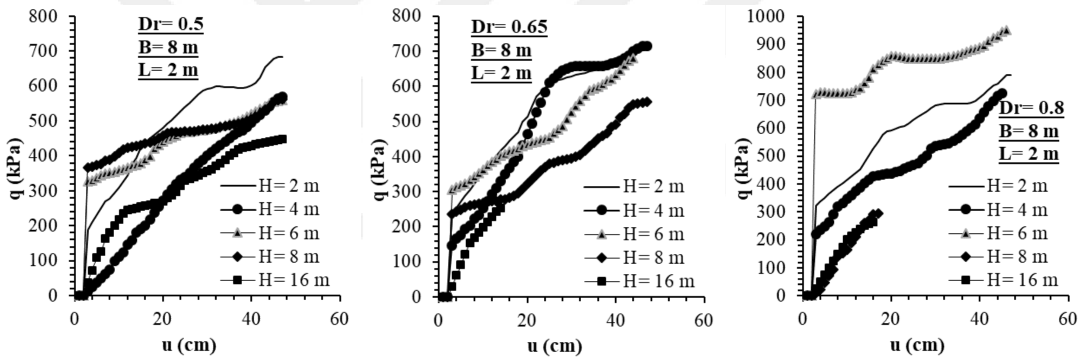

Figure 4.27. The change of displacement via the applied ultimate load magnitude for B=8 m and L= 2 m condition

The relationship between stress and displacement was obtained by considering the variations in slope heights with the aim of achieving different relative densities when B=8 m and L=4 m in Figure 4.28.

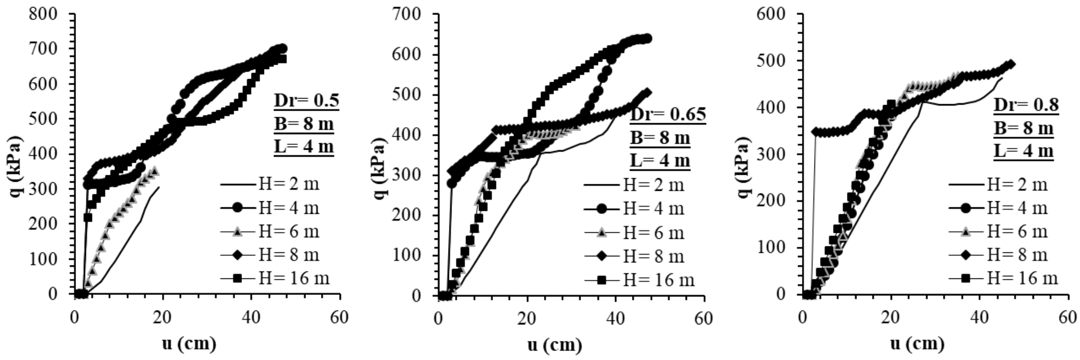

Figure 4.28. The change of displacement via the applied ultimate load magnitude for B=8 m and L= 4 m condition

The relationship between stress and displacement was obtained by considering the variations in slope heights with the aim of achieving different relative densities when B=8 m and L=8 m in Figure 4.29.

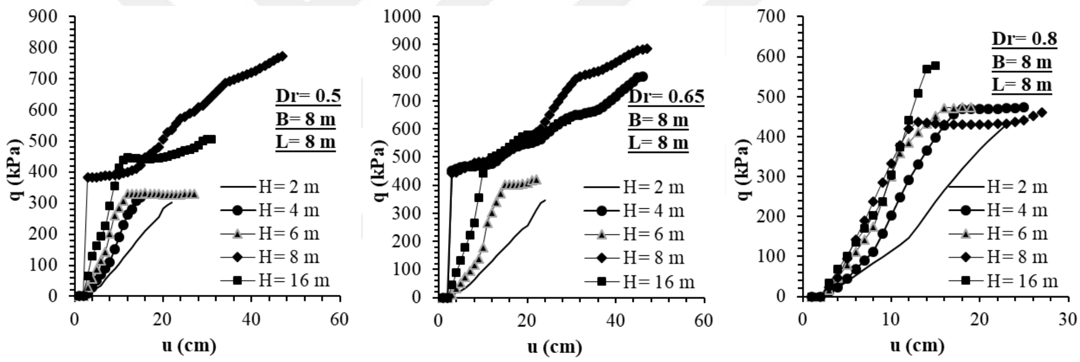

Figure 4.29. The change of displacement via the applied ultimate load magnitude for B=8 m and L=8 m condition

The relationship between stress and displacement was obtained by considering the variations in slope heights with the aim of achieving different relative densities when B=8 m and L=16 m in Figure 4.30.

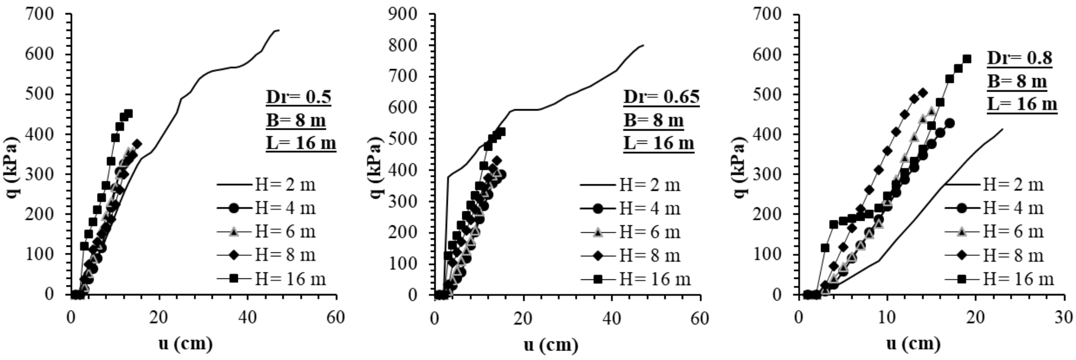

Figure 4.30. The change of displacement via the applied ultimate load magnitude for B=8 m and L= 16 m condition

The third step of the thesis work, which is the analysis of single footings within the slope, was carried out in a multivariate manner. However, for ease of comparison, the effect of varying slope heights was examined using a unit-width foundation element in different soil profiles. In this context, the safety numbers for the slope obtained from the analysis and the maximum load that can be carried by the foundation were presented in Table 4.5 Upon examining the table, it can be said that the safety number increases with an increase in relative density. However, when considering the varying slope heights, it is difficult to determine a specific rate of increase. When D_r=50%, an increase in slope height results in a relatively lower safety level for the slope. When looking at D_r=65%, there is a very high safety number at H=2 m. The increase in slope height has significant importance when considering this relative density value. Similarly, for D_r=80%, significant increases in safety numbers occur at H=2 m and H=4 m, while an increase in slope height results in a significant decrease in safety numbers. Additionally, at H=16 m, the safety number increases for D_r=80%. This suggests that the separation of failure mechanisms and the safety level of slope-foundation interactive systems may be attributed either to the potential failure of the slope or the mobilization of failure mechanisms under the loads imposed on the foundation.

Table 4.5. The safety numbers for the slope and the maximum load

	B= 1 m					
	D_r= 50%		D_r= 65%		D_r= 80%	
H (m)	FS_{slope}	q_{ult} (kPa)	FS_{slope}	q_{ult} (kPa)	FS_{slope}	q_{ult} (kPa)
2	1.602	73	15.338	98	11.6	137
4	1.441	78	1.867	103	8.02	144
6	1.461	63	1.541	94	1.584	129
8	1.412	82	1.483	122	1.611	163
16	1.329	73	1.437	102	2.222	141

In this step of the thesis, the mentioned conditions were examined by controlling incremental displacements of slopes at different heights but with the same relative density value in the safety phase. Figure 4.30 presents the possible critical failure planes for H = 2-4-6-8-16 m, corresponding to D_r= 50%. The foundation loads, assumed to act at the middle of the slope height, are considered when H = 2 m. In this case, the foundation induces a mobilization of a sliding plane that extends from the foundation to the toe, affecting the slope portion beneath the foundation.

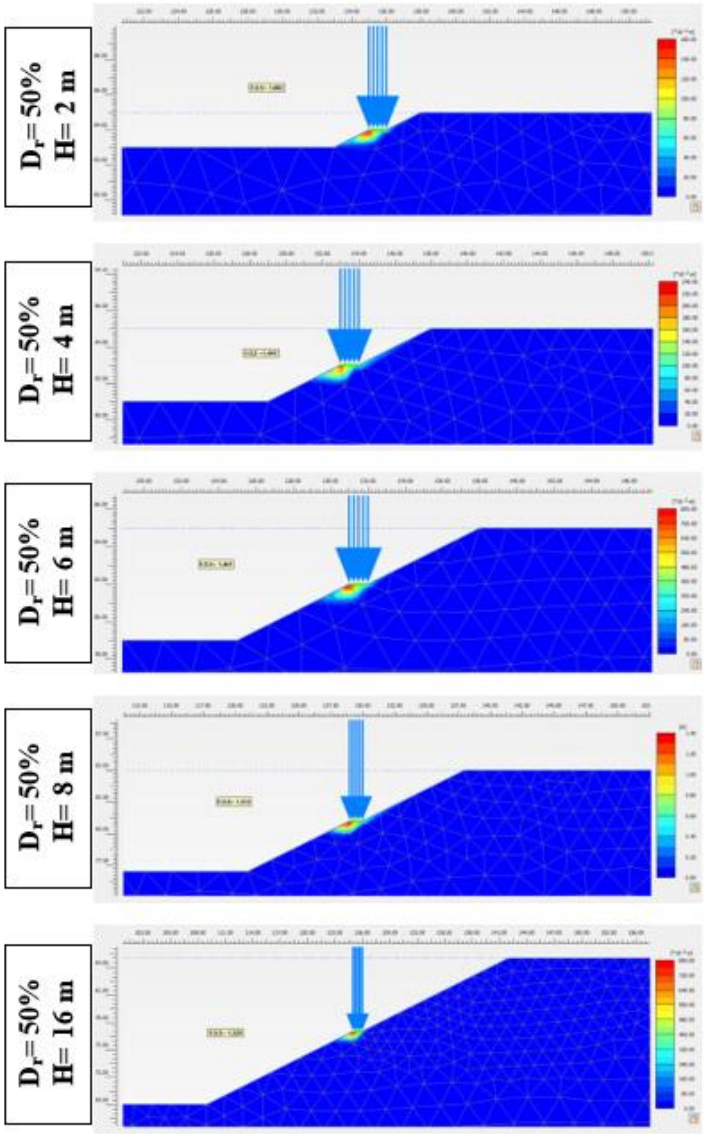

Figure 4.31. The possible critical failure planes for Dr=50%

When H= 4 meters, applying the load that brings the overall system to a safety factor of 1.0, the portion of the slope affected by the foundation loading has relatively decreased, leading to a decrease in deformation intensity. As the slope height continues to increase, there is an interactive behavior between the slope and the foundation, where the mechanism distributes from the foundation base towards the slope surface but primarily affects the upper portion of the slope in contact with the foundation.

In Figure 4.31, the same condition was investigated for D_r= 65%. When compared to the D_r = 50% case, it can be observed that the mobilized shear planes have expanded, transmitting their effects to the upper portion of the slope as well. However, in terms of the loads affecting the foundation, it can be evaluated that there is an increase in load intensity compared to $D_r = 50\%$, indicating an enhancement in the foundation's bearing capacity.

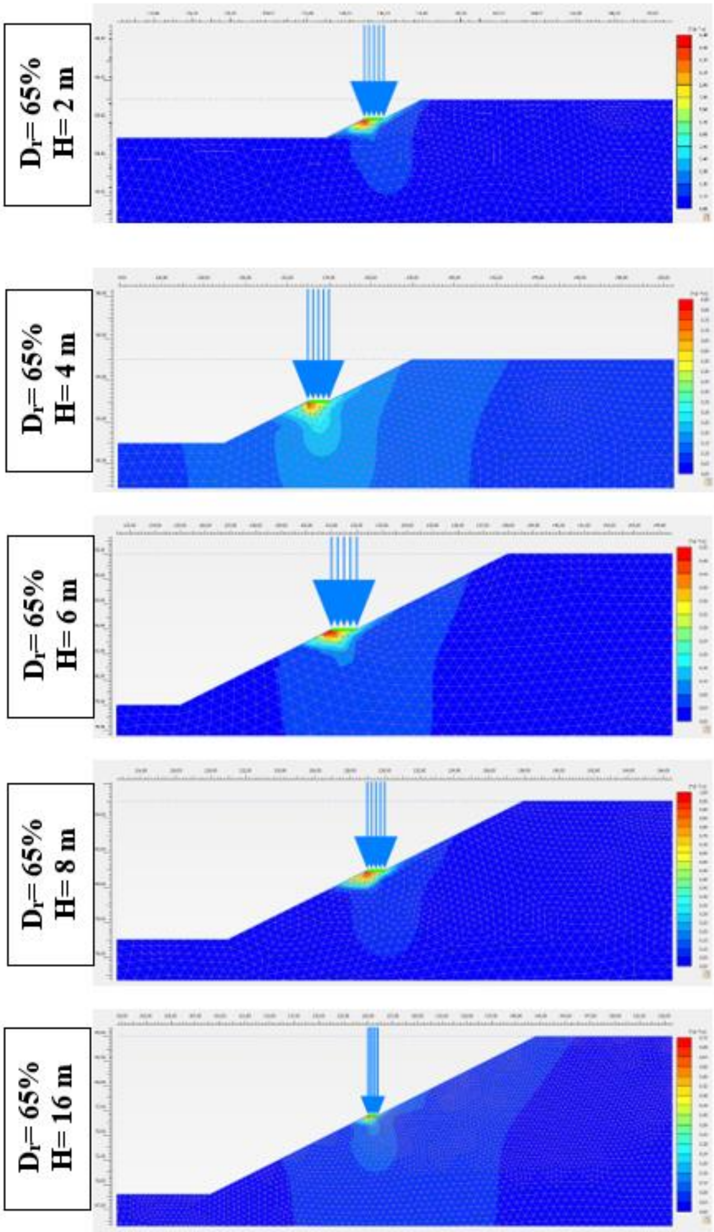

Figure 4.32. The possible critical failure planes for Dr=65%

In Figure 4.32, the condition of D_r = 80% was evaluated. As seen from Table ..., it can be observed that the load-bearing capacity has increased up to a height of H=16 m, but there is a slight decrease in capacity at H=16 m.

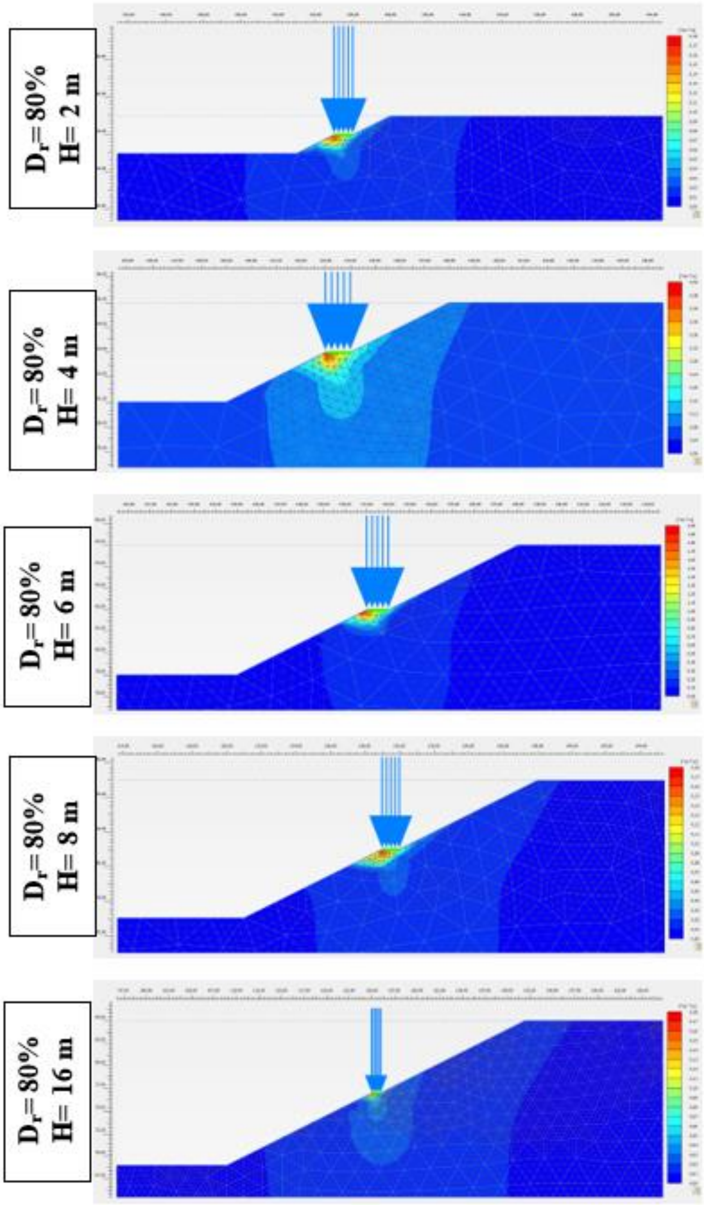

Figure 4.33. The possible critical failure planes for Dr=80%

The fourth step of the study involved analyzing adjacent foundations located on the slope. In this section, a different perspective was brought to the analysis. The number of analyzed foundations was doubled, and the maximum load capacities were determined through a trial and error method. Additionally, apart from the adjacent arrangement of the foundations, the analysis was repeated by spacing them at specific multiples of the foundation width.

Accordingly, the results have been presented in Table 4.6 for D_r=50%, Table 4.7 for D_r=65%, and Table 4.8 for D_r=80%.

Table 4.6. The analysis results of adjacent foundations located on the slope for D_r=50%

Dr = 50%

Constants	H=2 m			H=4 m			H=6 m			H=8 m			H=16 m		
L=0 m	FSslope	qult (kPa) F1	F2	FSslope	qult (kPa) F1	F2	FSslope	qult (kPa) F1	F2	FSslope	qult (kPa) F1	F2	FSslope	qult (kPa) F1	F2
Lf = 0 m	1.5	142	119	1.4	143	111	1.4	124	100	1.4	119	100	1.3	115	98
Lf = 1 m	1.5	65	61	1.4	63	58	1.4	63	56	1.4	61	56	1.3	60	55
Lf = 2 m	1.5	62	59	1.4	62	55	1.4	63	54	1.4	60	53	1.3	59	51
Lf = 4 m	1.5	58	53	1.4	60	52	1.4	61	53	1.4	58	51	1.3	57	49
Lf = 8 m	1.5	56	51	1.4	56	51	1.4	59	50	1.4	56	50	1.3	56	47
Lf = 16 m	1.5	52	48	1.4	56	48	1.4	57	47	1.4	55	50	1.3	54	46

Constants	H=2 m			H=4 m			H=6 m			H=8 m			H=16 m		
L=1 m	FSslope	qult (kPa) F1	F2	FSslope	qult (kPa) F1	F2	FSslope	qult (kPa) F1	F2	FSslope	qult (kPa) F1	F2	FSslope	qult (kPa) F1	F2
Lf = 0 m	1.5	231	216	1.4	219	210	1.4	212	200	1.4	198	187	1.3	190	184
Lf = 1 m	1.5	174	165	1.4	172	164	1.4	169	160	1.4	161	152	1.3	155	150
Lf = 2 m	1.5	172	161	1.4	165	161	1.4	159	158	1.4	156	152	1.3	153	143
Lf = 4 m	1.5	141	133	1.4	152	156	1.4	151	155	1.4	150	150	1.3	148	142
Lf = 8 m	1.5	139	130	1.4	151	150	1.4	149	150	1.4	147	149	1.3	146	141
Lf = 16 m	1.5	138	129	1.4	149	144	1.4	148	143	1.4	146	146	1.3	145	140

Constants	H=2 m			H=4 m			H=6 m			H=8 m			H=16 m		
L=2 m	FSslope	qult (kPa) F1	F2	FSslope	qult (kPa) F1	F2	FSslope	qult (kPa) F1	F2	FSslope	qult (kPa) F1	F2	FSslope	qult (kPa) F1	F2
Lf = 0 m	1.5	298	248	1.4	289	228	1.4	272	214	1.4	261	207	1.3	240	174
Lf = 1 m	1.5	264	248	1.4	261	232	1.4	249	217	1.4	242	211	1.3	227	180
Lf = 2 m	1.5	262	257	1.4	258	241	1.4	242	222	1.4	231	217	1.3	217	189
Lf = 4 m	1.5	259	269	1.4	246	245	1.4	229	227	1.4	224	221	1.3	210	200
Lf = 8 m	1.5	257	280	1.4	240	257	1.4	227	238	1.4	219	229	1.4	205	213
Lf = 16 m	1.5	245	280	1.4	238	268	1.4	215	241	1.4	214	238	1.3	203	228

Constants	H=2 m			H=4 m			H=6 m			H=8 m			H=16 m		
L=4 m	FSslope	qult (kPa) F1	F2	FSslope	qult (kPa) F1	F2	FSslope	qult (kPa) F1	F2	FSslope	qult (kPa) F1	F2	FSslope	qult (kPa) F1	F2
Lf = 0 m	1.5	374	341	1.4	362	334	1.4	354	325	1.4	348	317	1.3	336	305
Lf = 1 m	1.5	313	331	1.4	338	320	1.4	329	312	1.4	314	282	1.3	312	275
Lf = 2 m	1.5	307	316	1.4	331	309	1.4	324	303	1.4	312	275	1.3	298	264
Lf = 4 m	1.5	292	282	1.4	326	299	1.4	322	297	1.4	309	272	1.3	284	255
Lf = 8 m	1.5	281	269	1.4	322	293	1.4	319	288	1.4	298	264	1.3	277	243
Lf = 16 m	1.5	275	256	1.4	320	288	1.4	314	283	1.4	284	253	1.3	273	237

Constants	H=2 m			H=4 m			H=6 m			H=8 m			H=16 m		
L=8 m	FSslope	qult (kPa) F1	F2	FSslope	qult (kPa) F1	F2	FSslope	qult (kPa) F1	F2	FSslope	qult (kPa) F1	F2	FSslope	qult (kPa) F1	F2
Lf = 0 m	1.5	450	423	1.4	441	418	1.4	424	408	1.4	419	397	1.3	416	378
Lf = 1 m	1.5	288	225	1.4	286	222	1.4	293	235	1.4	302	258	1.3	322	266
Lf = 2 m	1.5	286	220	1.4	284	218	1.4	283	217	1.4	280	241	1.3	277	254
Lf = 4 m	1.5	282	213	1.4	279	216	1.4	281	213	1.4	273	226	1.4	275	249
Lf = 8 m	1.5	279	210	1.4	276	213	1.4	278	210	1.4	269	219	1.3	275	246
Lf = 16 m	1.5	277	209	1.4	275	212	1.4	277	209	1.4	267	216	1.3	272	242

Constants	H=2 m			H=4 m			H=6 m			H=8 m			H=16 m		
L=16 m	FSslope	qult (kPa) F1	F2	FSslope	qult (kPa) F1	F2	FSslope	qult (kPa) F1	F2	FSslope	qult (kPa) F1	F2	FSslope	qult (kPa) F1	F2
Lf = 0 m	1.5	526	449	1.4	493	421	1.4	470	404	1.4	443	381	1.3	429	367
Lf = 1 m	1.5	317	227	1.4	353	268	1.4	368	281	1.4	346	253	1.3	322	236
Lf = 2 m	1.5	314	221	1.4	339	245	1.4	342	251	1.4	325	239	1.3	312	217
Lf = 4 m	1.5	296	203	1.4	318	219	1.4	300	240	1.4	317	224	1.3	304	200
Lf = 8 m	1.5	292	197	1.4	302	211	1.4	296	217	1.4	306	216	1.3	289	184
Lf = 16 m	1.5	280	174	1.4	294	207	1.4	293	202	1.4	295	186	1.4	283	175

Table 4.7. The analysis results of adjacent foundations located on the slope for Dr=65%

Dr = 65%

Constants	H=2 m			H=4 m			H=6 m			H=8 m			H=16 m		
L=0 m	FSslope	qult (kPa) F1	qult (kPa) F2	FSslope	qult (kPa) F1	qult (kPa) F2	FSslope	qult (kPa) F1	qult (kPa) F2	FSslope	qult (kPa) F1	qult (kPa) F2	FSslope	qult (kPa) F1	qult (kPa) F2
Lf = 0 m	1.7	157	129	1.5	177	151	1.5	161	124	1.5	156	118	1.4	139	116
Lf = 1 m	1.7	98	91	1.5	100	89	1.5	99	83	1.5	96	85	1.4	93	88
Lf = 2 m	1.7	84	77	1.5	94	82	1.5	91	69	1.5	89	75	1.4	89	75
Lf = 4 m	1.7	93	83	1.5	98	86	1.5	101	68	1.5	94	73	1.4	91	81
Lf = 8 m	1.7	95	80	1.5	87	74	1.5	95	64	1.5	92	71	1.4	87	79
Lf = 16 m	1.7	95	74	1.5	109	85	1.5	93	90	1.5	93	95	1.4	89	91

Constants	H=2 m			H=4 m			H=6 m			H=8 m			H=16 m		
L=1 m	FSslope	qult (kPa) F1	qult (kPa) F2	FSslope	qult (kPa) F1	qult (kPa) F2	FSslope	qult (kPa) F1	qult (kPa) F2	FSslope	qult (kPa) F1	qult (kPa) F2	FSslope	qult (kPa) F1	qult (kPa) F2
Lf = 0 m	1.7	244	237	1.5	234	229	1.5	227	204	1.5	212	173	1.4	205	193
Lf = 1 m	1.7	226	217	1.5	231	231	1.5	217	209	1.5	178	175	1.4	202	197
Lf = 2 m	1.7	217	209	1.5	227	237	1.5	211	218	1.5	169	180	1.4	195	207
Lf = 4 m	1.7	196	204	1.5	194	240	1.5	204	227	1.5	167	186	1.4	176	220
Lf = 8 m	1.7	191	198	1.5	191	259	1.5	197	249	1.5	163	194	1.4	176	257
Lf = 16 m	1.7	204	263	1.5	184	273	1.5	197	283	1.5	157	229	1.4	173	293

Constants	H=2 m			H=4 m			H=6 m			H=8 m			H=16 m		
L=2 m	FSslope	qult (kPa) F1	qult (kPa) F2	FSslope	qult (kPa) F1	qult (kPa) F2	FSslope	qult (kPa) F1	qult (kPa) F2	FSslope	qult (kPa) F1	qult (kPa) F2	FSslope	qult (kPa) F1	qult (kPa) F2
Lf = 0 m	1.7	319	264	1.5	312	249	1.5	308	232	1.5	300	218	1.4	289	234
Lf = 1 m	1.7	313	267	1.5	309	263	1.5	297	238	1.5	284	222	1.4	272	243
Lf = 2 m	1.7	305	273	1.5	301	278	1.5	294	253	1.5	274	231	1.4	272	265
Lf = 4 m	1.7	299	280	1.5	294	292	1.5	283	269	1.5	269	242	1.4	259	287
Lf = 8 m	1.7	283	301	1.5	290	311	1.5	277	289	1.5	261	260	1.4	253	309
Lf = 16 m	1.7	257	316	1.5	278	333	1.5	243	308	1.5	255	293	1.4	241	336

Constants	H=2 m			H=4 m			H=6 m			H=8 m			H=16 m		
L=4 m	FSslope	qult (kPa) F1	qult (kPa) F2	FSslope	qult (kPa) F1	qult (kPa) F2	FSslope	qult (kPa) F1	qult (kPa) F2	FSslope	qult (kPa) F1	qult (kPa) F2	FSslope	qult (kPa) F1	qult (kPa) F2
Lf = 0 m	1.7	421	389	1.5	412	371	1.5	407	362	1.5	399	358	1.4	386	341
Lf = 1 m	1.7	397	395	1.5	408	379	1.5	404	370	1.5	388	362	1.4	384	350
Lf = 2 m	1.7	329	373	1.5	399	393	1.5	398	379	1.5	382	369	1.4	373	362
Lf = 4 m	1.7	290	352	1.5	376	410	1.5	384	407	1.5	375	379	1.4	360	381
Lf = 8 m	1.7	269	331	1.5	362	434	1.5	379	435	1.5	361	386	1.4	344	398
Lf = 16 m	1.7	257	329	1.5	349	468	1.5	346	435	1.5	347	402	1.4	326	433

Constants	H=2 m			H=4 m			H=6 m			H=8 m			H=16 m		
L=8 m	FSslope	qult (kPa) F1	qult (kPa) F2	FSslope	qult (kPa) F1	qult (kPa) F2	FSslope	qult (kPa) F1	qult (kPa) F2	FSslope	qult (kPa) F1	qult (kPa) F2	FSslope	qult (kPa) F1	qult (kPa) F2
Lf = 0 m	1.7	557	482	1.5	532	429	1.5	526	398	1.4	513	391	1.4	511	379
Lf = 1 m	1.7	355	390	1.5	417	431	1.5	443	379	1.5	473	385	1.4	439	351
Lf = 2 m	1.7	345	384	1.5	405	438	1.5	430	368	1.5	439	371	1.4	433	342
Lf = 4 m	1.7	334	351	1.5	378	455	1.5	421	350	1.5	430	356	1.4	419	334
Lf = 8 m	1.7	327	339	1.5	239	441	1.5	406	337	1.5	411	350	1.4	397	310
Lf = 16 m	1.7	323	339	1.5	227	425	1.5	399	335	1.4	386	339	1.4	362	294

Constants	H=2 m			H=4 m			H=6 m			H=8 m			H=16 m		
L=16 m	FSslope	qult (kPa) F1	qult (kPa) F2	FSslope	qult (kPa) F1	qult (kPa) F2	FSslope	qult (kPa) F1	qult (kPa) F2	FSslope	qult (kPa) F1	qult (kPa) F2	FSslope	qult (kPa) F1	qult (kPa) F2
Lf = 0 m	1.7	713	617	1.5	634	582	1.5	599	546	1.5	551	519	1.4	521	457
Lf = 1 m	1.7	441	209	1.5	431	198	1.5	427	347	1.5	423	340	1.4	418	376
Lf = 2 m	1.7	437	200	1.5	422	181	1.5	419	333	1.5	415	329	1.4	403	362
Lf = 4 m	1.7	391	184	1.5	416	175	1.5	407	325	1.5	401	320	1.4	374	341
Lf = 8 m	1.7	369	171	1.5	400	163	1.5	395	319	1.5	388	309	1.4	336	322
Lf = 16 m	1.7	369	150	1.5	381	159	1.5	391	316	1.5	372	300	1.4	314	300

Table 4.8. The analysis results of adjacent foundations located on the slope for Dr=80%

Dr = 80%

Constants	H=2 m			H=4 m			H=6 m			H=8 m			H=16 m		
L=0 m	FSslope	qult (kPa) F1	F2	FSslope	qult (kPa) F1	F2	FSslope	qult (kPa) F1	F2	FSslope	qult (kPa) F1	F2	FSslope	qult (kPa) F1	F2
Lf = 0 m	1.7	214	148	1.7	211	140	1.6	207	137	1.5	202	137	1.5	194	129
Lf = 1 m	1.7	144	148	1.7	135	147	1.6	143	150	1.5	132	153	1.5	130	136
Lf = 2 m	1.7	119	153	1.7	121	172	1.6	126	172	1.5	129	165	1.5	127	151
Lf = 4 m	1.7	111	191	1.7	118	189	1.6	123	181	1.5	125	179	1.5	127	165
Lf = 8 m	1.7	108	209	1.7	110	203	1.6	119	201	1.5	124	191	1.5	116	188
Lf = 16 m	1.7	107	238	1.7	116	231	1.6	119	242	1.5	120	233	1.5	112	227

Constants	H=2 m			H=4 m			H=6 m			H=8 m			H=16 m		
L=1 m	FSslope	qult (kPa) F1	F2	FSslope	qult (kPa) F1	F2	FSslope	qult (kPa) F1	F2	FSslope	qult (kPa) F1	F2	FSslope	qult (kPa) F1	F2
Lf = 0 m	1.7	337	267	1.7	334	256	1.6	329	250	1.5	294	136	1.5	271	181
Lf = 1 m	1.7	249	269	1.7	244	262	1.6	301	250	1.5	231	136	1.5	248	189
Lf = 2 m	1.7	245	278	1.7	241	274	1.6	287	257	1.5	228	147	1.5	244	196
Lf = 4 m	1.7	243	285	1.7	235	291	1.6	282	268	1.5	226	161	1.5	236	204
Lf = 8 m	1.7	238	300	1.7	235	303	1.6	278	291	1.5	222	199	1.5	233	218
Lf = 16 m	1.7	237	352	1.7	232	360	1.6	269	345	1.5	216	263	1.5	232	243

Constants	H=2 m			H=4 m			H=6 m			H=8 m			H=16 m		
L=2 m	FSslope	qult (kPa) F1	F2	FSslope	qult (kPa) F1	F2	FSslope	qult (kPa) F1	F2	FSslope	qult (kPa) F1	F2	FSslope	qult (kPa) F1	F2
Lf = 0 m	1.7	377	338	1.7	342	316	1.6	339	309	1.5	338	305	1.5	335	298
Lf = 1 m	1.7	374	347	1.7	339	321	1.6	336	315	1.5	338	312	1.5	278	208
Lf = 2 m	1.7	370	359	1.7	335	330	1.6	334	337	1.5	332	324	1.5	326	331
Lf = 4 m	1.7	364	364	1.7	329	347	1.6	330	359	1.5	328	338	1.5	323	347
Lf = 8 m	1.7	363	398	1.7	322	364	1.6	328	384	1.5	321	355	1.5	322	362
Lf = 16 m	1.7	339	436	1.7	320	396	1.6	294	399	1.5	314	387	1.5	318	389

Constants	H=2 m			H=4 m			H=6 m			H=8 m			H=16 m		
L=4 m	FSslope	qult (kPa) F1	F2	FSslope	qult (kPa) F1	F2	FSslope	qult (kPa) F1	F2	FSslope	qult (kPa) F1	F2	FSslope	qult (kPa) F1	F2
Lf = 0 m	1.7	523	444	1.7	507	428	1.6	500	411	1.5	491	400	1.5	479	383
Lf = 1 m	1.7	469	444	1.7	497	435	1.6	498	420	1.5	489	408	1.5	477	395
Lf = 2 m	1.7	417	455	1.7	494	446	1.6	494	432	1.5	484	419	1.5	473	409
Lf = 4 m	1.7	404	467	1.7	492	459	1.6	488	445	1.5	482	436	1.5	466	430
Lf = 8 m	1.7	400	483	1.7	488	472	1.6	480	468	1.5	476	453	1.5	462	464
Lf = 16 m	1.7	398	502	1.7	487	497	1.6	477	493	1.5	474	485	1.5	460	499

Constants	H=2 m			H=4 m			H=6 m			H=8 m			H=16 m		
L=8 m	FSslope	qult (kPa) F1	F2	FSslope	qult (kPa) F1	F2	FSslope	qult (kPa) F1	F2	FSslope	qult (kPa) F1	F2	FSslope	qult (kPa) F1	F2
Lf = 0 m	1.7	598	514	1.7	449	337	1.6	581	493	1.5	576	485	1.5	564	471
Lf = 1 m	1.7	531	519	1.7	493	379	1.6	490	375	1.5	523	488	1.5	558	483
Lf = 2 m	1.7	523	527	1.7	489	392	1.6	487	386	1.5	514	494	1.5	531	483
Lf = 4 m	1.7	519	540	1.7	487	406	1.6	477	398	1.5	510	506	1.5	529	496
Lf = 8 m	1.7	507	559	1.7	481	429	1.6	473	417	1.5	507	521	1.5	524	508
Lf = 16 m	1.7	492	573	1.7	480	455	1.6	473	440	1.5	497	543	1.5	327	358

Constants	H=2 m			H=4 m			H=6 m			H=8 m			H=16 m		
L=16 m	FSslope	qult (kPa) F1	F2	FSslope	qult (kPa) F1	F2	FSslope	qult (kPa) F1	F2	FSslope	qult (kPa) F1	F2	FSslope	qult (kPa) F1	F2
Lf = 0 m	1.7	761	637	1.7	436	351	1.6	653	569	1.5	632	537	1.5	616	499
Lf = 1 m	1.7	518	401	1.7	507	386	1.6	504	379	1.5	489	354	1.5	477	345
Lf = 2 m	1.7	514	379	1.7	504	377	1.6	487	376	1.5	472	351	1.5	461	342
Lf = 4 m	1.7	507	363	1.7	498	363	1.6	472	368	1.5	463	345	1.5	453	336
Lf = 8 m	1.7	499	357	1.7	495	349	1.6	465	353	1.5	457	332	1.5	449	328
Lf = 16 m	1.7	490	356	1.7	494	332	1.6	463	340	1.5	455	319	1.5	448	318

In the presented tables, it can be observed that there is a slight decrease in the safety factor with increasing slope height in all cases. This trend indicates that higher slope heights have a slight adverse impact on slope stability. Furthermore, the effect of varying relative density of the soil can be observed through an increase in the factor of safety of the slope as the relative density increases. This finding highlights the significance of relative density in influencing slope stability, with higher relative density contributing to improved safety. It should be emphasized once again that the safety factor analyses are applicable only to the slope and do not consider any structures present. After the incorporation of structures, loading values that bring the safety factor to its limit are used in design to interpret the mobilized shear planes and ultimate bearing capacity values in such cases. The influence of increasing soil-bearing capacity can be observed in the form of an increase in the ultimate load, assuming all other variables remain constant except for relative density. Additionally, moving away bases from the top of the slope results in an increase in the ultimate load in all cases. This effect occurs because the influence of load on slope stability diminishes as the distance from the slope increases. Conversely, the negative impact of slope height on bearing capacity is evident through a decrease in the ultimate load applied to the analysis cases. Higher slope heights are associated with reduced bearing capacity, leading to a lower ultimate load capacity. On the other hand, the distance between adjacent bases significantly affects the total ultimate load. When foundations are positioned close to each other, they behave as a single foundation with a unified field of influence and stress. Increasing the distance between bases results in the overlapping of two stress fields, diminishing slope stability and reducing the total ultimate load. The impact of this stress field overlap gradually diminishes with an increase in the distance between the two bases. In fact, it is observed that the load applied to the second base F2 increases in the last case at each height.

In order to bring a different interpretation to the case under consideration, some special scenarios were classified, and possible critical failure planes were obtained from the incremental displacements section of the analysis in the safety phase. Different sections with the same geometry and soil conditions were modeled for each distinct relative density value. Figure 4.34, is obtained for D_r=50%, Figure 4.35, for D_r=65%, and Figure 4.36, for D_r=80%. These figures are numbered sequentially up to ten (10). Case number one (1) is selected as the reference case for each figure, and possible critical failure planes are obtained by varying the parameters in each analysis. In the figures, the parameters used differently from the reference section are underlined. Additionally, in the case of a dual foundation system located on the slope, the maximum load values, or in other words, the foundation bearing capacity values that will cause the foundations to reach failure, are individually written on the figure. The characteristics of the section where the reference analysis represented by number one will be applied are chosen as follows: B=1 m, H=2 m, L=0, and L_f=0. In the second analysis represented by number 2, the interaction distance between the slope and the foundation, L, is increased to 8 m. In the third analysis represented by number 3, L is set to 8 m and the distance between the two foundations, L_f, is increased to 2 m. In the fourth analysis represented by number 4, L is set to 8 m and L_f is increased to 8 m, where the distance between the two foundations is 8 times the foundation dimension. In the fifth analysis represented by number 5, L is set to 0 and L_f is set to 2 meters. In the sixth analysis represented by number 6, the slope height, H, is increased to 8 m. In the seventh analysis represented by number 7, H is set to 8 m, L is set to 8 m, and L_f is set to 0. In the eighth analysis represented by number 8, the L_f dimension is modified to 2 m compared to the previous analysis. In the ninth analysis represented by number 9, the L_f distance is increased to 8 m. As for the tenth and final analysis, represented by number 10, H is set to 8m, L is set to 0 m, and L_f is set to 2 m. The same approach was followed for analyzing different relative density values, and the results are presented in consecutive figures. When the reference case is examined, a mobilized mechanism is observed due to the loads originating from the foundations for the contiguous foundation placed on the slope crest. However, due to the low height of the slope, a comprehensive mechanism has been activated, starting with the foundation bearing capacity issue and continuing with the questioning of slope stability, encompassing the slope as well. In case number 2, due to the increased interaction distance between the slope and the foundation, the load-bearing capacity of the foundations has increased by a ratio of approximately three times compared to case 1. The problem in the overall stability of the system has arisen solely from the foundation bearing capacity. The foundations have acted similar to the neighboring foundation located on the horizontal soil layers, and the slope stability issue has not affected the integrated system stability. In case number 3, both the change in slope-foundation interaction distance and the separation of the foundations from each other are present. In this scenario, the double foundation, which behaved as a rigid plate in case 2, has split into two separate parts and moved apart. The load-bearing capacity of the foundations has decreased, and a settlement mechanism that reduces the safety factor to 1.0 has been mobilized under excessive loading on one of the foundations. This situation still does not have an impact on slope stability. It simply presents a scenario that can be interpreted as the analysis of two different buildings interacting with each other on a horizontal soil layering. The result of the analysis indicates that the foundation-slope interaction distance, which is eight times the width of the foundation, is not an effective distance for the desired structure-foundation interaction being examined. Additionally, in case 4, the distance between the two foundations is also 8 meters. In this case, although the ultimate load-bearing capacities of the foundations do not change significantly, there is no longer any foundation-to-foundation interaction. In case number 5, only the interaction distance between the foundations has been changed compared to the reference case. In case number 6, once again, two foundations are positioned on the slope crest as contiguous foundations, with a height of 8 meters. The varying factor compared to the reference case is the height of the slope. In this case, the load-bearing capacity of the foundations has decreased compared to the reference case.

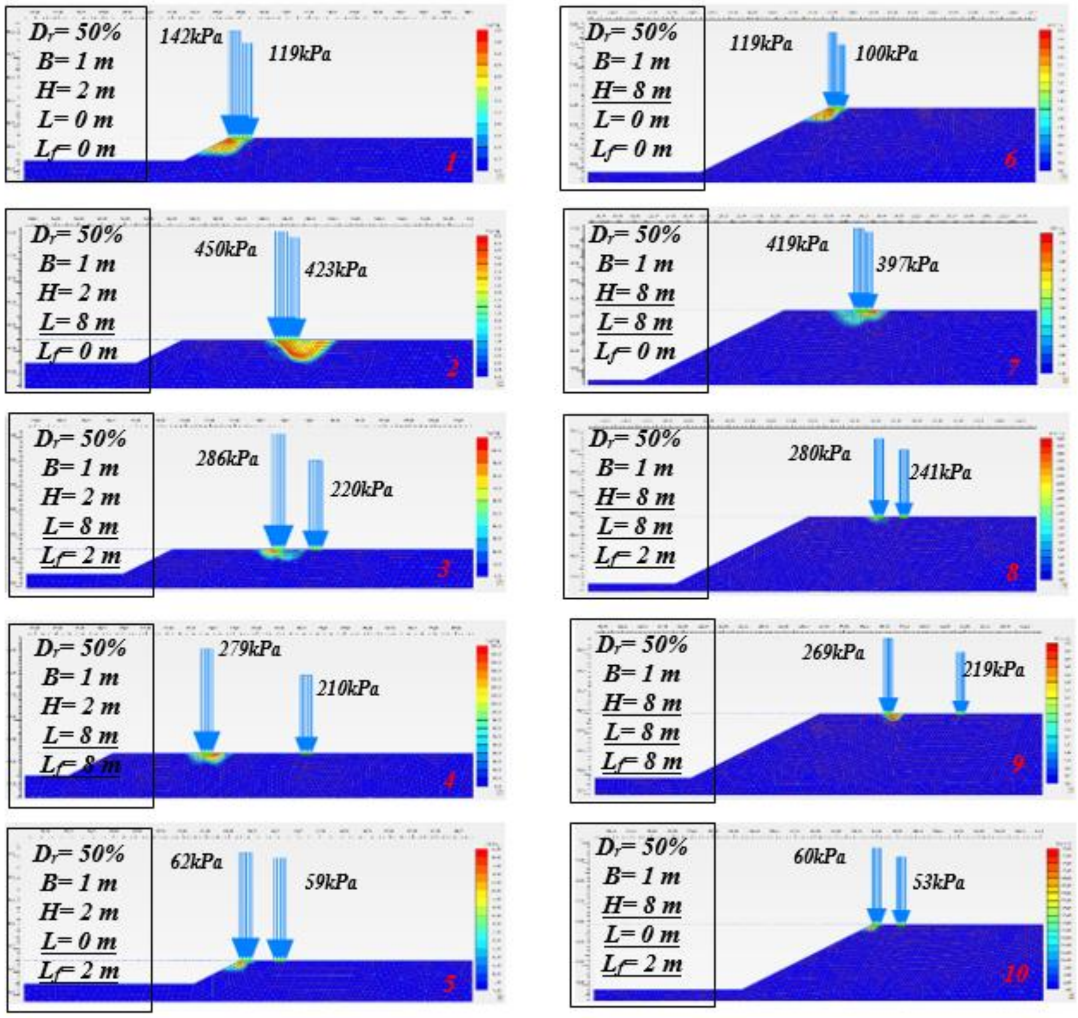

Figure 4.34. Different sections for foundations on slope with the same geometry and soil conditions for D_r=50%

A similar mechanism to the reference case is observed. The settlement behavior, which initially starts from the foundation bearing capacity, is spreading towards the slope, but it has not spread to the entire area due to the height of the slope. In case number 7, in addition to the height of the slope, the distances between the foundations and the slope have been changed. Upon examining this situation, it can be concluded that similar to case 2, the load-bearing capacity has increased, and the slope stability is not affected by the foundation loads. In case number 8, the analysis focuses on the separation of the foundations from the slope crest and from each other. It is observed that in this scenario, compared to the reference case, the load-bearing capacity values have increased. However, when compared to case 3, which was designed with the same logic but with a lower slope height, it can be said that the load-bearing capacities have slightly decreased. In case number 9, the foundations have been separated by a distance of 8 meters. In this case, the load-bearing capacities remain similar to the previous case, case 8. This result can be attributed to the fact that the foundation dimensions are 1 meter, resulting in the distance between the foundations that affects each other being less than twice the foundation width. In case number 10, the separated foundations placed on the slope crest are the focus of the problem. In this scenario, compared to the reference case, the load-bearing capacities have decreased. However, this decrease has occurred relatively independently of the slope height. This observation is a specific evaluation that can be made only for this particular case when comparing it with case 5. Indeed, the ultimate load capacities in case 5 and case 10 are of similar magnitudes, and it cannot be argued that a settlement mechanism triggered by slope stability is present.

In Figure 4.35, the same cases were analyzed for D_r = 65%. When comparing the cases internally, it was observed that similar behaviors and proportional load-carrying capacity values were obtained with a D_r= 50%. As the relative density of the sandy soil increased, the foundations' ultimate load-carrying capacities also increased due to the corresponding increase in stiffness properties and strength parameter values.

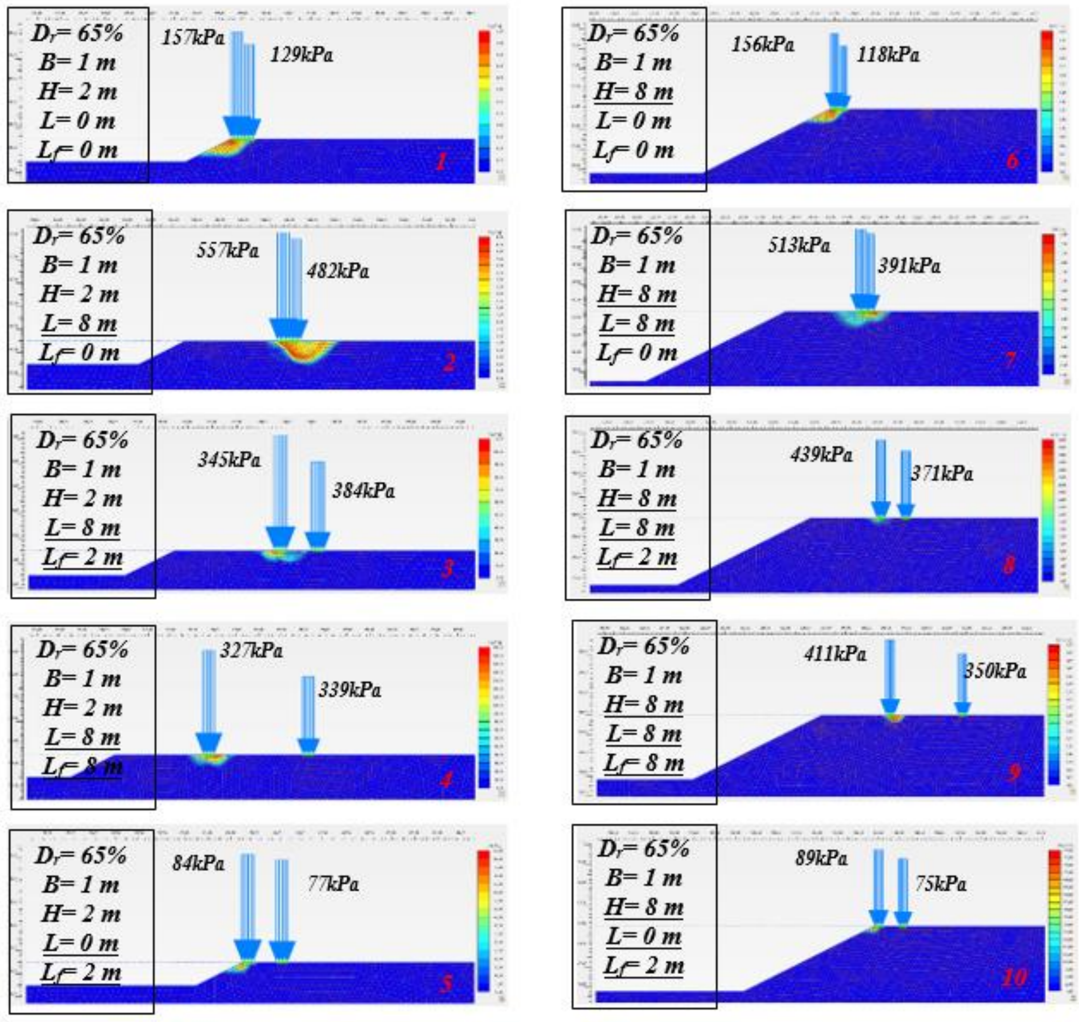

Figure 4.35. Different sections for foundations on slope with the same geometry and soil conditions for Dr=65%

In addition, analysis results for D_r=80% are provided in Figure 4.36, In this case, similar qualitative failure mechanisms were observed in the analyses conducted for the soil profiles created using D_r=65% and D_r=50% values. However, when compared to D_r=50%, the load-bearing capacities of the foundations have significantly increased for the D_r=80% condition. From the representations created for the purpose of predicting the differences in behavior due to changes in soil properties, it can be understood that the shape of possible critical failure planes mobilized in the foundations or the influence of the soil on triggering forces appears to be relatively low. Although the change in soil formation affects the level of load-bearing capacity and safety factor values of the foundations, the triggering effects of mechanism formation remain similar for 1-meter-wide foundations that are thought to be suddenly loaded under undrained conditions.

Considering the cases analyzed within the scope of the thesis study, it can be observed that the mechanisms activated are primarily due to the load-bearing capacity when the foundation-slope interaction distance is small, which subsequently affects the slope and leads to failure. However, when the foundation-slope interaction distance exceeds twice the foundation width, it can be evaluated that the effects caused by load-bearing capacity would not have an impact on an already stable slope. It has to be noted that this interpretation provided is based on the information provided in the question, and the technical details and context may vary. It is always recommended to consult with relevant experts for a comprehensive analysis and evaluation of specific cases.

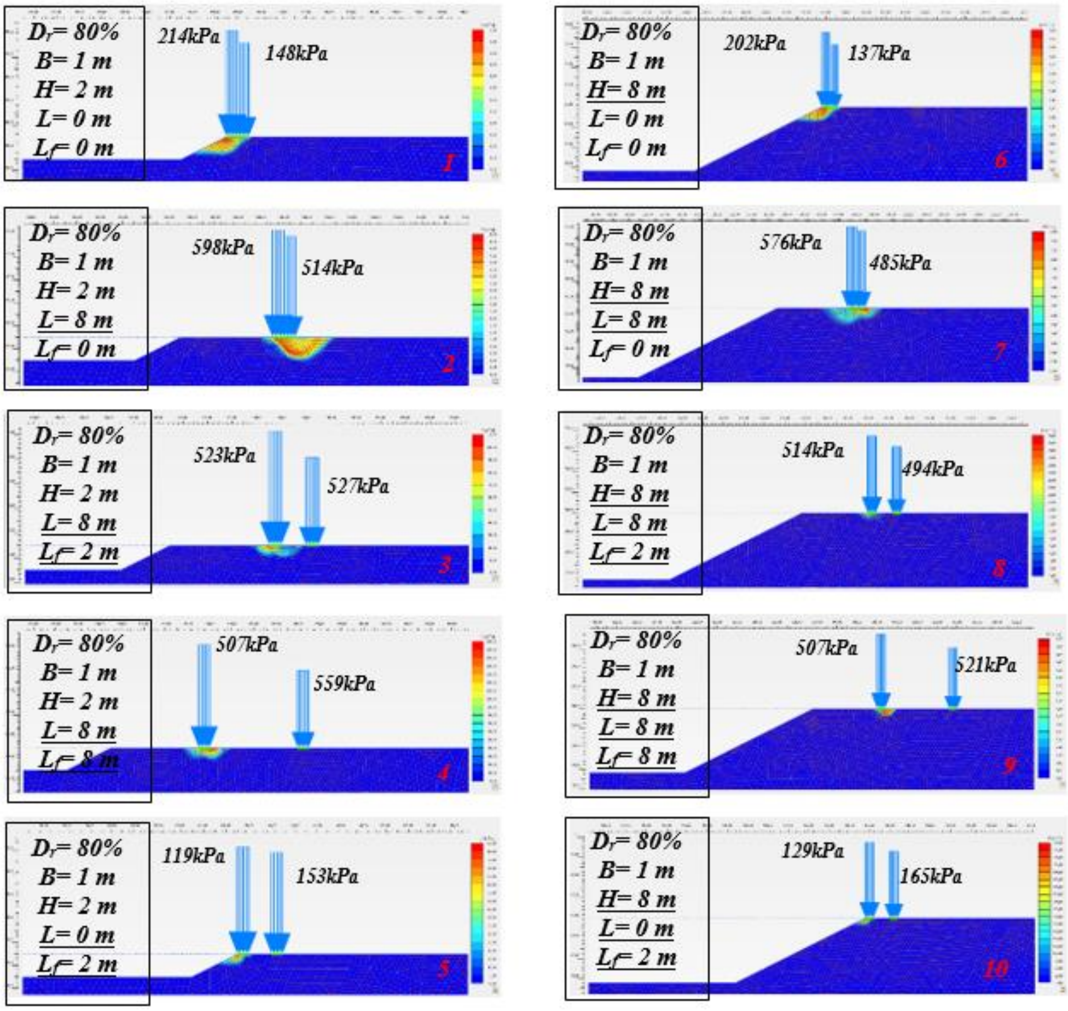

Figure 4.36. Different sections for foundations on slope with the same geometry and soil conditions for Dr=80%

The last step of the study is to analyze double foundations resting in the sloped ground. Analyzes mentioned in Figure 4.37, were conducted for multiple foundations within the slope.

Below, some details of these analyses are compiled and presented for the purpose of comparison. In this context, the analysis of two adjacent shallow foundations within the slope has been conducted. The foundations are positioned at coordinates corresponding to half of the slope height. The distance between the two adjacent foundations has been varied in the analyzed cases, but the relevant distance is evaluated horizontally. In other words, the structures have been constructed between two slopes that have the same inclination. Below, three comparative figures have been constructed based on the variations in D_r. Figure 4.37, represents the reference case with D_r=50%, B=1 m, H=2 m, and L_f=0 m. The other cases are interpreted with changes in these parameters. In Case 1, adjacent contiguous foundations have been used, and the lower portion of the 2-meter slope height, which remains at a height of 1 meter, is fully influenced by the foundation loads. The combination of the 1-meter portion of the slope and the foundation has led to the mobilization of the slope failure mechanism. The presence of the foundation load, combined with the slope geometry and characteristics, has influenced the stability of the slope and triggered the mobilization of the failure mechanism.

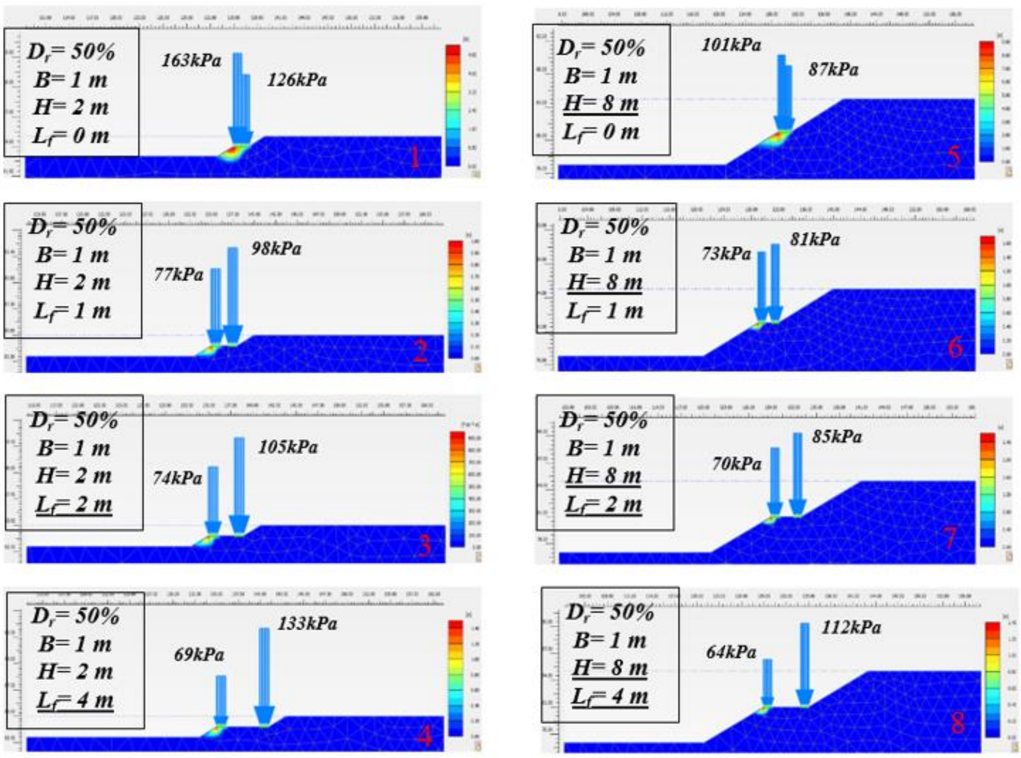

Figure 4.37. Different sections for foundations within slope with the same geometry and soil conditions for Dr=50%

In the second case, increasing the distance between the foundations to 1 meter has resulted in a decrease in the load-carrying capacity of the foundations. However, a similar mechanism as in the first case has led to the formation of a failure plane caused by the adjacent foundation interacting with the slope. Despite the reduced load capacity, the interaction between the foundation and the slope has still triggered the mobilization of the failure mechanism. In the third and fourth cases, an increase in the distance between the foundations is observed. This situation has reduced the interaction between the two foundations, and the triggering mechanism that is active originates from the first foundation, affecting the first step of the slope. When examining the cases 5, 6, 7, and 8 in Figure 4.38, it can be observed that the situation occurs independently of the change in slope height and the shape of the failure mechanism remains consistent with an increase in the interaction distance between the foundations. In Figure 4.38, the condition of D_r = 65% has been evaluated.

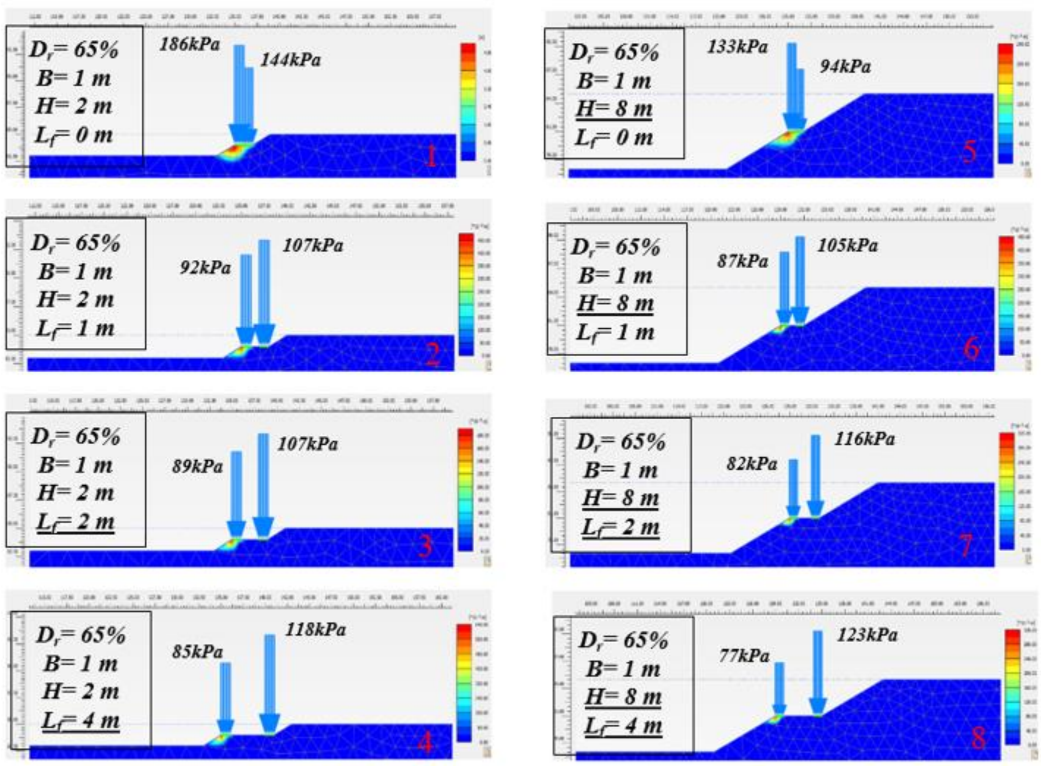

Figure 4.38. Different sections for foundations within slope with the same geometry and soil conditions for Dr=65%

When comparing the D_r = 65% condition in Figure 4.38, with the D_r = 50% condition, it can be observed that the magnitude of the ultimate bearing capacity of the foundations has increased for both foundations. However, in terms of the activated shear mechanisms, the contributions of the first and second foundations to the mobilized mechanism show similar characteristics to those observed in the Dr = 50% case. The cases with D_r = 80% were examined in Figure 4,39.

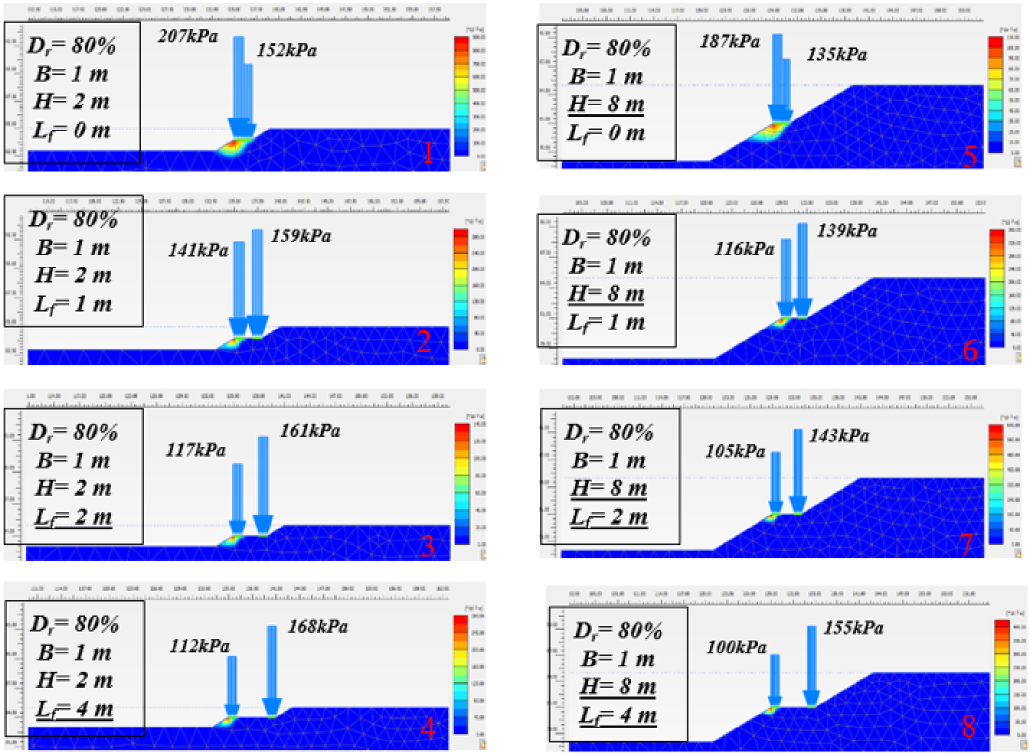

Figure 4.39. Different sections for foundations within slope with the same geometry and soil conditions for Dr=80%

The mechanism formation in Figure 4.37, and Figure 4.39, is the same, and the ultimate bearing capacity of the foundations has increased as expected due to the increase in shear strength parameters.

5. DISCUSSION

Previous research studies on the design of a foundation on or within a slope have primarily focused on the ultimate bearing capacity and settlement characteristics of the foundation. However, the behavior of a foundation on or within a slope is governed by either the bearing capacity of the foundation or the stability of the slope. An integrated approach that combines foundation bearing capacity behavior with slope stability analysis facilitates the design and analysis of a foundation-slope interactive system. In this context, the use of numerical analysis programs as tools for solving complex system geometries and design parameters has become a commonly employed method. This allows for time savings compared to manual design processes. Additionally, the evaluation of parametric analysis results using numerical analysis program outputs can provide valuable insights for designers to address potential issues they may encounter. The objective of this thesis is to interpret and analyze effective parameters in the design process by approaching slope-foundation interaction analysis from different perspectives. Within this scope, scenarios have been developed and analyzed for single and multiple foundations located within and on the slope, starting with slope stability analyses. The results determine the load levels that bring the slope-foundation system to its limit state and evaluate the relationship between slope and foundation parameters. Factors such as soil properties, foundation locations and numbers, interaction distances, and ultimate foundation bearing capacity values are taken into consideration. Furthermore, activation models of failure surfaces mobilized depending on the foundation locations and the applied ultimate foundation pressure have been analyzed. When evaluating the existing literature, it can be observed that there are limited studies that closely resemble this thesis in terms of their approach to interpreting the slope-foundation system with detailed parameters and interactive neighboring foundation analyses. In this context, for the guidance of designers and researchers, some of the results obtained within the scope of this thesis are comparatively interpreted below as specific cases.

The first comparative case examines the presence of a shallow foundation on the slope. In this case, different positioning of a single shallow foundation with a width of B=1 m, relative density of 65%, and the same slope height on a sandy soil is investigated.

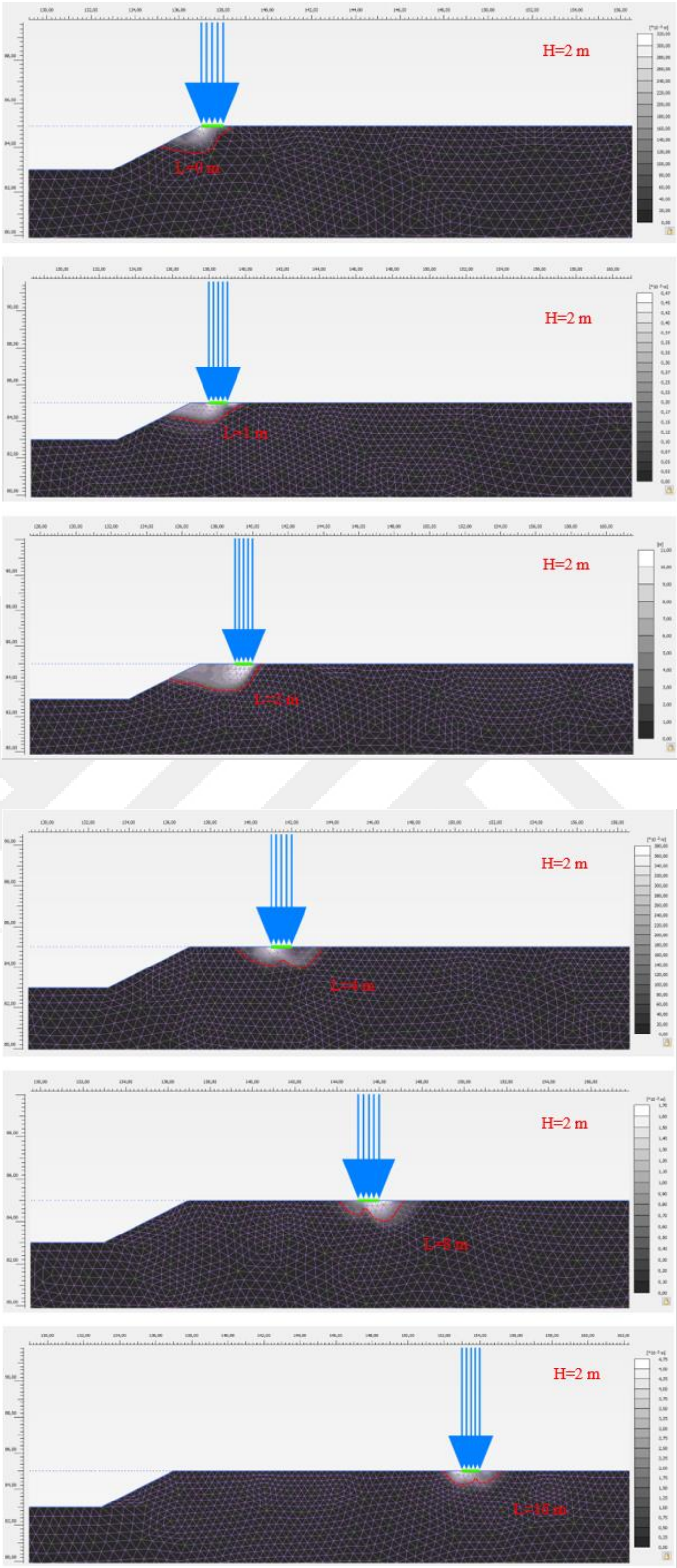

Figure 5.1. The incremental displacements for a single foundation on the slope at H=2m, B=1 and different interaction distances

Figure 5.1, presents the incremental displacement mechanisms mobilized after foundation loading for L=0-1-2-4-8-16 m. In cases where L=0-1-2 m, it can be observed that the triggering of the sliding mechanism in the slope can lead to the overall system reaching the limit equilibrium condition due to insufficient bearing capacity of the foundation-soil system. The reason for the insufficient bearing capacity of the foundation soil, as mentioned in many literature sources, is the absence of a passive zone that provides resistance against destabilizing effects in the overall failure mechanism. Due to the presence of the slope, the passive resistance zone is not present in the system. Without the passive resistance zone, the foundation soil cannot symmetrically respond to structural loads. Therefore, the bearing capacity value of shallow foundations constructed on horizontally layered soils is higher than that of shallow foundations constructed on slope. In this situation, it is necessary to address both the bearing capacity of the foundation-soil system and the slope instability problem together. However, when the interaction distance L exceeds twice the size of the foundation (interactions between 2-4B were not examined in this case), the slope-foundation system does not interact, and only a sliding mechanism can be activated due to insufficient bearing capacity of the foundation-soil system. In this case, slope instability is not a concern. The analysis conducted in the previous section has shown that the mentioned distance is not dependent on the soil properties.

Another case examined is the presence of shallow foundations with different widths on a slope. In this case, B=2 m (constant), H=2 m, and the relative density of the sandy soil is considered to be 65%. The variations occurring in the critical failure plane mobilized due to changes in the slope-foundation interaction distance are analyzed and presented in Figure 5.2. The effect of different foundation widths, B=1 m and B=2 m, on the mobilized failure mechanism is visibly significant. With an increase in foundation width, the increased bearing capacity value leads to an increase in the width and depth of the soil affected by the loading. It can be observed that the slope-foundation system influences each other's behavior up to an interaction distance of nearly L=8 m. However, once this distance is exceeded, the failure mechanism occurs due to insufficient bearing capacity of the foundation soil. Indeed, as the interaction distance reaches twice the foundation width, the mobilized slip circle deepens. This can be attributed to the increase in the stress level that can be sustained by the soil. When the interaction distance between the foundation and slope exceeds 8 times the foundation width, the foundation and slope behave as separate systems.

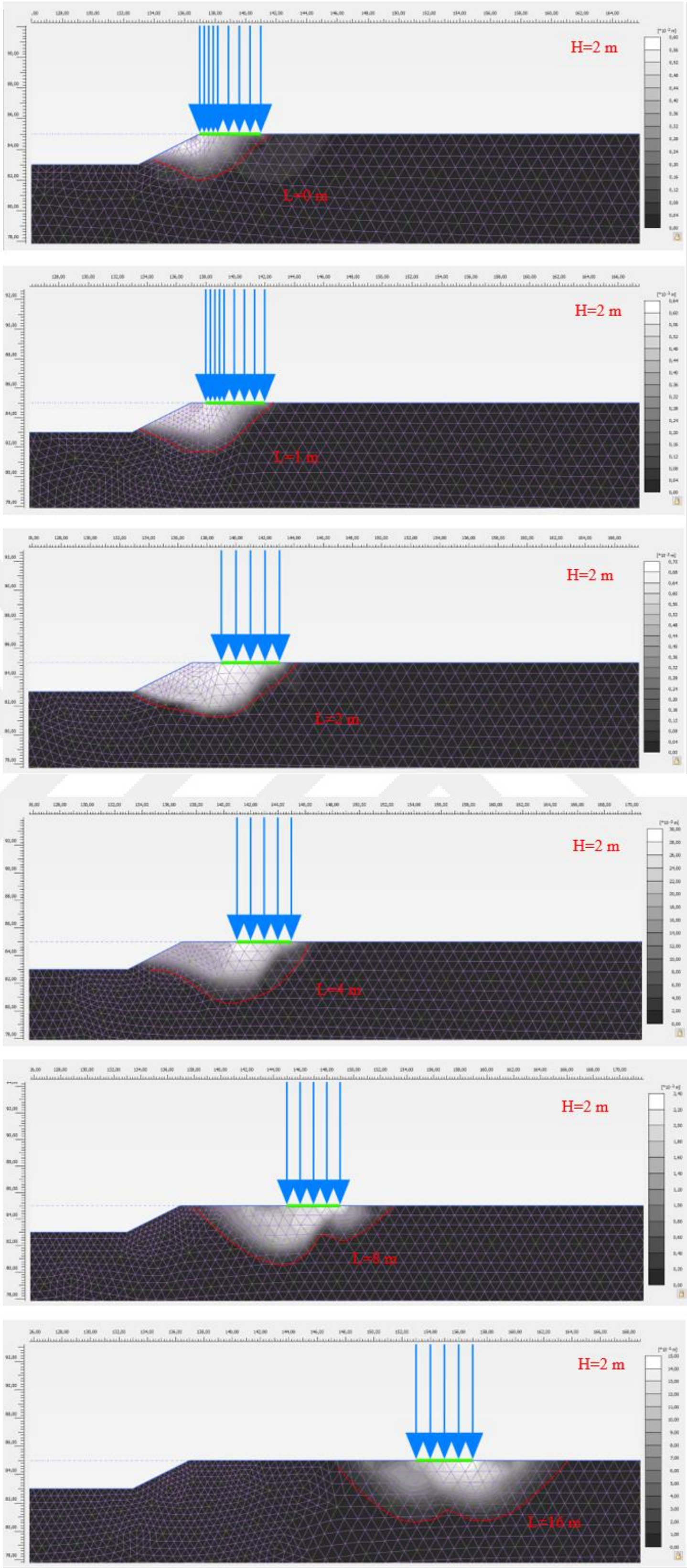

Figure 5. 2. The incremental displacements for a single foundation on the slope at H=2m, B=2 and different interaction distances

In the case where single footings on the slope are examined, another scenario involves increasing the slope height to determine the dimensions of the loaded area or to identify the boundaries of the mobilized failure mechanism.

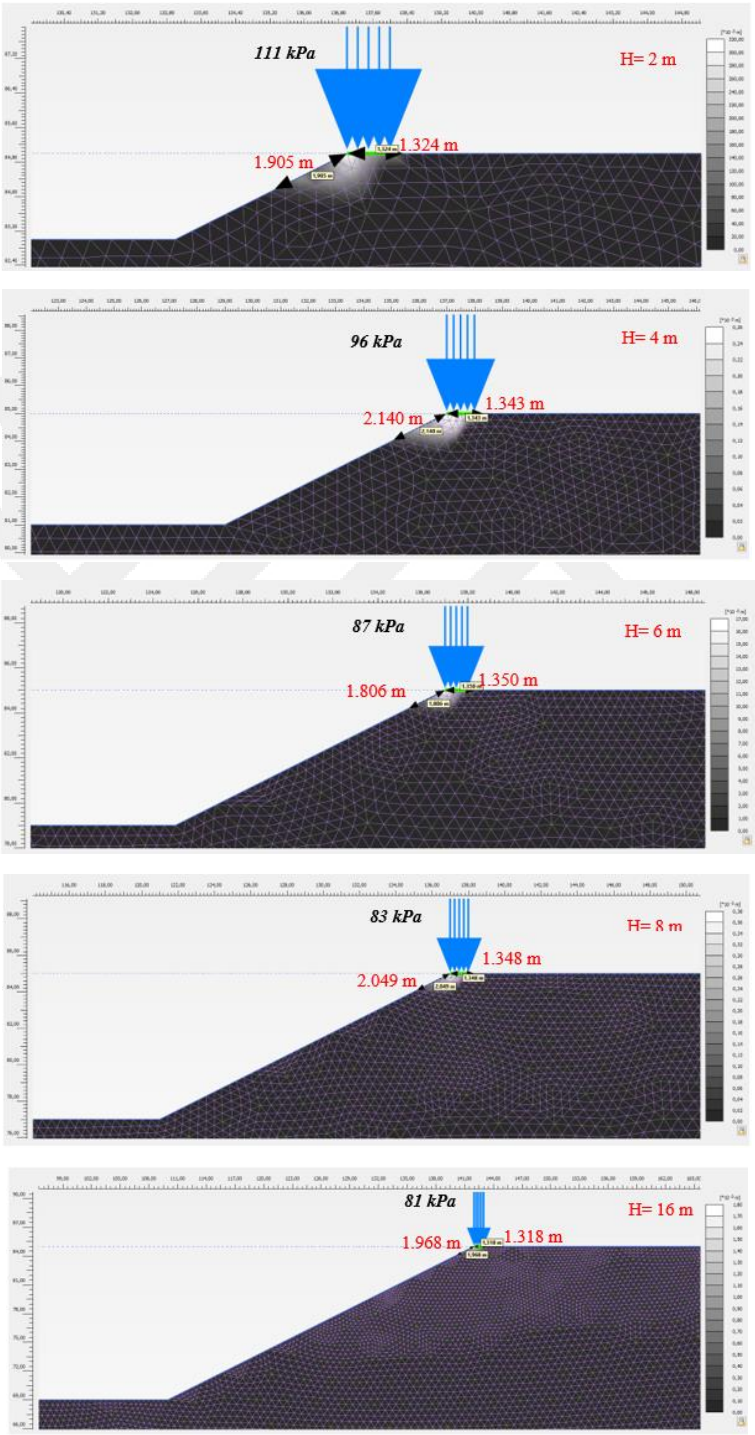

Figure 5. 3. The boundaries of the mobilized failure mechanism for different heights for single foundation on the slope.

In Figure 5.3, the change in the bearing capacity of the soil and the influence of the loading condition are determined as the slope height is increased, considering a relative density value of 65% for the foundation soil. The critical slip plane mobilized under the influence of the slope length and foundation length along with the applied loading condition is determined. It is observed that as the slope height increases, the ultimate load capacity decreases. However, the increase in slope height does not alter the boundaries of the mobilized mechanism, independent of the applied load magnitude. Along the slope length, the effect is observed within the range of 1.8-2.1 m, and the distance influenced by the foundation in the horizontal soil environment is 1.3 m, considering the applied load for each case separately.

In Figure 5.4, the analysis of the footings located within the slope composed of sand soil with a relative density of 65% is presented. In this figure, with a constant footing width of B=1 m, the variation of the ultimate load values and the boundaries of the potential critical failure planes are examined as the slope height is increased. In this case, it should be noted that the foundation is constructed at the middle height of the slope and lays on a bench ditch. The slope is formed on both sides of the foundation. In this scenario, the ultimate load values remain approximately the same regardless of the variation in height. The range of variation in the ultimate load value is 94-122 kPa. It should be noted that extremely accurate measurements were not taken in the Plaxis program under these loading conditions, indicating that the boundaries of the activated mechanism are of similar nature. Therefore, the mechanism that occurs only affects the stability of the slope portion located below the foundation.

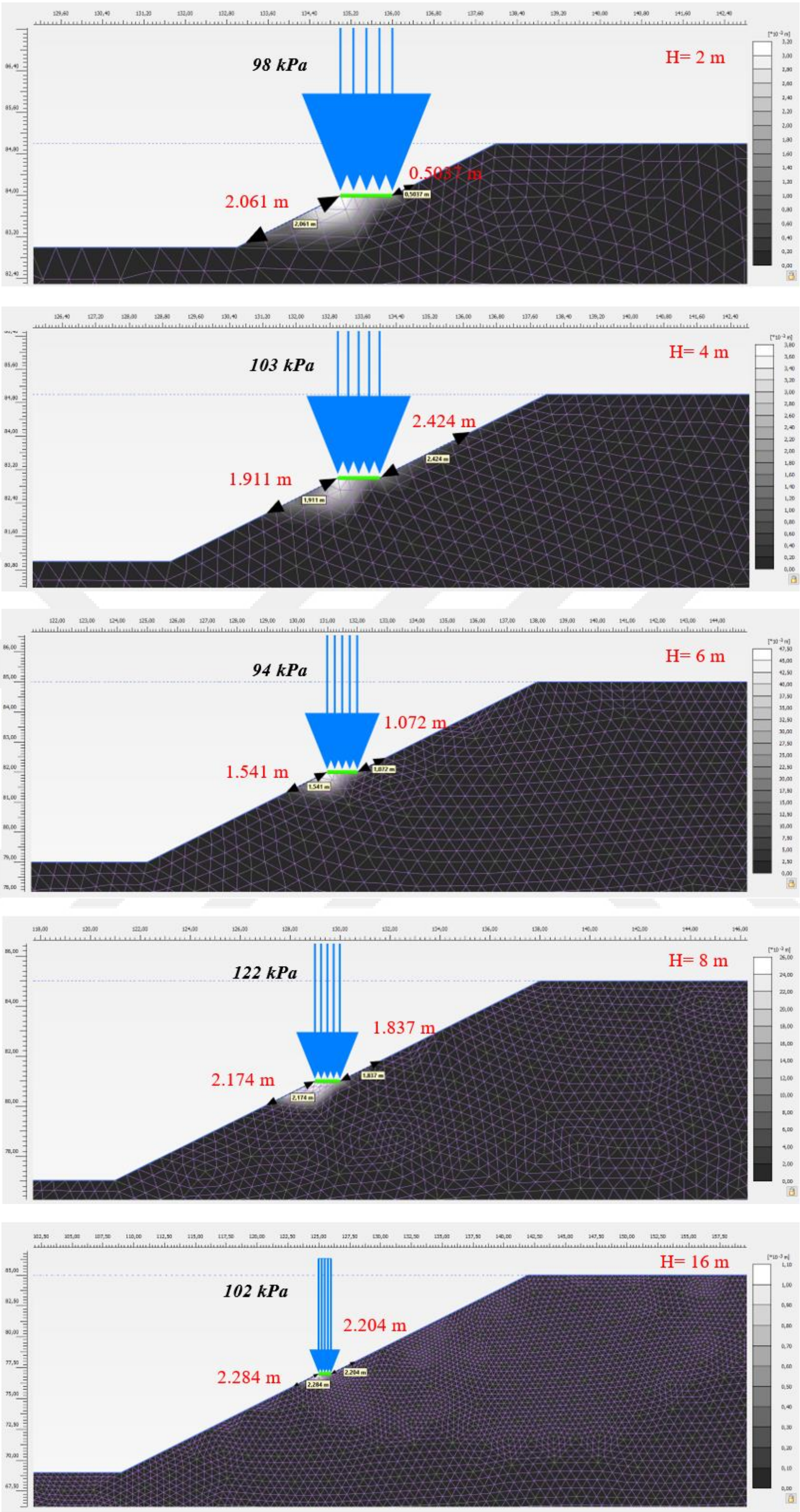

Figure 5.4. The boundaries of the mobilized failure mechanism for different heights for single foundation within the slope.

The first case examined for the analysis of multiple foundations on a slope involves studying the critical slip planes that would mobilize when the interaction distance between unit-length foundations (B=1 m) placed on the slope crest (L=0 m) is increased. In Figure 5.5, the maximum load capacities that can be carried and the limits of mobilized failure mechanisms are provided for different inter-foundation distances, namely L_f=0-1-2-4-8-16 m. These limits have been investigated considering the slope length, interaction distance between foundations, and the length of influence along the depth. This scenario was examined for a relative density value of 65% for the underlying soil and a slope height of 2 meters. In the case of unit-length (B=1 m) foundations modeled as a dual foundation system in a fully adjacent arrangement, the foundations exhibited a single plate behavior and reached the maximum load capacity. In the case of L_f = 0m, the mechanism initiated by the foundation's load-bearing capacity transformed into a comprehensive instability mechanism that included the slope due to the low height of it. In this case, a wider and deeper failure plane was activated compared to all other options examined within the scope of only this part of the study. However, as the interaction distance between the foundations increased, this comprehensive stability problem transformed into a situation of load-bearing capacity insufficiency, driven by the loads imposed on the first foundation. The mechanisms that would lead to the failure of the foundations also diverged as the interaction distance was shifted by B, and the boundaries of the areas posing stability issues became independent of further increases in the interaction distance due to the absence of a passive zone for the first foundation.

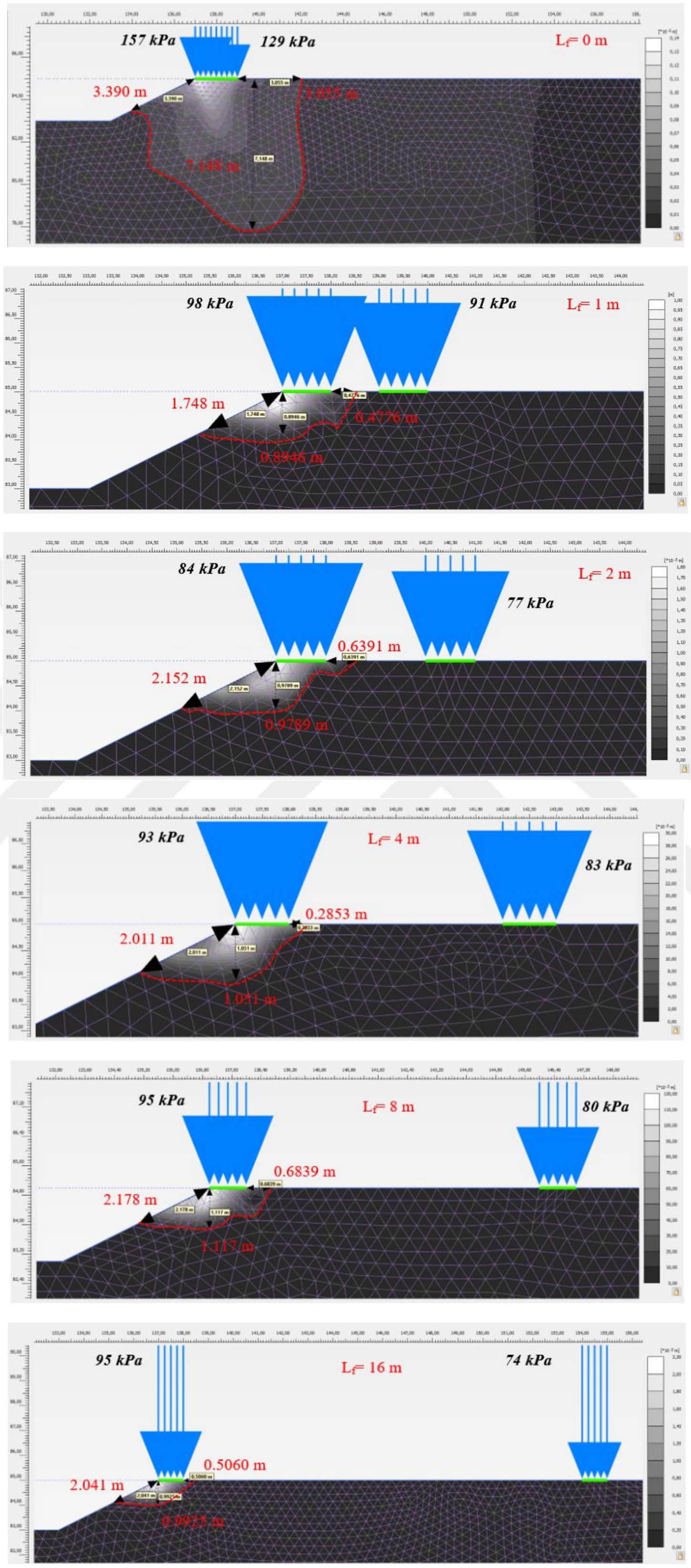

Figure 5.5. The maximum load capacities and the limits of mobilized failure mechanisms for different inter-foundation distances

Another case considered for multiple foundations on a slope is the evaluation of system stability by varying the slope-foundation interaction distance. In this context, assuming B=1 m, D_r=65%, H=4 m, and L_f=0 m. In Figure 5.6, the load-bearing capacity values of the foundations and the dimensions related to the activated critical failure planes are provided for this situation. Increasing the slope-foundation interaction distance is expected to increase the load-bearing capacity of the underlying soil. In the cases where the interaction distance reaches twice the foundation width, the mobilized failure mechanism is primarily driven by the load-bearing capacity of the foundation, affecting the slope as well. However, as the distance increases, the slope area affected by the foundation loading decreases, and after the failure extends beyond L=4B distance (behavior for distances between L=4-8m was not examined in these analyses), the problem turns into a foundation load-bearing capacity problem.

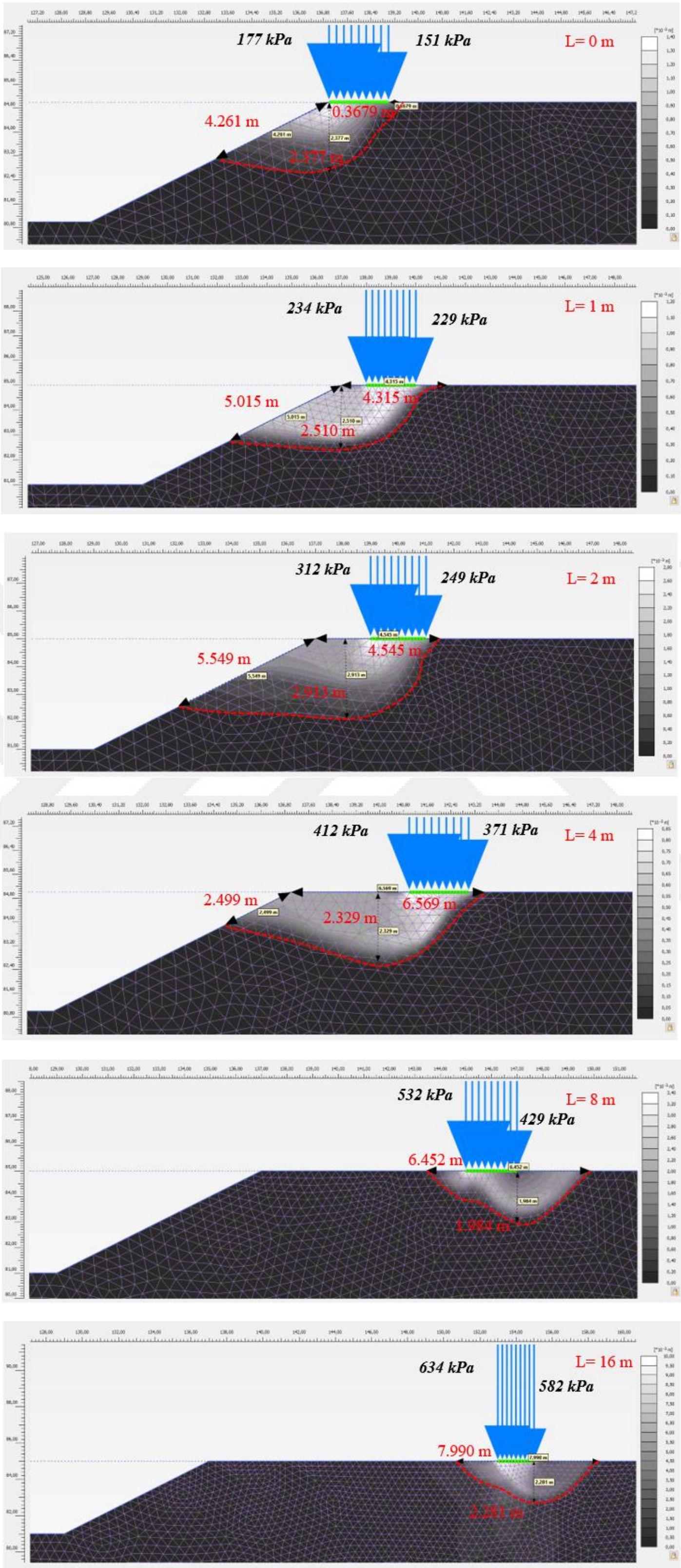

Figure 5.6. The maximum load capacities and the limits of mobilized failure mechanisms for multiple foundations

The analysis of plural foundations constructed within the slope was conducted by evaluating different slope height conditions, and the incremental displacements shown in Figure 5.7, were obtained. In these analyses, the relative density of the foundation soil was considered as 65%, the foundation width was B=1 m, and the interaction distance between the foundations was Lf=0 m. The increase in slope height has led to a decrease in the load that can be carried by the foundation soil or transferred from the structure.

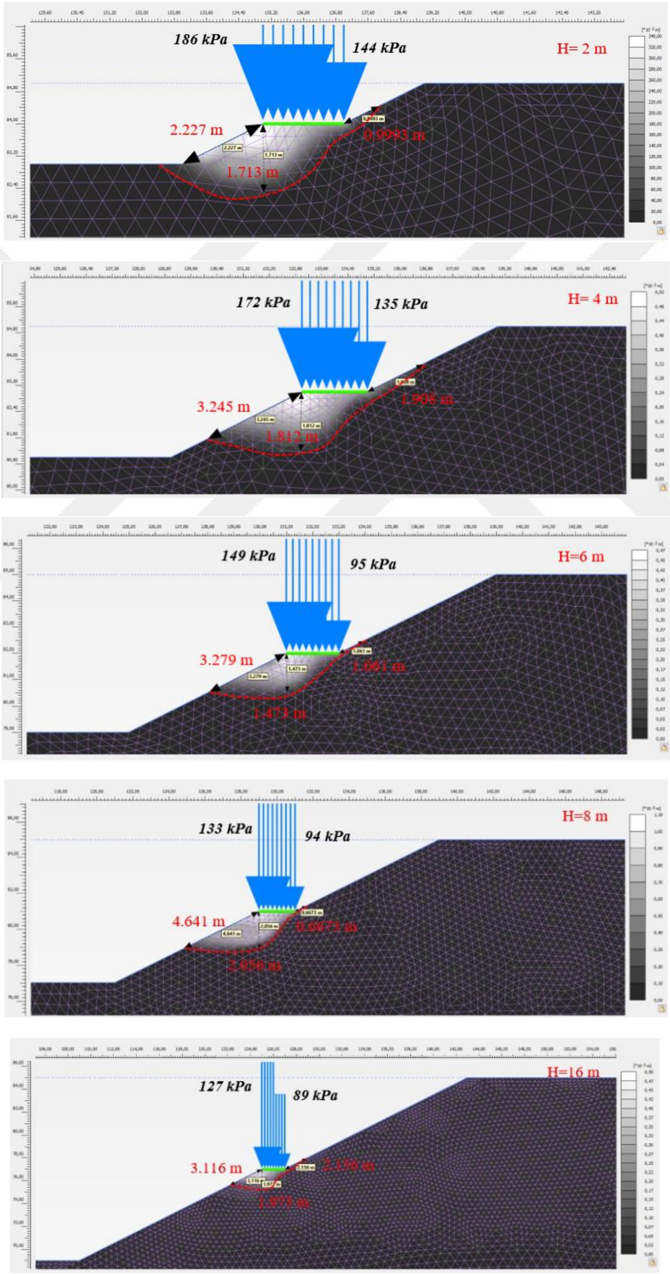

Figure 5.7. The maximum load capacities and the limits of mobilized failure mechanisms for multiple foundations within the slope

The increased slope height has had a relatively limited effect on the boundaries of the mobilized sliding mechanism, and a general approach to the effect of height variation on these mechanism boundaries could not be reached. However, unlike individual foundations within the slope, in the case of plural foundations within the slope, it can be said that the upper part of the slope is also affected by deformations and forms a boundary for the potential mobilized critical sliding plane.

The last case to be considered in the study is the effect of changing the interaction distance between plural foundations within the slope on the formation of the sliding plane. For the analysis of this situation, H=4 m, D_r=65%, and B=1 m are assumed.

The interaction distance between the foundations, L_f, is assumed to be 0-1-2-4 m respectively. The construction of these foundations, similar to singular foundations, is performed on the horizontal soil layer between the slopes and at the mid-height of the slope. Increasing the interaction distance between the foundations has led to a decrease in the load-bearing capacity of the first foundation, particularly at the level of load it can carry. However, there has not been a significant change in the load-bearing capacity of the second foundation. In the case of adjacent neighboring foundations, the upper part of the slope involved in the sliding mechanism has exhibited behavior independent of and unaffected by the foundation loads, as the interaction distance between the foundations increased. The observed sliding mechanism in the case of adjacent foundations has the deepest dimensional characteristics within the presented figure 5.8. When the distance between the first and second foundations exceeds the value of B (foundation width), the foundations have shown a tendency towards sliding behavior due to the mobilized shear stresses under their respective loads. In the considered case, the first foundation has also influenced the slope portion on which it is located, contributing to the overall sliding behavior.

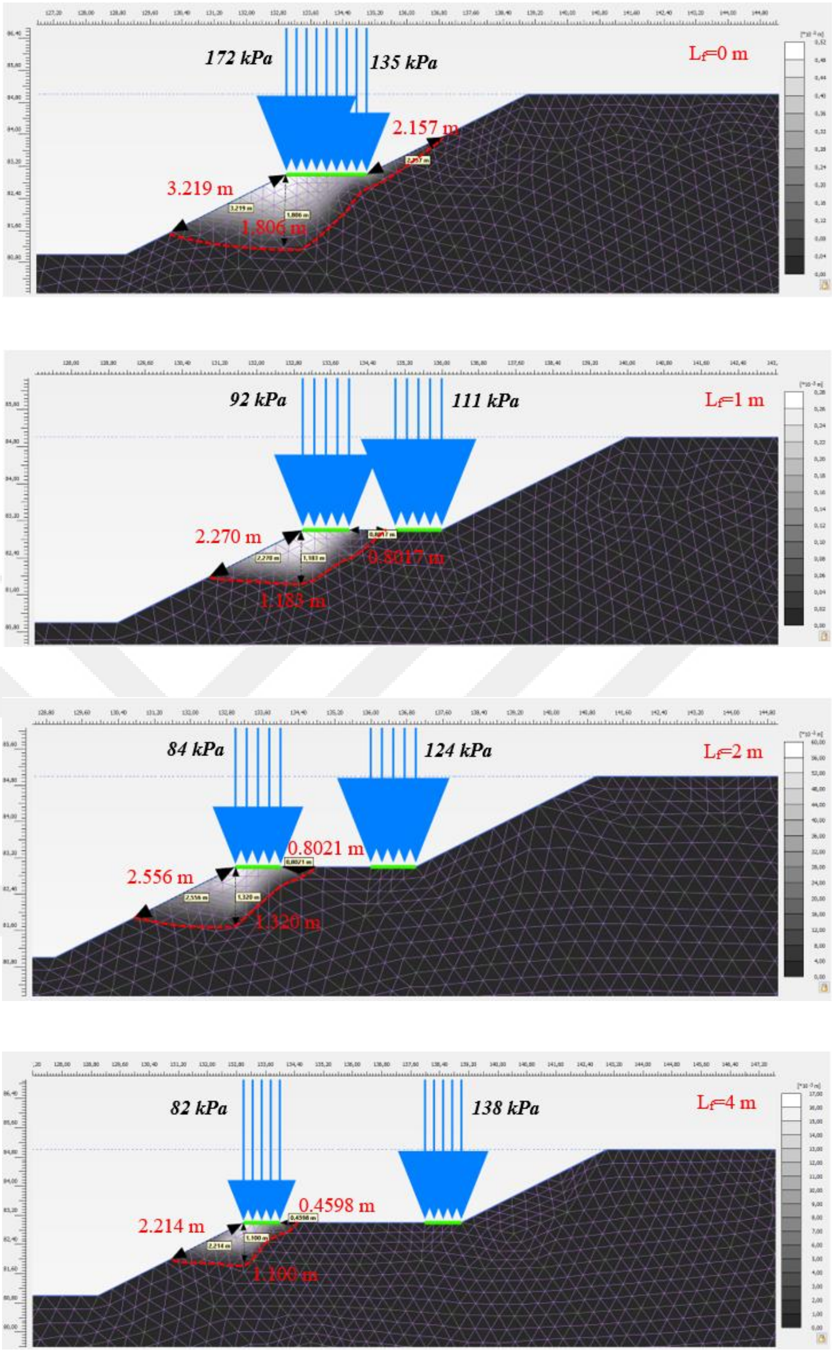

Figure 5.8. The maximum load capacities and the limits of mobilized failure mechanisms for multiple foundations within the slope for different inter-foundation distances

6. CONCLUSION AND RECOMMENDATIONS

The study utilized the finite element technique to develop a numerical model for investigating the influential parameters affecting the bearing capacity of single and adjacent foundations located both on and within slopes. A comprehensive parametric analysis was conducted, considering variables such as slope height (H), foundation width (B), distance between double foundations (L_f), and distance from the foundation to the edge of the slope (L). To facilitate practical design considerations, design procedures, and charts were developed to aid engineers in predicting optimal foundation locations based on specific slope geometries and soil conditions, ensuring stability for both the foundation and slope. The study also presented practical design examples as illustrative cases. Based on the findings, several conclusions can be drawn. Firstly, an increase in slope height was found to correspond with a decrease in the bearing capacity of the foundation. Conversely, the bearing capacity showed an increase with increasing distances from the slope and/or higher relative soil density. Moreover, the distance between bases exhibited varying effects on the bearing capacity. Specifically, as the distance increased, an overlapping effect between the stress fields occurred, resulting in a decrease in the bearing capacity of one base compared to the other. However, as the distance further increased, the interfering effect gradually diminished until reaching a point where the influence of this overlap was negligible.

These conclusions provide valuable insights for engineers and designers, enabling them to make informed decisions regarding foundation placement in relation to slope characteristics and soil conditions, ultimately ensuring the stability of both the foundation and the slope system.

There is potential for extending the study by considering the behavior of foundations at different levels on the slope within the same experimental context. Additionally, within every case, it could be extended to consider the effect of differences in the dimensions of the Adjacent foundations. moreover, an exploration of the response exhibited by foundations in layered soil conditions is also feasible.

REFERENCES

[1]. Baskharon, M., 2019, *Numerical Modeling for Shallow Foundation near Slope*, Thesis (MASc), Concordia University.

[2]. Haghgouei, H., Kargar, A.R., Khosravi, M.H., Amini, M., 2021, *A 2D semi-analytical analysis of the time-dependent settlement of a shallow foundation placed near the soil slope*, Journal of Analytical and Numerical Methods in Mining Engineering 11 (29), 41-54.

[3]. Yang, S., Leshchinsky, B., Cui, K., Zhang, F., Gao, Y., 2019, *Unified Approach toward Evaluating Bearing Capacity of Shallow Foundations near Slopes*, Journal of Geotechnical and Geoenvironmental Engineering, 145 (12).

[4]. Brinkgreve, R.B.J., 2005, *Selection of soil models and parameters for geotechnical engineering application*, Soil Constitutive Models, Congres Austin, Texas, 24/01/05, Reston,Virginia, American Society of Civil Engineers (ASCE), ISBN: (0-7844-0771-1), 69-98.

[5]. Brinkgreve, R.B.J., Engin, E., Engin, H.K., 2010, *Validation of empirical formulas to derive model parameters for sands*, Numerical methods in geotechnical engineering Numge 2010., Leiden: CRC Press, 137-142 6 p.

[6]. Javdanian, H., 2017, *On the behaviour of shallow foundations constructed on reinforced soil slope – a numerical analysis*, International Journal of Geotechnical Engineering, 24 (8).

[7]. Haghgouei, H., Kargar, A.R., Khosravi, M.H., Amini, M., 2021, *Semi-Analytical Study of Settlement of Two Interfering Foundations Placed on a Slope*, Journal of Mining and Environment (JME), 12 (2), 457-470.

[8]. Raj, D., Singh, Y., Kaynia, A.M., 2018, *Behavior of Slopes under Multiple Adjacent Footings and Buildings*, International Journal of Geomechanics, 18 (7).

[9]. ACHARYYA, R., DEY, A., 2020, *Assessment of interaction mechanism and bearing capacity of strip footings located on slope face*, Indian Academy of Sciences, Sådhanå 37, 11.

[10]. Baah-Frempong, E., Shukla, S.K., 2018, *Stability analysis and design charts for a sandy soil slope supporting an embedded strip footing*, International Journal of Geo-Engineering 9, 13.

[11]. Xiao, S., Chen, T., Guo, W.D., 2020, *Bearing capacity of rigid strip footings near soil slopes*, Proceedings of the Institution of Civil Engineers - Engineering and Computational Mechanics, 173:4, 173-187

[12]. Xiao, S., Chen, T., 2022, *Bearing capacity of shallow rigid strip foundations near slopes based on generalized log-spiral shear mechanism*, licensed under a CC BY 4.0 License.

[13]. Acharyya, R., Dey, A., 2021, *Assessment of bearing capacity and failure mechanism of single and interfering strip footings on sloping ground*, International Journal of Geotechnical Engineering, 15:7, 822-833.

[14]. Qarmout, M., Ghrairi, F.H.A., Lavasan, A.A., König, D., Wichtmann, T., 2020, *Bearing Capacity of Embedded Strip Footing Placed Adjacent to Sandy Soil Slopes*, International Conference on Geotechnical Engineering-Iraq.

[15]. Leshchinsky, B., 2015, *Bearing Capacity of Footings Placed Adjacent to c′-ϕ′ Slopes,* Journal of Geotechnical and Geoenvironmental Engineering, 141(6).

[16]. Dey, A., Acharyya, R., Alammyan, A., 2019, *Bearing capacity and failure mechanism of shallow footings on unreinforced slopes: a state-of-the-art review*, International Journal of Geotechnical Engineering, 15:10, 1284-1297.

[17]. CÜRE, E., 2013, *Ultimate Loads Of Eccentrically Loaded Model Strip Footing Adjacent To Slope On Sand*, Thesis (PhD), Karadeniz Technical University.

[18]. Acharyya, R., Dey, A., 2020, *Assessment of interaction mechanism and bearing capacity of strip footings located on slope face*, Sådhanå 45, 89.

[19]. Skempton, A.W., Macdonald, D.H., 1956, *The Allowable Settlements of Buildings*, Proceedings of the Institution of Civil Engineers, 5:6, 727-768.

[20]. Çimen, Ö., Türkmen, M., Urhan, A., 2015, *A Case Study of Different Settlement Problem on Low Rise Building*, AKU Journal of Science and Engineering, 15, 1-10.

[21]. Uzuner, B. A., 1995. *Temel Mühendisliğine Giriş*, Derya Kitabevi, 27-92.

[22]. Moayedi, H., Hayati, S., 2018, *Modelling and optimization of ultimate bearing capacity of strip footing near a slope by soft computing methods*, Applied Soft Computing, 66, 208-219.

[23]. Liu, Y., 2013, *Effects of Mesh Density on Finite Element Analysis*, SAE Technical Papers. 2.

[24]. Shields, D., Chandler, N., Garnier, J., 1990, *Bearing Capacity of Foundations in Slopes*, Journal of Geotechnical Engineering, 116, 3.

[25]. Mansouri, T., Abbeche, K., 2019, *Experimental bearing capacity of eccentrically loaded foundation near a slope*, Studia Geotechnica et Mechanica, 41(1): 33–41.

[26]. Javdanian, H., 2020, *On the behaviour of shallow foundations constructed on reinforced soil slope-a numerical analysis*, Geotechnical Engineering, 14(2): 188–195.

[27]. Acharyya, R., Dey, A., 2017, *Finite Element Investigation of the Bearing Capacity of Square Footings Resting on Sloping Ground*, INAE Lett, 2, 97–105.

[28]. Leshchinsky, B., 2015, *Bearing capacity of footings placed adjacent to C-ϕ slopes*, Journal of Geotechnical and Geoenvironmental Engineering, 1(1), 1–20.

[29]. Keskin, S.M., Laman, M., 2013, *Model studies of bearing capacity of strip footing on sand slope*, KSCE J Civ Eng **17**, 699–711.

FIRST PAGE OF THE PLAGIARISM REPORT

4801180690-Bashar BADAWI

ORİJİNALLİK RAPORU

%17	%15	%12	%3
BENZERLİK ENDEKSİ	İNTERNET KAYNAKLARI	YAYINLAR	ÖĞRENCİ ÖDEVLERİ

BİRİNCİL KAYNAKLAR

1	spectrum.library.concordia.ca İnternet Kaynağı	%5
2	www.researchgate.net İnternet Kaynağı	%3
3	Submitted to The Scientific & Technological Research Council of Turkey (TUBITAK) Öğrenci Ödevi	%1
4	idoc.pub İnternet Kaynağı	%1
5	ebin.pub İnternet Kaynağı	%1
6	ro.ecu.edu.au İnternet Kaynağı	<%1
7	anm.yazd.ac.ir İnternet Kaynağı	<%1
8	"Proceedings of the Indian Geotechnical Conference 2019", Springer Science and Business Media LLC, 2021 Yayın	<%1

ETHICS COMMITTEE PERMISSION

WARNING: It is mandatory to obtain an Ethics Committee Permission for all research topics related to living subjects.

☐ **Ethics Committe permission is required.**

☒ **Ethics Committe permission is not required.**

Bashar BADAWİ

INSTITUTIONAL PERMISSIONS

WARNING: It is mandatory to obtain Institutional Permission for all research topics related to living and dead subjects. In cases involving confidentiality and privacy, the name of the institution should be closed.

☐ **Institutional permission is required.**

☒ **Institutional permission is not required.**

Bashar BADAWİ